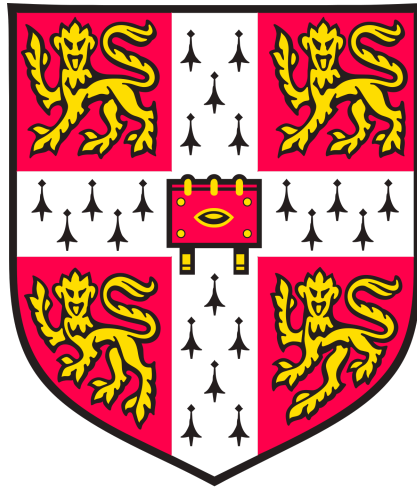


Elucidating p53's physiological and tumourigenic roles



Chun-Ming Lam

Hughes Hall, University of Cambridge

**Department of Biochemistry
University of Cambridge**

This dissertation is submitted for the degree of Doctor of Philosophy

January 2020

**BLANK
PAGE**

PREFACE

I declare that this dissertation represents my own work and includes nothing that is the outcome of work done in collaboration except as declared in **Preface** (as below) and specified in the text.

- **Figure 2.15 (a): Western blot of Spleen in Chapter 2** was executed under my supervision by Ms. Maria-Myrsini Tzoni, then a rotatory student in Evan group, for the purpose of her training. The results were used in this dissertation with her consent.

This dissertation is not substantially the same as any that I have submitted, or, is being concurrently submitted for a degree or diploma or other qualifications at the University of Cambridge or any other university or institution except as declared in **Preface** and specified in the text. I further state that no substantial part of my dissertation has already been submitted, or, is being concurrently submitted for a degree or diploma or other qualifications at the University of Cambridge or any other university or institution except as declared in **Preface** and specified in the text.

This dissertation does not exceed the limit of 60,000 words and meets the requirements set by the relevant Degree Committee.

Chun-Ming Lam

January 2020

**BLANK
PAGE**

ABSTRACT

The key role of p53 as a tumour suppressor is widely acknowledged and based on many observations that p53 suppresses oncogene-mediated transformation of rodent fibroblasts and is the most frequently mutated gene in human cancers. However, the p53 family of transcription factors is evolutionarily very ancient and already found in primordial metazoans where it acts as a pivotal coordinator of reparative responses to cellular stress, cell and DNA damage (“the Guardian of the Genome”). The best guess is that the tumour suppressor functions of p53, principally induction of cell death and senescence, are later additions that serve to rein in rogue somatic cells. The extent to which the immediate stress response and tumour suppression functions of p53 augment or antagonise each other is hotly debated, not the least because of occasional studies that indicate a paradoxical positive selective retention of p53 in some early stage cancers, suggesting that p53 function is indeed in some way beneficial for nascent tumours. Such inherent antagonistically pleiotropic properties make classical genetic analysis of p53 function complicated – as does the confounding presence in the mammalian genome of at least two additional paralogues of p53, p63 and p73 whose functions partially overlap. Therefore, to address the potentially distinct functions of p53 in development, maintenance and repair of normal adult tissues and in tumour suppression, I have built a unique, temporally switchable mouse model in which p53 function may be reversibly toggled between wild type and null states at will in vivo. I show that acute systemic repression of p53 in adult mice elicits no overt symptoms or somatic pathologies. However, spontaneous tumours emerged in the same cellular compartments and with a similar latency to those observed in germline p53-null mice. Detailed analyses of tissues and tumours have yet to be conducted. Temporal dissection of p53’s functions at different stages of chemically-induced skin cancer revealed a window during the initiation stage where p53 retention promoted early carcinogenesis (skin papillomas) while loss of p53 promoted the development of later squamous carcinomas. The ability to rapidly and reversibly switch p53 functional status and to identify windows of p53 pro-tumorigenic and tumour suppressive function will provide new insights into the diverse and perhaps antagonistic roles of p53 in development, tissue homeostasis, cancer and ageing.

ACKNOWLEDGEMENTS

First and foremost, I would like to thank my supervisors Prof. Gerard Evan and Dr. Trevor Littlewood, who offered me the opportunity to work in this laboratory in Cambridge as an MPhil and then a PhD student. Throughout the course of my study, not only has Gerard guided me and offered advice for the project, but also inspired me to become a proper scientist who is perceptive to ask the right questions as well as creative yet careful to address them. Trevor has always been there to offer his guidance and practical advice as well as to discuss ideas for the project; this project would not have reached this far otherwise. Both Gerard and Trevor are attentive and supportive supervisors who care for my general wellbeing beside my academic progress. It was a great pleasure to undertake my graduate study under their supervision.

I also would like to thank Dr. Philip Johnston, my tutor from Hughes Hall, for his advice and support throughout the course of my graduate study. I thank Cambridge Trust and Hughes Hall, my affiliate college in Cambridge, for funding my PhD study.

I would like to take this opportunity to thank my colleagues who had been helpful and supportive in the group. In particular, I thank Dr. Debbie Burkhart for all her invaluable advice regarding the making of the mouse model, Southernns and other countless experiments, the numerous discussions we had about this project as well as the experiments she had done in my place when I was not available. I would like to thank Ms. Deborah Breiner, Ms. Michaela Griffin, Ms. Stephanie Mackie and Ms. Molly Craxton for their help in genotyping and processing of mouse tissues and Ms. Alessandra Perfetto and the animal technicians in the Cambridge Stem Cell Institute, Gurdon Institute and CRUK Cambridge Institute for their help in general maintenance of mice and *in vivo* experiments. I thank Mr. Ken Jones and Mr. Dominik Spensberger for their guidance in conducting mouse stem cell experiments and targeting. I thank Dr. Houjiang Zhou, who is a good friend, for he

taught me everything about Western blotting. I thank Ms. Maria-Myrsini Tzioni for her participation and efforts in this project. I would also like to thank Dr. Catherine Wilson, Dr. Luca Pellegrinet, Dr. Tania Campos and Dr. Frank McCaughan for the helpful discussions we had about experiments and prospectives of the project. I especially thank Dr. Nicole Sodir and Ms. Ban Dodin for not only their professional advice but generous support and friendships. I would also like to thank Ms. Fiona Goodman for the numerous times she helped me with paperwork, procedures and tracking down Gerard.

I would also like to thank Dr. Dan Lu, Dr. Adam Guterres, Dr. Nick Salisbury, Dr. Roderik Kortlever, Dr. Ana Rebocho, Dr. Ivonne Gamper, Dr. Linsey Porter, Dr. Megan Bywater, Dr. Helena Rannikmae, Dr. Phil Barry, Dr. Lucia Correia, Ms. Manuela Urbischek, Mr. Thomas Foet, Ms. Kerstin Fentker and Ms. Heidi Funke, alongside whom I had the privilege to work, for all the fun we had together and the joy you brought me. I also thank Ms. Ceci Li for her support during the writing of this dissertation. And I thank Mr. Tom Gray who has been a supportive friend with unfailing British humour. Finally, I thank Mr. Ng. Chap-Fai - my high school biology teacher - for he was the first to believe in me as well as the first to inspire my interest in biology and research through his marvellous classes.

At the very last, and mostly importantly, I would like to express my utmost gratitude to my family - my parents, aunt Amy and my sister - who have always been unconditionally supportive and encouraging in my pursuit of dream. They are a constant anchor in the vast torrent of the world and life onto which I can always trustingly hold. I could not have made this far without any of them. Thank you.

TABLE OF CONTENTS

Preface	I
Abstract	II
Acknowledgement	III
Table of Contents	V

List of Abbreviations	X
------------------------------	----------

Introduction	1
---------------------	----------

I.1	Cancer as a disease	2
I.1.1	Historical perspective	2
I.1.2	Cancers are genetic diseases	2
I.1.3	Existing therapeutic options	3
I.1.4	Therapeutic challenges	4
I.2	Tumorigenesis, oncogenes and tumour suppressors	5
I.3	The p53 protein	8
I.3.1	Structure and function of the p53 protein	8
I.3.2	Regulation of p53 by post-translational modifications	10
I.3.3	Isoforms of p53 mRNA and protein	11
I.4	p53 tumour suppression	13
I.4.1	The discovery of p53	13
I.4.2	p53 is a tumour suppressor	13
I.4.3	Mechanisms of p53 tumour suppression	17
I.4.4	Exploring p53-based cancer therapies	18

Introduction (continued)

I.5	Non-tumour suppressive functions of p53	21
I.5.1	Ancient function of p53 - what has it evolved to do?	21
I.5.2	Developmental functions of p53	22
I.5.3	p53 plays a key role in somatic stem cell maintenance	23
I.5.4	p53 and cellular stresses - metabolism, hypoxia and autophagy	24
I.6	Questions to address regarding p53 biology and experimental approach	27
I.6.1	Importance of p53 in adulthood physiology	25
I.6.2	Clarifying the paradigm of p53 tumour suppression	28
I.6.3	Aims of the project and experimental approaches	30
I.6.4	<i>In vivo</i> models to be used	31

Methods and Materials

M.1	Molecular cloning and DNA manipulations	34
M.1.1	PCR amplification, restriction digestion and ligation of DNA	34
M.1.2	BAC preparation and verification	38
M.1.3	Preparing electro-competent EL350, electroporation and recombineering of DNA in EL350	39
M.1.4	Gibson Assemble	40
M.1.5	Antibiotics used in molecular cloning	40
M.2	Mouse embryonic stem cells (mESC) culture and targeting	41
M.2.1	Culture of mESC	41
M.2.2	DNA electroporation into mESC	41
M.2.3	Isolation of antibiotic-resistant clones of mESC	41
M.2.4	Preparation of mESC for blastocyst injection	42
M.2.5	Lipofectamine transfection of mESC	42
M.2.6	mESC culture media composition	43

Methods and Materials (continued)

M.3	Primary mouse embryonic fibroblasts (MEFs) culture	43
M.4	Southern blot	44
M.5	RNA extraction and qPCR analysis	46
M.6	Protein extraction and Western blot	48
M.7	Mice	49
M.7.1	Genetic backgrounds and strains of mice	49
M.7.2	Maintenance of mice	49
M.7.3	Chemical induction of skin cancer	50
M.7.4	Collection and preparation of mouse tissues	50
M.8	Immunofluorescence staining of mouse tissues	51

Chapter 1: A model for reversible repression of endogenous <i>Trp53</i> expression	53
---	-----------

1.1	Why is a new switchable p53 model needed?	54
1.2	Designing and optimising the <i>TRE-p53</i> repression system	57
1.3	Generation of <i>Trp53</i> targeting vector	59
1.3.1	Cloning of <i>TRE-LoxP-Neo-LoxP</i> cassette into pL452	59
1.3.2	Preparation of DTA targeting vector to capture <i>Trp53</i> promoter/intron sequence	59
1.3.3	Capturing <i>Trp53</i> promoter/intron sequence from BAC into DTA vector	63
1.3.4	Insertion of <i>TRE-LoxP-Neo-LoxP</i> cassette into DTA3/4/5	65
1.3.5	Isolation of DTA-TRE3/4/5-NeoR vectors	69
1.4	Targeting <i>Trp53</i> gene in mouse embryonic stem cells (mESC)	71
1.5	Analyses of positional effect of TRE insertion	76
1.6	Generation of TRE-p53 mice	83
1.7	Reconstituting the repression system <i>in vivo</i>	85

Chapter 2: Validation of the TRE-p53 model	87
---	-----------

2.1	Validating the repression system in mESC	88
2.1.1	Creating homozygous <i>Trp53</i> ^{TRE3/TRE3} ;CAG- <i>rtTS</i> ^{tg} mESC	88
2.1.2	Kinetics of <i>Trp53</i> repression and de-repression in mESC	91
2.2	Repression of <i>Trp53</i> in primary MEFs	93
2.3	Repression of <i>Trp53</i> <i>in vivo</i>	100
2.3.1	Does <i>TRE</i> insertion interfere with normal <i>Trp53</i> mRNA expression in tissues?	100
2.3.2	Verifying <i>rtTS</i> mRNA expression <i>in vivo</i>	102
2.3.3	Repression of <i>Trp53</i> mRNA expression by Dox <i>in vivo</i>	103
2.3.4	Kinetics of <i>Trp53</i> mRNA repression by Dox	103
2.3.5	Kinetics of <i>Trp53</i> mRNA de-repression following removal of Dox	106
2.3.6	Repression of p53 protein levels by the <i>TRE</i> system	108
2.3.7	Regulation of p53 transcription activity	110
2.4	The antisense gene <i>Wrap53</i>	120
2.4.1	<i>Wrap53</i> mRNA expression <i>in vivo</i>	122
2.4.2	Strategies to address the co-repression of <i>Wrap53</i>	124
2.5	Discussion	127
2.5.1	The TRE-p53 model and its applicability	127
2.5.2	Significance of the results in this Chapter	126

Chapter 3: Investigation of <i>Trp53</i> functions	129
3.1 Effect of systemic p53 denial in adulthood	130
3.1.1 Transient p53 denial in adult mice has no effect	130
3.1.2 Long-term <i>Trp53</i> repression in adults results in tumour formation	131
3.2 Assessment of <i>Trp53</i>'s roles in early stage skin cancer	135
3.2.1 Temporal dissection of <i>Trp53</i> function in chemically induced skin cancer	136
3.2.2 Refined temporal dissection of <i>Trp53</i> 's roles in chemically induced SCC	142
3.2.3 Does p53 play a similar role in other cancers?	144
General Conclusion	149
List of References	151

List of Abbreviations

4OHT	4-hydroxytamoxifen
BAC	Bacterial artificial chromosome
BCA assay	Bicinchoninic acid protein assay
BGS	Bovine growth serum
bp	Base pair
BSA	Bovine serum albumin
cDNA	Complementary DNA
DMBA	7,12-dimethyl-benz[a]anthracene
DMEM	Dulbecco's modified Eagle's medium
Dox	Doxycycline
Doxo	Doxorubicin
d.p.c.	Day post-coitum
DTT	Dithiothreitol
F1	First generation of mouse progenies from chimeras
g	Gravity
gDNA	Genomic DNA
GMEM	Glasgow Minimum Essential Medium
IGG	Immunoglobulin G
IP injection	Intraperitoneal injection
kbp	kilobase pair
MEFs	Mouse embryonic fibroblasts
mESC	Mouse embryonic stem cells
mRNA	Messenger RNA
<i>NeoR</i>	Neomycin resistance gene
OD	1. Optical density (in the context of bacterial culture) 2. Oligomerisation domain (in the context of p53 protein structure)
ORF	Open reading frame
p53	p53 protein (mouse and human)
PBS	Phosphate buffered saline
PCR	Polymerase chain reaction
PTM	Post-translational modification
qPCR	Real time polymerase chain reaction
<i>R26</i>	<i>Rosa26</i> promoter/gene locus
ROS	Reactive oxygen species
<i>rtTS</i>	Reverse tetracycline-controlled trans-repressor gene
SDS	Sodium Dodecyl Sulfate
TAM	Tamoxifen
Tet	Tetracycline
<i>TP53</i>	Human endogenous p53 gene
TPA	12-O-tetradecanoyl-phorbol-13-acetate
<i>TRE</i>	<i>Tetracycline responsive element</i>
<i>Trp53</i>	Mouse endogenous p53 gene
TSS	Transcription start site

I. Introduction

I.1 Cancer as a disease

I.1.1 Historical perspective

Cancer has been documented since antiquity. Papyri from 1600 BC contain descriptions of breast cancer and a procedure to remove it by cauterisation (American Cancer Society 2009). Hippocrates, a physician from the Age of Pericles of Classical Greece, named the disease *Karkinos* (Greek word for crab in reference to the cross surface of a tumour that appears “with vein stretched on all sides as the animal the crab has feet”). Our current word “cancer” derives from this. Since the last century, we have acquired a deeper understanding of cancer in terms of its pathologies, causes and molecular mechanisms. However, the disease remains incurable for many patients and remains the second leading cause of mortality - after cardiovascular diseases - in the world, accounting for one in six deaths. In the UK, one in every two people will eventually develop some form of cancer (Cancer Research UK 2019).

I.1.2 Cancers are genetic diseases

Cancer is not a single disease but a collective of genetic diseases that share the feature of abnormal, uncontrollable propagation and expansion of the defective cancer cells. Cancers are probably all genetic by origin, involving relatively subtle abnormalities in regulation and/or function of key growth-regulatory genes that arise by mutations that accumulate in somatic cells over time. These DNA mutations frequently corrupt the amino acid sequences of specific gene products (though some are known to affect non-coding RNA such as Long Non-coding RNAs (Do & Kim 2018)), altering the encoded protein’s structure and how it interacts with other macromolecules that control its function and regulation. Other oncogenic mutations directly inactivate genes by frameshift or nonsense mutations in their coding sequences. Furthermore, mutations of transcriptional regulatory *cis*-elements can lead to alteration in expression of the genes. While some mutations precociously activate signalling pathways that promote

proliferation of cells (oncogenes), others inhibits pathways that restricts cells from proliferation or promotes cell death and differentiation (tumour suppressor genes). Accumulation of such mutations confers on (pre-)cancer cells an enhanced propensity to survive and/or proliferate promiscuously, thereby eroding their dependence upon their original designated somatic niches. Such rogue clones are thenceforth subject to various selective pressures that limit uncontrolled proliferation within their local somatic environments. In this way, incipient cancer clones gradually accumulate combinations of mutations that drive their evolution into malignant cancer cells. Such malignant cells expand uncontrollably and compete in organs for space occupancy and resources such as supply of nutrients and oxygen. Their outgrowth also blocks ducts and vessels, compromising architecture and function of the organ in which the tumour resides. Cancer cells may also spread and invade other parts of the body, developing into secondary tumours (metastasis) that are not always operable. Eventually the tumour-occupied organs or even the whole system fails, resulting in the patient's death.

I.1.3 Existing therapeutic options

Nowadays, there are multiple treatment options for cancers. Surgical removal of the primary tumour mass remains the most effective one - it can eliminate and cure some types of cancers - but is only effective at the earliest stages of malignant outgrowth of solid tumours, before they have metastasised. Other treatment options such as chemotherapy, radiotherapy, targeted therapy and immunotherapy can be applied more systemically but are less effective at curing the disease and often elicit more severe side-effects, although they do allow disease management and prolong survival of patients. The challenge of treating cancers is multifold. First, the diverse pathologies of different types of cancer and variations amongst individual patients, each of whom have distinct genetic makeups. Second, biological signaling pathways exhibit both robustness and redundancy, making it difficult to target individual oncogenic processes effectively. As a consequence, even similar types of cancer can be driven by

substantially different underlying molecular mechanisms in different patients. As a result, there are almost no general treatments for all cancers and individual patients likely respond differently to the same treatment (even for the same type of cancer). Existing therapies targeting specific oncogenic signalling pathways may eliminate some (even most) cancer cells but some cancer cells survive, adapt, evolve and re-wire, regenerating tumours that are no longer sensitive to the initially effective therapy, and the patient relapses.

I.1.4 Therapeutic challenges

These current challenges in curing human cancers could, however, perhaps be overcome by rational design of therapies that target the non-redundant “nodes” at which all oncogenic signalling pathways converge (e.g. inhibition of the pleiotropic oncogenic transcription factor c-MYC or reactivation of intrinsic tumour suppressors, such as p53 and its attentive pathways). The idea behind this is that cancers are aberrantly activated variants of normal developmental or regenerative somatic programmes and therefore share common underlying mechanisms that drive or inhibit them. In this unorthodox view of cancer, the apparent, diverse differences between individual cancers arise because most oncogenic mutations arise in the robust, redundant upstream signal networks that drive the underlying common cancer engines. Indeed, multiple studies have tested this hypothesis in mouse models in the past two decades and proved the validity of this, at least in principle. Thus, Soucek *et al.* demonstrated that systemic repression of c-Myc by a dominant negative mutant induced general regression of Ras-driven lung tumours within one week by blocking proliferation and inducing apoptosis specifically in the cancer cells (Soucek et al. 2008). Follow-up studies expanded the applicability of the notion that c-Myc is a shared signalling node upon which cancer cells vitally depend to other types of murine cancer (Sodir et al. 2011; Soucek et al. 2011). Similarly, other studies demonstrated in mouse models that carefully timed restoration of the tumour suppressor p53 results in regression of tumours, though to different extents in different tumour types and via different

pathways, such as senescence versus apoptosis (Martins et al. 2006; Xue et al. 2007; Ventura et al. 2007; Junttila et al. 2010; Feldser et al. 2010). A more thorough and comprehensive understanding of the biology of these shared oncogenic and tumour suppressive pathways, as well as the underlying mechanisms by which they operate, awaits further analysis in order to determine its applicability to human cancer patients.

I.2 Tumorigenesis, oncogenes and tumour suppressors

Tumorigenesis describes the process by which cancers arise and evolve to macroscopic size. The process is thought to involve the same general processes as macroscopic evolution – random genetic diversification through mutation followed by selection for increased fecundity. However, in cancer, the process is confined to somatic cell clones, the selective pressures are those that normally limit untoward expansion of somatic cells and remain only partially understood, and the ultimate impact of such excessive somatic cell growth is ironically detrimental to the survival of the host. It is axiomatic that this oncogenic evolutionary process does not take place in normal tissues, mainly because normal somatic cells are under strict restraints that limit their growth, propagation and survival to discrete somatic organ niches. It is these somatic restraints, most notably the inhibitory actions of key tumour suppressors such as p53, that serve as the selective pressures that shape the evolution of incipient cancer clones. Such is the basic mechanism underlying the evolution of cancer cells.

DNA mutation, an inescapable consequence of the intrinsic chemical reactivity of nucleic acids, become relevant to tumorigenesis when they result either in activation of oncogenes or inactivation of tumour suppressor genes. Classically, oncogenes are operationally defined as genes whose mutagenic activation drives precocious expansion of somatic cell clones. The normal (non-mutated) proto-oncogene counterparts of oncogenes are typically (although not exclusively) involved in promoting proliferation or survival of somatic cells in response to mitogenic growth and survival factors during development and in maintenance and repair of

INTRODUCTION

adult tissues. A more inclusive definition of an oncogene also includes genes that, while not necessarily themselves mutated, nonetheless transduce the pro-proliferative/pro-survival signals from upstream activated oncogenes. A good example of this latter class is the transcription factor Myc. Myc is seldom directly mutated in human cancers, at least in their early stages. However, due to its normal role as the non-redundant link connecting diverse upstream mitogenic signals to the disparate downstream transcriptional effector programmes that implement somatic cell proliferation, it serves as an obligate conduit for many, perhaps all, upstream oncogenic mutations. Thus, MYC, expression is frequently deregulated in human cancers due to relentless upstream oncogenic signals channelled by RTK-Ras, Wnt- β -catenin or Notch (Soucek & Evan 2010).

However, acquisition of oncogenic activities, or the abnormal proliferative activities they elicit, are under constant scrutiny and restraint imposed by so-called tumour suppressors. The term tumour suppressor is rather misleading since few or none of these appear to have evolved to suppress tumourigenesis: virtually all are evolutionarily ancient and present in unicellular organisms and short-lived invertebrates in which cancer is, respectively, either a meaningless concept or unlikely to be a significant source of morbidity. Rather, tumour suppressor genes appear to have evolved originally as intrinsic checks, antagonists or attenuators of the signals and processes that drive proliferation of normal cells. Hence, their roles as suppressors of cancer appear to be either exapted consequences or subsequent re-purposing of their primordial functions. In adult vertebrates, somatic cell proliferation is restricted to a few continuously renewing tissues and to regeneration following injury or pathogen damage. In adult vertebrate tissues, the majority of cells have differentiated into a quiescent state that performs specialised niche functions to maintain systemic homeostasis. Certain sub-populations of somatic cells in most tissues, stem cells, do retain a certain capacity to proliferate and replenish organs as cells gradually diminish in the tissue from wear and tear or damage. However, these are under tight control. Maintenance of the overall balance between

proliferative potential in development and systemic homeostasis afterwards is a primary function for many tumour suppressor genes. Nonetheless, the fact that various tumour suppressors are frequently inactivated in human cancers attests to their indisputable importance in stalling genesis and evolution of cancer cells

p53, in particular, has been acknowledged as a pivotal tumour suppressor since the late 80s/early 90s when studies confirmed the protein's capacity to suppress oncogene-mediated transformation of mouse fibroblasts (Eliyahu et al. 1989; Finlay et al. 1989) and identified frequent mutations of the *TP53* gene in diverse human cancers (Baker 1989; Nigro et al. 1989). These early studies were soon reinforced by the signature phenotype of germline p53-knockout mice, which revealed a mostly normal physiology but with drastically increased susceptibility to spontaneous tumourigenesis, principally lymphoma (Donehower et al. 1992).

I.3 The p53 protein

I.3.1 Structure and function of the p53 protein

Before introducing the p53 signaling networks, I will first discuss current knowledge of p53 protein structure and functions. The human p53 protein is a 393 amino acid-long transcription factor (390 in the mouse analog) whose sequence may be divided into six structural/functional domains - two N-terminal *Trans-activation domains* (TADI and TADII), followed by a proline-rich region, a core *DNA-binding domain* (DBD), an oligomerisation domain (OD), and a regulatory domain at the C-terminus (CTD) (**Figure I.1**). Also present is a nuclear localisation signal within the OD. The N-terminal TADI (amino acid 1 - 42) and TADII (amino acid 43 - 63) interact independently as well as cooperatively with a variety of proteins that are each involved in different aspects of transcription control, such as histone modification and transcriptional initiation, and which determine target gene preference (Lemon & Tjian 2000). For instance, TAD1 interacts with the transcription components TAF6 and chromatin modifier PRMT1 (Thut et al. 1995; An et al. 2004), while TAD2 interacts with the chromatin modifier GCN5 and DNA metabolism proteins PC4 and RPA (Gamper & Roeder 2008; Rajagopalan et al. 2009). Both TAD1 and TAD2 interact with the negative p53 regulators MDM2 and MDMX. The requirement for transactivation activity from the two TADs is not the same for all target genes. TADI is solely required for transactivation of certain canonical p53 target genes, including *CDKN1A*, *PUMA* and *NOXA*, but is dispensable for transcriptional activation of other targets such as *ABHD4*, *BAX* and *SIDT2*. TAD2 appears to be particularly important for the tumour suppressive activity of p53 (Raj & Attardi 2017).

The proline-rich region (amino acids 64-92) plays a critical and specific role in activation of apoptosis and related processes such as reactive oxygen species production through induction of the *PIG3* gene yet appears dispensable for transactivation of other key p53 targets, such as *CDKN1A* and *MDM2* (Walker & Levine 1996; Sakamuro et al. 1997; Venot et al. 1998; Zhu et al. 1999; Flatt et al. 2000; Baptiste et al. 2002; Lee et al. 2010).



Figure I.1 Functional domains of the p53 protein. TADI: transactivation domain one, amino acids 1 - 42; TADII: transactivation domain two, amino acids 43 - 63; Pro-rich: proline-rich region, amino acids 64 - 92; DBD: core DNA-binding domain, amino acids 102 - 292; OD: oligomerisation domain, amino acids 307 - 355; NLS: nuclear localisation signal, amino acids 316 - 325; CTD: C-terminal regulatory domain, amino acids 356 - 393.

The core DBD (amino acid 102-292), as its name suggests, mediates p53 sequence-specific DNA binding and is essential for the protein's function as a transcription factor (Pavletich et al. 1993; Wang et al. 1993). Its well-conserved loop-sheet-helix motif of the domain interacts with residues in the DNA major groove and the principal mutational hot-spot for the many p53-inactivating mutations found in cancers. Such mutations alter, or entirely abrogate, the sequence-specific binding capacity of p53, underscoring the significance of this domain for the protein's tumour-related functions (Cho et al. 1994).

The C-terminal OD (amino acid 307-355) mediates tetramerisation of the p53 protein. Though monomeric p53 protein monomer can bind to DNA, tetramerisation increases the DNA binding affinity of p53 some 10-100 fold (Balagurumoorthy et al. 1995). Tetrameric p53 also interacts with various other proteins more efficiently – for example, casein kinase 2 (Götz et al. 1999) and the adenovirus E4orf6 protein (Delphin et al. 1997).

The function of the CTD (amino acid 356 - 393) remains the most controversial amongst the domains. First described as a negative regulator of sequence-specific binding to DNA (Anderson et al. 1997; Ayed et al. 2001; Hupp et al. 1992; Hupp & Lane 1994; Jayaraman & Prives 1995), the CTD has since been shown to promote p53 binding to chromatin (Espinosa & Emerson 2001) and its linear diffusion along the DNA molecule (McKinney et al. 2004; Tafvizi et al. 2011). A study recently published by Laptenko *et al.* supports the notion that the p53 CTD is indeed an important determinant of sequence-specific binding by the DBD to DNA that enhances the stability of the p53-DNA complex (Laptenko et al. 2015).

I.3.2 Regulation of p53 by post-translational modifications

The intracellular level of p53, along with its various functions, are in the main, if not entirely, regulated by post-translational modifications (PTMs) at different amino acid residues throughout the protein. A major class of such modifications is phosphorylation at serine and threonine residues, many of which are important modulators of p53 activity. For example, phosphorylation of serine-15, threonine-18 and serine-20 block binding of MDM2. MDM2 is an E3 ubiquitin ligase that acts as a pivotal negative regulator of p53 stability: hence phosphorylation at serine-15, threonine-18 and serine-20 stabilises p53 and leads to its rapid accumulation (Shieh et al. 1997; Böttger et al. 1999; Chehab et al. 1999; Craig et al. 1999; Dumaz & Meek 1999; Unger et al. n.d.; Sakaguchi et al. 2000; Dumaz et al. 2001; Schon et al. 2002). The same phosphorylation event also promote interaction of p53 with p300/CBP, thereby enhancing p53 transactivation activity (Lambert et al. 1998; Dumaz & Meek 1999; Dornan et al. 2003; Finlan & Hupp 2004).

Another important class of PTMs of p53 is ubiquitination, the process by which single or multiple ubiquitin units are added to target lysine residues. Thus, (poly-)ubiquitination of the six lysine residues at the C-terminus of p53 by MDM2 targets p53 for proteasomal degradation and is essential to maintain low levels of p53 in unstressed or undamaged cells (Horn & Vousden 2007). Mono-ubiquitination of one of these lysine residues also promotes nuclear export of p53 (Li et al. 2003; Nie et al. 2007), though the functional implication of this remains unclear.

Many p53 lysine residues subject to ubiquitination, such as the six C-terminal lysine residues discussed above, can also be acetylated by the p300/CBP complex (Carter & Vousden 2009), thereby enhancing p53's binding to specific sequences of DNA and transactivation of associated target genes (Grossman 2001). As acetylated lysine residues cannot be ubiquitinated, this suggests that competition between the two PTMs for the same lysine residues is critical for determining p53 stability and transcriptional activity (Ito et al. 2002; Le Cam et al. 2006).

Other PTMs such as SUMOylation (conjugation of the small ubiquitin-like modifier) and methylation are also observed on some lysine residues of p53, though their biological relevance is not well defined (Carter & Vousden 2009). However, it is clear from such analyses that p53 protein is heavily regulated by PTMs and that these modifications are critical determinants of the protein's stability, level and function.

I.3.3 Isoforms of p53 mRNA and protein

It has been reported that the human *TP53* mRNA is expressed in some nine isoforms through a combination of alternative usage of two transcription start site and alternative splicing, while a total of twelve p53 protein isoforms is translated from these mRNA isoforms due to further variation introduced by usage of internal ribosomal entry sites in some mRNA isoforms (Joruiz & Bourdon 2016). As these isoforms have been identified in different cellular contexts and conditions, investigators have attempted to draw inferences as to differential functionality of these many isoforms. However, evidence to support such differential isoform function is scarce and to date the only reasonably firm conclusion is that the balance of p53 isoform expression might define p53's post-damage/-infection downstream responses (Bourdon et al. 2005; Joruiz & Bourdon 2016). For example, systemic constitutive expression at high-level of a shortened isoform of p53, named p44 (translated from an mRNA lacking exons 1-3), from a randomly inserted transgene in mice led to ageing phenotypes and shortened lifespan (Maier et al. 2004). The investigators speculated that such systemic overexpression of p44 leads to proliferation deficit, cellular senescence and organismal ageing to aberrant insulin-like growth factor (IGF) signalling. However, several caveats weaken this study. First, while it is formally possible that this p53 isoform exists in a physiological setting with the speculated functions, there is no evidence that it is normally expressed at the level required to elicit its phenotypic impact. Also, there remains the possibility that the *p44* isoform transgene has disrupted some endogenous genes.

INTRODUCTION

The Evan Laboratory recently generated a mouse model in which a full-length mouse *Trp53* mRNA construct (with preservation of intron 4) was knocked into the ubiquitously and constitutively expressed *Rosa26* locus. The ectopic allele of *Trp53*, *R26-p53*, was shown to be expressed at levels similar to that of the endogenous *Trp53* alleles in all tissues *in vivo* and in derived embryonic fibroblasts *in vitro*. Furthermore, the p53 protein expressed from the ectopic allele exhibited identical functionality to that expressed from the endogenous alleles in terms of p53 transcription activities. Importantly, animals carrying two *R26-p53* alleles but no endogenous *Trp53* appeared identical phenotypically to *Trp53* wild type mice in all aspects examined; all developmental and physiological abnormality exhibited by the germline *p53*-null mice, including sensitivity to whole body irradiation, were rescued by the ectopic *R26-p53* alleles (unpublished data). As the *R26-p53* allele likely expresses only one isoform of mRNA and protein, it challenges the speculated importance of mRNA/protein isoforms on biology of p53.

I.4 p53 tumour suppression

2019 marks the 40th year of p53's discovery, with more than 100,000 hits returning from a search of p53 on PubMed. Nonetheless, it appears we are still only beginning to glimpse the physiological and pathological functions of p53. This is perhaps unsurprising considering the entire research field took a decade-long early detour after mistakenly classifying p53 as a proto-oncogene! The paradigm was corrected some 30 years ago: even so, our understanding of p53 remains patchy.

I.4.1 The discovery of p53

p53 was originally identified in 1979 by several laboratories as a protein interacting with the oncogenic SV40 viral large T-antigen in SV40-infected cells (Lane & Crawford 1979; Linzer & Levine 1979). As the protein level of p53 appeared to be regulated by large T-antigen in these cells, it was presumed that the protein was oncogenic and played a part in SV40 LT-mediated transformation (Linzer et al. 1979). Shortly thereafter, p53 cDNA clones were successfully isolated from tumour cells and were shown to be capable of transforming normal rodent fibroblasts together with dominant oncogenes such as *Ras*^{V12} (Eliyahu et al. 1984; Jenkins, Rudge, Redmond, et al. 1984; Jenkins, Rudge & Currie 1984; Eliyahu et al. 1985). This, again, supported the notion that p53 was an oncogenic protein. Around the same time, Maltzman and Czyzyk showed that p53 protein expression level was induced by DNA damage (Maltzman & Czyzyk 1984), providing the first hint as to the actual function of the protein, as determined in the early 90s.

I.4.2 p53 is a tumour suppressor

The turning point for the paradigm of p53 as an oncoprotein came in 1989 when two reports showed that wild type p53 cDNA transfected and expressed is capable of suppressing oncogene-mediated transformation of rodent fibroblasts cells *in vitro* while the mutant versions

INTRODUCTION

- which indeed had been cloned instead of the wild type in the previous reports in 1984 - transform the cells (Eliyahu et al. 1989; Finlay et al. 1989). This was further supported by the identification of point mutations in the *p53* gene in both human and mouse cancers as well as in cancer cell lines (Baker et al. 1989; Hollstein et al. 1991; Wolf & Rotter 1984; Ben David et al. 1988; Mowat et al. 1985; Wolf & Rotter 1985). Furthermore, it was shown that inheritance of mutant a *TP53* allele is the underlying cause of Li-Fraumeni syndrome, which predisposes patients to early (before 30-year old) development of cancer (Malkin et al. 1990; Srivastava et al. 1990). Finally, Donehower *et al.* showed in 1992 that germline *p53*-knockout mice were viable and fertile but developed spontaneous tumours at an average age of 20 weeks (earliest 12 weeks) (Donehower et al. 1992). Together, these findings firmly established the paradigm of *p53* as a tumour suppressor.

In the 90s, research on *p53* took off and yielded some foundational understanding of *p53*'s cellular functions. First, several studies reported that *p53* protein is induced by DNA damage signals and, when so activated, stops cell-cycle progression and triggers apoptosis (Yonish-Rouach et al. 1991; Hall et al. 1993; Lowe, Schmitt, et al. 1993; Lowe, Ruley, et al. 1993). Based on the hints that *p53* protein binds to DNA at a specific consensus sequence (Bargonetti et al. 1991; Kern et al. 1991; El-Deiry et al. 1992), Kastan *et al.* established that *p53* is a transcription factor inducible by ATM kinase (back then only known as a ataxia-telangiectasia gene product) upon DNA damage signals and directly induces transcription of the growth arrest and DNA damage protein 45 (*GADD45*) by binding to its coding gene (Kastan et al. 1992). It was at around this time that *p53* was dubbed the title "guardian of the genome", a hypothesis centralising *p53*-mediated DNA damage response as its principal mechanism of tumour suppression (Lane 1992). The Guardian of the Genome hypothesis soon turned to dogma.

The next few years saw the progressive unveiling of *p53*'s attendant pathways as well as the mechanisms that regulate its activity. In 1993, El-Deiry *et al.* discovered that *p53* directly induces expression of the *CDKN1A* gene, which encodes *p21^{Cip1}* (alternatively *p21^{Waf1}*), a potent

inhibitor of the cyclin-dependent kinases whose activities are necessary for cell cycle progression. This linked p53 activation directly to cell cycle arrest (El-Deiry 1993). Next, the gene encoding the E3 ubiquitin ligase MDM2 was revealed as a direct target of p53 while the MDM2 protein was shown to be a key mediator of p53 degradation (Momand et al. 1992; Barak et al. 1993; Wu et al. 1993). This placed p53 and MDM2 in a direct negative feedback loop – p53 induces MDM2, which inhibits p53. Further investigation showed that MDM2 is absolutely and continuously required to keep p53's protein level low in the absence of upstream p53-activating signals (Barak et al. 1993; Wu et al. 1993; Kubbutat et al. 1997; Haupt et al. 1997; Momand et al. 1992). Germline knockouts of MDM2 were embryonically lethal in early gestation but this lethality was rescued by co-deletion of p53 (de Oca Luna et al. 1995; Jones et al. 1995; **Table I.1**).

Other important milestones in our understanding of p53 biology include uncovering the diverse upstream signalling pathways that transduce various stress and damage insults, including DNA damage and oncogene activation, to regulation of the p53 protein. Three reports published between 1997-2000 established that upon DNA damage signals protein kinases ATM, Chk1 and Chk2 phosphorylate p53 at multiple sites, disrupting the Mdm2-p53 complex and releasing p53 from its negative regulation by Mdm2, thereby triggering rapid p53 accumulation (Siliciano et al. 1997; Canman et al. 1998).

Then the protein ARF (also named p14^{ARF} in human and p19^{Arf} in mouse), encoded by the *INK4ARF* gene, was shown to bind and ubiquitinate MDM2, causing its dissociation from p53 and subsequent degradation by the proteasome pathway. p53 released from MDM2 is no longer ubiquitinated and degraded and thus is accumulated to high level (Quelle et al. 1995; Kamijo et al. 1997; Zhang et al. 1998; Kamijo et al. 1998; Pomerantz et al. 1998). Remarkably, Zindy *et al.* demonstrated in mouse embryonic fibroblasts that Myc induces p19^{Arf} and thereby triggers p53-dependent apoptosis (Zindy et al. 1998). The ability of ARF to survey oncogenic signals was further confirmed by a report in which the investigators visualise p19^{Arf} expression

in vivo in mice by replacing the first exon of the mouse endogenous gene with a GFP-expressing open reading frame (ORF). It was shown that oncogenic signals such as ectopic overexpression of Ras and Myc stimulate p19^{Arf} expression (Zindy et al. 2003). Together, these data showed that the p53 network has evolved a dedicated faculty with which to detect and eliminate cells that exhibit aberrant oncogenic signals, persistent and obligate attributes of (proto-)cancer cells.

Year	Discovery	Reference
1979	- p53 interacts with the oncogenic SV40 viral Large T-antigen and so characterised as an oncogene.	Lane & Crawford 1979; Linzer & Levine 1979; Linzer et al. 1979
1984 - 1985	- p53 can transform rodent fibroblasts together with some oncogenes. - p53 is inducible by DNA damage.	Eliyahu et al. 1984; Jenkins, Rudge, Redmond, et al. 1984; Jenkins, Rudge & Currie 1984; Eliyahu et al. 1985; Maltzman & Czyzyk 1984
1989	- Correct cloning of WT p53 which was confirmed to suppress transformation of cells by oncogene; thus confirming p53 function as tumour suppressor.	Eliyahu et al. 1989; Finlay et al. 1989
1990	- Inheritance of one allele of <i>TP53</i> is the underlying cause of Li-Fraumeni syndrome.	Malkin et al. 1990; Srivastava et al. 1990
1992	- Germline p53-knockout mice are born viable and fertile but develop spontaneous tumours at young age	Donehower et al. 1992
1991 - 1993	- Activated by DNA damage, p53 stops cell-cycle progression and triggers apoptosis. - p53 consensus sequence.	Yonish-Rouach et al. 1991; Hall et al. 1993; Lowe, Schmitt, et al. 1993; Lowe, Ruley, et al. 1993 Bargonetti et al. 1991; Kern et al. 1991; El-Deiry et al. 1992
1992 - 1993, 1995	- p53 is a transcription factor activated by ATM kinase upon DNA damage and induces transcription of GADD45. - Dabbed the name "The Guardian of the Genome". - MDM2-p53 negative feedback loop. - <i>CDKN1A</i> as a p53 target gene and link to cell cycle arrest. - Germline knockout of MDM2 is embryonically lethal.	Kastan et al. 1992 Lane 1992 Momand <i>et al</i> 1992; Barak et al. 1993; Wu et al. 1993 El-Deiry 1993 de Oca Luna et al. 1995; Jones et al. 1995
1997 - 1998	- DNA damage signal is relayed to p53 from ATM kinase via Chk1 and Chk2 kinases that phosphorylate p53 at multiple sites, disrupting MDM2 binding and inhibition.	Siliciano et al. 1997; Canman et al. 1998
1995, 1997, 1998, 2003	- ARF protein frees p53 from MDM2 and allows p53's accumulation in response to oncogenic Myc signal and triggers apoptosis.	Quelle <i>et al.</i> 1995, Kamijo <i>et al.</i> 1997, Zhang <i>et al.</i> 1998, Kamijo et al. 1998; Pomerantz et al. 1998, Zindy et al. 1998, Zindy et al. 2003

Table I.1 Milestones in p53 research that establishes its role in DNA damage response and as a tumour suppressor.

I.4.3 Mechanisms of p53 tumour suppression

The extent to which the p53 DNA damage response versus ARF-p53 oncogenic signalling contribute to p53's tumour suppressive nature has long been hotly debated. In keeping with Lane's "guardian of the genome" notion (Lane 1992), many reports have argued that p53 inhibits tumorigenesis by sensing episodic or ongoing DNA damage in evolving tumour cells and directing affected cells to senescence or apoptosis. For example, two reports published in 2005 noted a correlation between the activation of the ATM-Chk2-p53 apoptosis pathway in different human early (pre-invasive) cancerous lesions and frequent mutations and/or inactivation of this pathway in lesions of later stages. Based on such observations, the authors speculated that the ATM-Chk2-p53-mediated DNA damage response is the principal axis of p53-mediated tumour suppression (Bartkova et al. 2005; Gorgoulis et al. 2005). This view, however, was challenged by Christophorou *et al.* who, using a reversibly switchable p53 mouse model showed that the p53-mediated response to DNA damage inflicted by whole body irradiation is irrelevant for suppression of lymphoma induced by the irradiation: rather, the tumour suppressive effect of p53 was entirely dependent on ARF (Christophorou et al. 2006). A complementary study showed that oncogenic signals sensed and relayed by ARF to p53 are alone essential for the extra protection against induced cancers conferred by an extra germline copy of p53 (Efeyan et al. 2006). ARF appears to have evolved specifically to monitor oncogenic signalling. In addition, however, ARF is reported to direct p53-independent functions, such as the sumoylation and negative regulation of MDM2 and nucleophosmin (NPM or B23 is a nuclear protein involved in ribosome biogenesis) (Tago et al. 2005), perhaps suggesting that its original evolution trajectory was independent of p53. Given the evidence suggesting that p53 family proteins may initially have evolved to regulate aspects of damage/stress sensing during development (discussed below in **Section I.5.1**), it seems plausible that p53 and ARF evolved independently and their roles then later converged to potentiate the emerging necessity to rein in rogue somatic cells in larger, longer-lived organisms.

While sufficiently effective in preventing tumorigenesis through reproductive age, ARF-p53-mediated tumour suppression is not without its shortcomings. Thus, two reports published respectively in 2007 and 2008 demonstrated that ARF suppresses tumorigenesis by sensing aberrantly high levels of growth signals in cells. The problem being that aberrantly persistent growth signals are the underlying cause of oncogenesis whereas elevation of signals is an indirect byproduct of the mutations that commonly cause signal deregulation: elevated oncogenic signaling flux is a “frequent but not unfailing correlate of the true attribute” of oncogenesis (Sarkisian et al. 2007; Murphy et al. 2008; Juntila & Evan 2009). Such suboptimal design for tumour suppression appears peculiar - why has the system not evolved to ensure more accurate surveillance of rogue cells driven by oncogenic signalling? Possibly, the ARF-mediated sensing system that has evolved is adequate to suppress cancer through reproductive age, after which it is evolutionarily irrelevant? Alternatively, perhaps ARF evolved initially not for surveillance of tumorigenesis but some other, currently obscure, function? Answers to these questions are sure to offer additional fundamental insights to how p53 suppresses cancers.

1.4.4 Exploring p53-based cancer therapies

Despite our incomplete understanding of p53-mediated tumour suppression, it is clear that restoration of p53 in late stage p53-negative murine cancers is remarkably effective at eliminating existing tumours, as indicated by several reports published through 2006-2010. The rapid elimination of tumours, by apoptosis or senescence, upon restoration of p53 in different murine cancer models formally illustrated the therapeutic feasibility of restoring wild type p53 in tumours in which endogenous p53 is mutated or inactivated. Importantly, such observations confirmed that p53-activating signals persist in tumours that have evolved in the absence of p53 and that the downstream p53-dependent tumour suppressive pathways remain functional in such cells (Martins et al. 2006; Ventura et al. 2007; Xue et al. 2007; Juntila et al. 2010; Feldser et al. 2010). Nonetheless, the differential responses of tumours at different stages of their

progression - early stage tumours were largely unresponsive to p53 restoration whereas later stage lesions underwent profound regression - indicated that additional factors need to be considered when implementing p53-based therapy. Provocatively, there is also evidence that retention of p53 confers selective advantages on early stage tumours (see below).

A parallel approach to exploring the mechanisms underlying p53's tumour suppressive nature is to enhance the general activities of p53, i.e. increasing p53-mediated tumour surveillance. Tyner *et al.* showed that a mutant p53 lacking its N-terminus conferred augmented tumour suppression in mice when co-expressed with wild type p53, although such animals also exhibited features of premature ageing (Tyner *et al.* 2002). The authors attributed these observations to increased baseline p53 activity of the mutant. While such results are intriguing in the sense that p53 activity may possibly be fine-tuned pharmacologically to provide enhanced tumour suppression, it remains unclear whether the observed phenotypes were indeed a result of increased p53 activity, as the authors claimed. A copy of the mutant allele by itself failed to match wild type p53 in terms of suppression of spontaneous tumorigenesis. Moreover, it was later realised that the Tyner mutant mouse also had some 24 other endogenous genes inadvertently deleted (Gentry & Venkatachalam 2005). Nonetheless, an elegant study by Garcia-Cao *et al.* showed that increasing p53 activities by adding an extra transgenic copy of *Trp53* driven at relatively normal native levels of transcription (a "super p53" mouse) did confer extra protection against induced tumours without leading to premature ageing (Garcia-Cao 2002). The difference in terms of the ageing phenotype in the two studies is explicable by the argument that the augmented p53 activities in the "super p53" model remained subject to normal factors that regulate p53, such as by Mdm2 and ARF while the structurally altered Tyner mutant p53 might not be so regulatable. Remarkably, a follow up study combining "super p53" with the p19^{Arf}-knockout model showed that the extra protection bestowed on by the additional *Trp53* allele is entirely dependent on oncogenic activation through ARF (as discussed above), underscoring the importance of the ARF-p53 axis for p53's

INTRODUCTION

tumour suppressive activities (Efeyan et al. 2006). This same idea of enhancing p53-mediated tumour suppression by constitutively enhancing p53 activity was explored in a different way in mice by another approach - using a hypomorphic mutant of the p53 inhibitor MDM2 (Mendrysa et al. 2006). This also showed enhance protection against tumours, but without associated premature ageing. Taken together, these findings confirm the validity of augmenting p53's level and activities as a preventive therapeutic approach.

Mouse model	Genetic modification	Phenotype*	Reference
p53 KO	<i>Trp53</i> gene deletion	Increased tumour susceptibility	Downhower <i>et al.</i> 1992
p53m	<i>Trp53</i> exon 1 to 6 deletion	Premature ageing phenotype	Tyner <i>et al.</i> 2002
Super p53	An extra, ectopic copy of <i>Trp53</i> gene	Increased tumour resistance	García-Cao <i>et al.</i> 2002
p19 ^{Arf} KO	<i>Ink4Arf</i> deletion	Increased tumour susceptibility	Kamigo <i>et al.</i> 1997
Mdm2 KO	<i>Mdm2</i> gene deletion	Embryonic lethality rescuable by p53 KO	Luna <i>et al.</i> 1995; Jones <i>et al.</i> 1995
Hypomorphic Mdm2	Reduced expression of Mdm2	Anemia and increased radiosensitivity rescuable by p53 KO	Mendrysa <i>et al.</i> 2003
p53 ^{Flox}	Cognate sequence of Cre recombinase flanking exon 2 to 11	<i>Trp53</i> exon 2 to 11 deletion in the presence of Cre	Ventura <i>et al.</i> 2007
p53ER	In-frame fusion of estrogen receptor sequence to 3' of <i>Trp53</i>	p53ER functions like wild type in the presence of tamoxifen ligand. Otherwise is null.	Christophorou <i>et al.</i> 2005
TRE.shp53	cDNA of shRNA to <i>Trp53</i> added to genome as transgene	The shRNA is expressed in the presence of tetracycline ligand and transcription activator rtTA	Xue <i>et al.</i> 2010

Table I.2 Summary of some mouse genetic models of p53. *Only the phenotype of homozygous animals are described here.

I.5 Non-tumour suppressive functions of p53

Since being dubbed as the “guardian of the genome” by David Lane (1992), p53 has been viewed by most primarily as a tumour suppressor that uses the DNA-damage response as its principal sensing mechanism. However, such a hypothesis is not logically plausible from an evolutionary point of view given the evolutionary age of p53 (and its siblings p63 and p73). There is emerging evidence suggesting p53’s functional involvement in diverse development and physiological processes in addition to DNA damage response – notably, metabolism and autophagy and a wide variety of responses to injury (Antoniades et al. 1994) and infection (Siegl et al. 2014).

I.5.1 Ancient function of p53 - what has it evolved to do?

p53 and/or its siblings p63 and p73 are evolutionarily ancient and their common ancestor is found, together with their MDM2 controllers, across a wide diversity of simple eukaryotic lifeforms, including choanoflagellates, cnidaria and Placozoa, many of which are the simplest animals with no evident differentiated lineages (Chen et al. 2017; Rutkowski et al. 2010; Pankow & Bamberger 2007; Lane et al. 2010). Such evolutionary evidence suggests that p53 evolved initially as a transcriptional integrator of responses to stress/damage/developmental signals rather than for its evolutionarily relatively recent role of tumour suppression. The common ancestor gene of the *p53/p63/p73* family more closely resembles *p63* and *p73* than *p53* itself. It seems plausible that this ancestral gene functioned principally to preserve the integrity of gamete genomes by eliminating defective germ cells, a function conserved (mostly in p63 and p73) in higher eukaryotic lifeforms such as invertebrates and vertebrates (Suh et al. 2006; Belyi et al. 2010). Presumably, in more complex organisms p53 inherited this primordial germline function and extended it to the elimination of aberrant somatic cells whose uncontrolled clonal outgrowth would fatally corrupt embryonic and adult

tissue function. This role would be especially important in tissues with high rates of cell division and, hence, high rates of intrinsic DNA damage (Takimoto & El-Deiry 2001; Aranda-Anzaldo & Dent 2003).

Functional analyses of the *Drosophila melanogaster* p53 homologue, Dmp53, have yielded further insights into the gene's likely evolutionary trajectory. Germline deletion of *Dmp53*, like that of *Trp53* deletion in mouse, is not embryonic lethal but generates offspring with reduced viability and fertility (Lee et al. 2003; Bauer et al. 2005). However, in contrast to *Trp53*-null mice *Drosophila* do not develop cancers whether *Dmp53* has or has not been deleted, even after irradiation. This suggests that *Dmp53* does not act as a conventional tumour suppressor in the fruit fly (Bauer et al. 2005). Of course, this could be an indirect secondary consequence of the fruit fly developmental programme – its short lifespan and limited cell proliferation in adults would greatly limit the chances of somatic cells arising with the compound ensemble of interacting mutations necessary for malignant outgrowth. Nonetheless, *Dmp53* remains essential for inducing apoptosis in response to genotoxic stress. However, it appears to be dispensable for cell cycle arrest in response to genotoxic injury. This could indicate that the apoptotic function of p53 predates its cell cycle arrest function (Kondo 1998; Sogame et al. 2003). On the other hand, protostomes like arthropods have undergone extensive lateral evolutionary diversification since splitting from their deuterostome cousins. Hence, traits that differ between insects and vertebrates are as likely to reflect horizontal specialisation as they are chronological sequence.

1.5.2 Developmental functions of p53

As discussed above, it seems plausible that p53 has evolved to facilitate certain processes in embryonic development and adult tissue maintenance – either a dedicated developmental role for p53 itself or perhaps through functional overlap with the activities of p63 and/or p73. Such putative physiological functions of p53 have, of course, been

overshadowed by the initial reports on germline p53-null mice that indicated no demonstrable phenotype other than greatly increased tumour rates and radio-resistance (Donehower et al. 1992; Clarke et al. 1993; Lowe et al. 1993). However, subsequent reports detailed a variety of developmental deficits in p53-null mice, albeit with variable penetrance. These included a range of developmental defects that cause occasional miscarriage or persist to adulthood such as neural tube closure defects leading to exencephaly and craniofacial abnormalities (Armstrong et al. 1995; Kaufman et al. 1997), and abnormalities in lung, urinary tract and kidney as well as dwarfism (Tateossian et al. 2015; Saifudeen et al. 2009; Baatout et al. 2002). *Trp53*^{-/-} female mice are also less fecund due to lack of expression of *Lif1*, the p53-dependent gene encoding Leukaemia Inhibitory Factor, a cytokine critical for embryo implantation (Hu et al. 2007). Importantly, the variable penetrance developmental phenotypes observed in *Trp53*^{-/-} mice probably fail to reflect the complete scope of p53's involvement in these complex developmental processes due to some degree of compensation by the closely related and functionally degenerate p63 and p73 (Jain & Barton 2018), both of which have been shown to play more direct, prominent roles in mouse development than p53 (Mills et al. 1999; Yang et al. 1999; Yang et al. 2000).

1.5.3 p53 plays a key role in somatic stem cell maintenance

More recent studies have shown the involvement of p53 in somatic stem cell homeostasis, including the regulation of haematopoietic cell fates, renewal and differentiation of mammary stem cells and repression of hepatic stem cells (Liu et al. 2009; Bondar & Medzhitov 2010; Colaluca et al. 2008; Tosoni et al. 2015; Tschaharganeh et al. 2014). p53 also plays key roles in various signalling pathways that, respectively, regulate pluripotency and induce differentiation. For instance, p53 is required to maintain the balance of DNA methylation that is important in preserving mouse embryonic stem cell homogeneity *in vitro* (Tovy et al. 2017). Notably, p53 is reported to induce mouse embryonic stem cell differentiation by

repressing expression of *Nanog* (a homeobox transcriptional factor that maintains embryonic stem cell pluripotency by suppressing cell fate determination factors; (Lin et al. 2005)), while Wang *et al.* demonstrated a specific role for p53 and its family members in modulating mesendoderm differentiation of mouse embryonic stem cells by coordinating Wnt and Nodal signalling (Wang et al. 2017).

1.5.4 p53 and cellular stresses - metabolism, hypoxia and autophagy

Discoveries of the direct p53 target genes *TIGAR* (*TP53*-induced glycolysis and apoptosis regulator) and *DRAM* (damage-regulated autophagy modulator) in 2006 established the first links between p53 and cellular metabolism. p53's role in metabolism mirrors that of its DNA damage responses: in the presence of mild and transient metabolic stresses, redox imbalance or hypoxia, p53 facilitates responses that protect cells and allows them to cope with the insults, so promoting cell survival. However, if the insult persists or the damage inflicted cannot be resolved, p53 switches its role to promote cell death or, possibly, irreversible arrest (i.e. cellular senescence) (Humpton & Vousden 2016). Thus, when a cell is subject to a transient glucose scarcity, AMPK (AMP-activated protein kinase) acts through p53 to facilitate metabolic cell-cycle arrest (Jones et al. 2005). p53 transactivates *TIGAR*, which in turn facilitates metabolic reprogramming by reducing the glycolytic rate and increasing oxidative phosphorylation. In concert, p53 also directly adjusts expression of glycolytic enzymes accordingly. The net outcome is prioritisation of metabolic pathways that sustain survival of cells over counterproductive expenditure through proliferation-related pathways (Humpton & Vousden 2016).

Another common source of stress in cells is increased reactive oxygen species (ROS). Following a mild increase in ROS, p53 protects cells by mediating ROS detoxification. Upon induction by upstream signals, p53 increases *TIGAR* expression, which promotes production of NADPH (which helps with ROS removal) via the pentose phosphate pathway and induces expression of antioxidant genes, such as aldehyde dehydrogenase 4 (*ALDH4*) that reduces

intracellular ROS level (Yoon et al. 2004). On the other hand, Fitzgerald *et al.* showed that upon irradiation, p53-dependent expression of *CDKN1A* in a human cancer cell line increased the ROS level and led to more senescence (Fitzgerald et al. 2015). Although it has been shown in haematopoietic stem cells (HSC) that p53 is induced by thioredoxin-interacting protein (TXNIP) - a ROS sensor - upon mild ROS stress, how p53 is induced in other contexts is still not known (Jung et al. 2013; Budanov 2011).

p53 functions analogously during hypoxia. When hypoxic stress is mild and transient, p53 protects by helping cells to cope with the stress and to survive (Alarcón et al. 1999; Li et al. 2004; Feng et al. 2011). However, in cells undergoing a severe lack of oxygen (anoxia), p53 activation correlates with cell death. However, no consistently proven mechanistic relationship is known that links hypoxia sensors (such as HIF1 complex) and p53. Consequently, the p53 response to severe hypoxia may well be an indirect consequence of oxygen deprivation – perhaps via DNA damage (Hammond et al. 2002; Pan et al. 2004).

p53 also plays an important role in autophagy, the cellular catabolic process that recycles intracellular components such as macro-molecules and organelles to facilitate survival of cells. Autophagy is an important transient survival mechanism in circumstances such as nutrient deficiency as it allows rationing and re-allocation of resources. Given p53's role in mediating metabolic stresses, as discussed, it is not unsurprising that p53 is also an activator of autophagy through direct transactivation of autophagy-related genes such as *DRAM* (Crighton et al. 2006). Interestingly, p53 is also known to induced other autophagy genes such as *Ulk1* and *Atg7* upon DNA double strand breaks amongst other DNA damage response genes (Kenzelmann Broz et al. 2013).

Nonetheless, although it is becoming clear that p53 plays a pivotal function as a coordinator of responses to stress in the soma, some fundamentally important questions remain unanswered: what are the upstream activators of p53 when subject to such diverse forms of insult? Since p53 is a but single protein yet facilitates differential signalling of so many

INTRODUCTION

diverse effector pathways, how is each type of insult coded so as to be relayed by p53 to trigger the most effective response? For example, is it facilitated by different sets of phosphorylation, acetylation and/or ubiquitination on p53? Or by different parallel modulatory signals? Different chromatin accessibility? What governs the thresholds at which p53 function shifts from protective to apoptotic? Is there a common threshold for all the stresses or distinct thresholds for each? Answers to these questions, along with many more, are central to crafting a comprehensive functional picture of p53 biology.

I.6 Questions to address regarding p53 biology and experimental approach

I.6.1 Importance of p53 in adulthood physiology

While its developmental roles have been fairly well characterised, p53's importance in adulthood physiology is not well established, despite numerous published studies that implicate p53 in a wide range of physiological processes. And given the existence of the closely related and functionally overlapping p53-family members p63 and p73, how essential and/or non-redundant is p53 in the maintenance of adult tissues and organs in the face of injury, insults and infection? Such questions might be effectively addressed by acutely and reversibly repressing p53's expression and activities in adulthood. For example, acute repression of p53 in adult mice would uncover any possible roles for endogenous p53 in its basal, non-activated state, particularly in tissues known to express low level of p53 most of the time. More sustained p53 suppression might reveal its role in maintaining tissues homeostasis, including any role in governing stem cell proliferation, differentiation and survival.

I.6.2 Clarifying the paradigm of p53 tumour suppression

The discussions in **Section I.5** call into question p53's role in tumourigenesis. While the ARF-p53 pathway is tumour suppressive, it appears to be an "improvised" evolutionary adaptation rather than a primordial evolved function of p53. Indeed, as discussed earlier, the tumour suppression function of p53 therefore appears sub-optimally "designed" since it fails to detect the actual cause of tumourigenesis – the aberrant persistence of growth signals – but instead senses the supraphysiologically high signal flux generated by the most frequent oncogenic mutations, such as amplification or promoter hijacking (Murphy et al. 2008). Moreover, despite being the most frequently mutated gene in human cancers, *TP53* is often not completely inactivated or deleted like other prominent tumour suppressors such as *RB* and *APC* in human cancers; instead, missense mutations are common that, while abrogating aspects of p53 function nonetheless preserve other aspects of its functionality (Fodde 2002; Du & Searle 2009; Aranda-Anzaldo & Dent 2007). These observations suggest p53 may not solely play the part of suppressor of tumourigenesis but might also contribute to genesis and evolution of cancer cells via its other, non-tumour suppressive functions, for example those mediating protective responses to injury or stress. It seems plausible that these protective p53 functions would be selectively retained, at least in early stages of tumourigenesis until the point where additional oncogenic mutations drive oncogenic signals to the level where they breach the ARF-p53 detection threshold. This unorthodox notion is consistent with observations that inactivation of *TP53* appears to arise (i.e. be positively selected) only relatively late in most human cancers, and is supported by a remarkable and counterintuitive study in the early 90s in which investigators compared the early development of chemically induced skin cancer in germline p53-null versus WT mice. Unexpectedly, they noted that an absence of p53 significantly impedes the oncogenic process by greatly reducing the incidence of papillomas (**Figure I.2**) (Kemp et al. 1993). At the time, this observation was perplexing and contrary to the deeply rooted paradigm of p53 as a potent tumour suppressor. However, a role for p53 in

protecting early stage cancers is entirely consistent with these observations. Undoubtedly, further careful testing of the hypothesis, for example by suppressing p53 activities in early stages of tumourigenesis, will yield an essential understanding of the dynamic roles p53 plays in different phases of carcinogenesis.

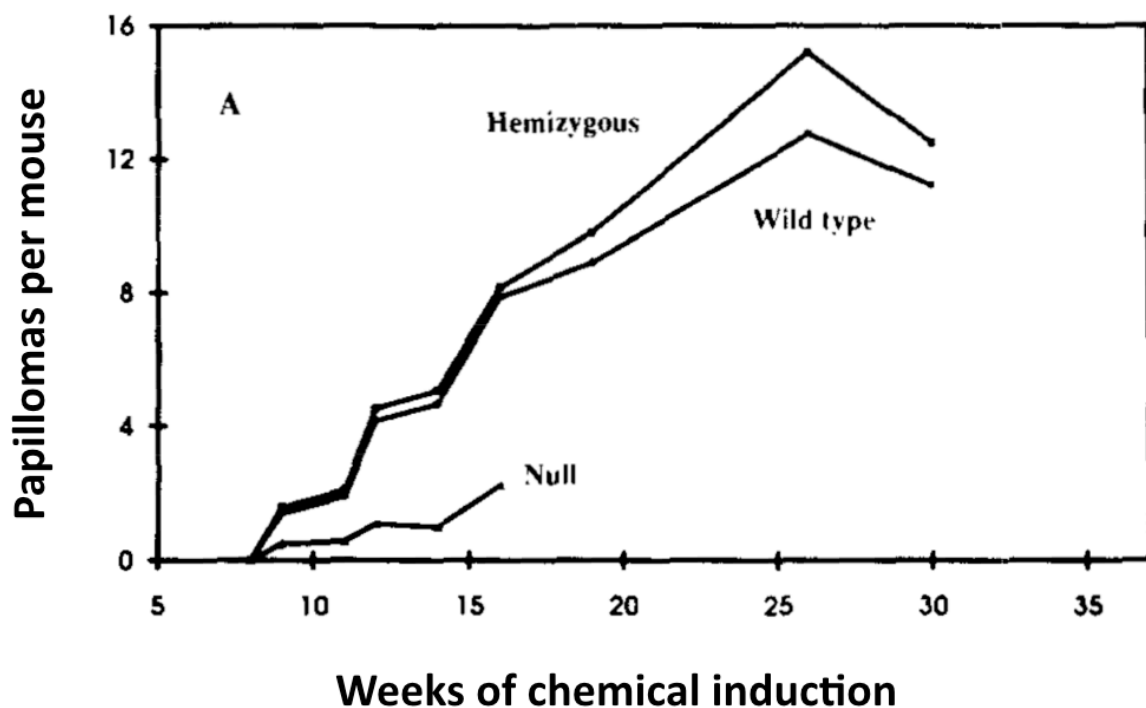


Figure 1.2 Rate of papilloma genesis in p53 wild type (*Trp53^{+/+}*), hemizygous (*Trp53^{+/-}*) and null (*Trp53^{-/-}*) mice. Note that only the number of papillomas was plotted; once a papilloma evolved to later stage carcinoma, it was not included. The curve for p53-null mice stops at 18 weeks because either all papillomas had converted to carcinomas or the animal succumbed to spontaneous tumours (Figure from Kemp *et al.* 1993).

I.6.3 Aims of the project and experimental approaches

The two main questions regarding p53’s physiological and tumourigenic roles to address in this thesis are:

- (1) What are the immediate consequences, if any, of acute blockade of p53 function in adult mice – both systemically and tissue-by-tissue? Does prolonged suppression of p53 functions in adult mice impact maintenance of tissue homeostasis?
- (2) Does p53 confer any advantages to the genesis and/or early stage development of chemically induced skin cancer? What aspects of p53’s functions are involved?

The experiments designed to address these questions are illustrated in **Figure I.3** below.

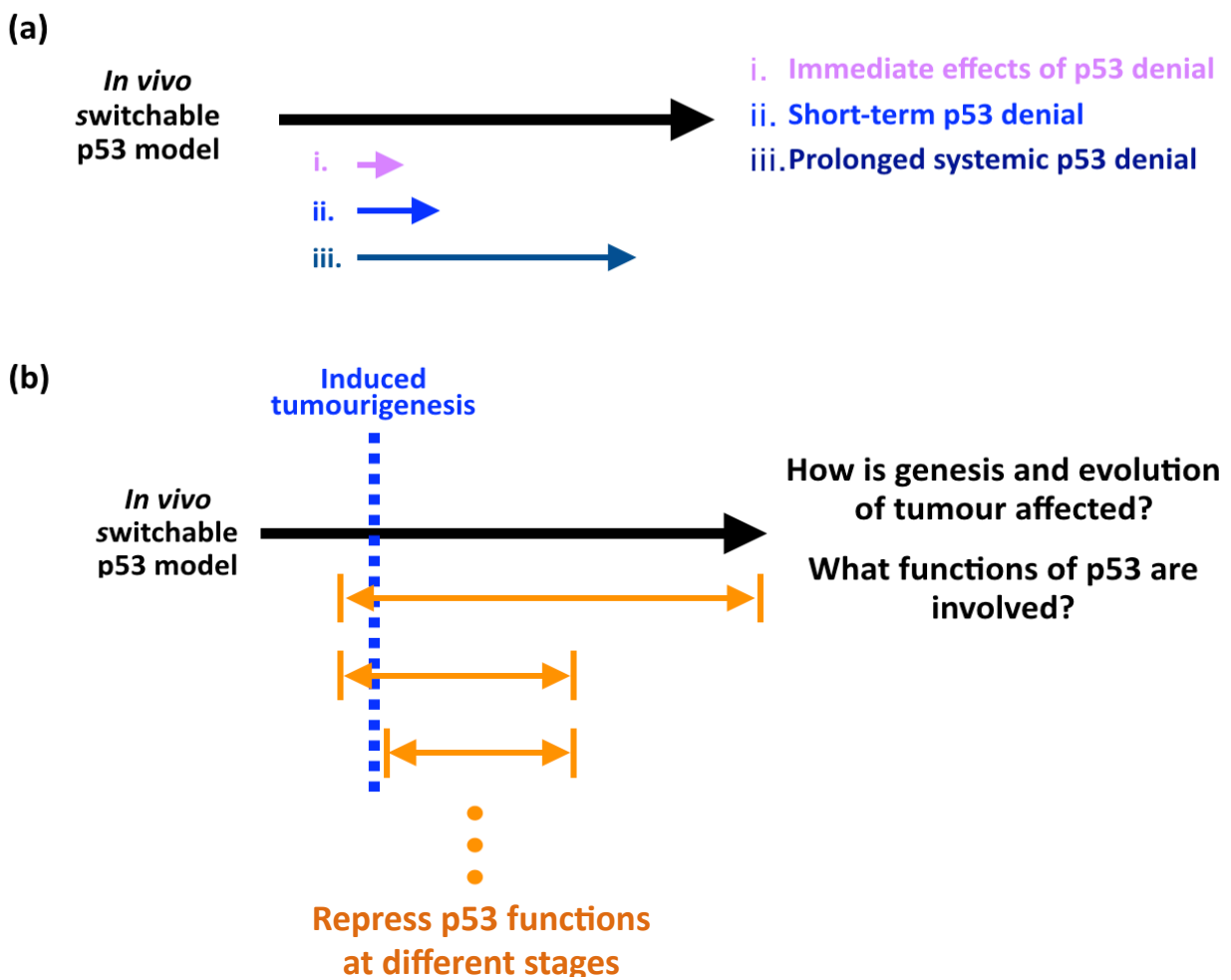


Figure I.3 Schematic diagrams of experiments to address questions regarding p53’s functions in (a) physiological processes and (b) at different stages of tumourigenesis.

I.6.4 *In vivo* models to be used

To efficiently address the questions regarding p53's physiological functions and its roles in tumorigenesis, an *in vivo* switchable model of p53 is required and it must fulfil several prerequisites:

- (1) Rapidly and reversibly switchable repression of all endogenous *Trp53* alleles. This permits dissection of physiological and tumorigenic functions of p53 in its native contexts with precise temporal resolution.
- (2) Minimal impact exerted by the implemented repression system on the normal expression and regulation of *Trp53* and so when the repression system is not in use the animals behave exactly as wild type. It also permits normal development of experimental animals without potential compensation from other genes such as *Trp63* and *Trp73*.

Although existing genetic mouse models of p53 employing different switchable molecular technologies such as Cre recombinase-mediated gene excision and ligand-activatable estrogen receptor protein domain are available, none fulfils the posted criteria due to their caveats and limitations (discussed in details in **Chapter 1 Section 1.1**). Hence, it is necessary to develop a novel, improved reversibly switchable system of p53 to address the important questions regarding p53's functions in physiological processes and tumorigenesis.

The chemically induced skin cancer model of skin squamous cells carcinoma (Abel et al. 2009) used in the Kemp study (1993) will also be used here too as the induced skin cancer develop with a well-defined, visually assessable progression, providing an ideal perform for temporal dissection of p53's functions at different stages.

**BLANK
PAGE**

Methods and Materials

M.1 Molecular cloning and DNA manipulation

M.1.1 PCR amplification, restriction digestion and ligation of DNA

PCR was used to amplify DNA fragments throughout the cloning process using Q5 High-Fidelity DNA Polymerase (NEB). General PCR composition and reaction cycles recommended by the manufacturer are summarised in **Tables M.1a** and **M.1b** respectively. Colony-PCRs used for screening plasmid constructs in *E. coli* using the same reaction conditions were carried out with Taq Polymerase (NEB) following the manufacturer's instructions (not shown). **Table M.1c** shows the primers used in all PCR reactions in this thesis.

Table M.1a General PCR reaction composition

Reagent	Volume
DNA template (Plasmid to be verified)	0.5 μl
10x ExTaq Buffer (Thermo Scientific)	5 μ l
2.5 mM dNTP (Thermo Scientific)	4 μ l
Primer 1 (depends on gene to be amplified)	2 μ l
Primer 2 (depends on gene to be amplified)	2 μ l
Q5 or Taq DNA Polymerase	0.25 μ l
MiliQ water	To 50 μ l

Table M.1b General PCR reaction cycle

Step	Temperature	Duration	
1	95°C	3 minutes	
2	95°C	25 seconds	
3	T °C (Depend on primer melting temperature) *	25 seconds	Repeats 29 times
4	72°C	t minutes #	
4	72°C	5 minutes	
5	10°C	2 minutes	

* T = \sim 2 °C lower than the T_m of the primer with a lower T_m

t depends on size of fragment to be amplified; generally 60 second/1000 bp.

Table M.1c List of PCR primers used

Direction	Primer sequence	Description	T _m (°C)
Forward	5'-CTTCTACAGATCCTTCTGT-3'	BAC verification PCR 1. Figure 1.6.	54.9
Reverse	5'-GTAGTGTGCTTGCCTGT-3'		56.2
Forward	5'-TTCTGACCTCTGCATGTC-3'	BAC verification PCR 2. Figure 1.6.	57.1
Reverse	5'-CCCAAGTAAAAAGTTGGA-3'		55
Forward	5'-CTAGGGAAACAAGCTCGT-3'	BAC verification PCR 3. Figure 1.6.	57
Reverse	5'-CGACAGTCTTGAATCTCAA-3'		55.3
Forward	5'-TTAGCTAATGAGGGGAAA-3'	BAC verification PCR 4. Figure 1.6.	54.8
Reverse	5'-GCTTTGTGCATGTTATT-3'		51.4
Forward	5'-AAAAAA-GTCGAC-TAGGCACACTGACATGCCTA-3'	To clone 200 bp homology sequence upstream of the 10 kbp fragment into the DTA3 vector. Figure 1.7.	62
Reverse	5'-TTTTTT-AGATCT-GTTGTTTGAGACAGGGTTTC-3'		58.6
Forward	5'-AAAAAA-AGATCT-GCTTACATATGACCTGCAC-3'	To clone 200 bp homology sequence downstream of the 10 kbp fragment into the DTA3 vector. Figure 1.7.	59.6
Reverse	5'-TTTTTT-GGTACC-TCAACTGTAGCAGCAGGTTA-3'		58.7
Forward	5'-AAAAAA-GTCGAC-GCTTCACAGTAAGACCCTGT-3'	To clone 200 bp homology sequence upstream of the 10 kbp fragment into the DTA4 vector. Figure 1.7.	58.4
Reverse	5'-TTTTTT-AGATCT-GTTGTTTGTGAGATGGGGTC-3'		60.8
Forward	5'-AAAAAA-AGATCT-CCCTTCAGATAGATACCGG-3'	To clone 200 bp homology sequence downstream of the 10 kbp fragment into the DTA4 vector. Figure 1.7.	60
Reverse	5'-TTTTTT-GGTACC-GGCAGGTGAATGACTCTTTAT-3'		59.6
Forward	5'-AAAAAA-GTCGAC-ATAAGATCGTCTCAAAGGCG-3'	To clone 200 bp homology sequence upstream of the 10 kbp fragment into the DTA5 vector. Figure 1.7.	60.8
Reverse	5'-TTTTTT-AGATCT-ATCATTGTACACCCAAGT-3'		59.3
Forward	5'-AAAAAA-AGATCT-CCCAGAACCCTTCTTATA-3'	To clone 200 bp homology sequence downstream of the 10 kbp fragment into the DTA5 vector. Figure 1.7.	58.1
Reverse	5'-TTTTTT-GGTACC-GAGGTAGGCTCTTCTTATC-3'		56.1
Forward	5'-TGCTTCCCTCAAGACAGATTCTTAAGTAGCCCTGGCTGT CCTAGAAGTGGACCCATGG-TCGAGTTTACCACTCCCT-3'	To add homology sequences of 60 bp upstream and downstream of insertion site C3 to the two ends of the <i>TRE-LoxP-Neo-LoxP</i> cassette. Figure 1.9.	57.1
Reverse	5'-TTAATCTCAGCACTCTGGGGGAAGAAGCAGGCAGATGTGT GAGTCCAGGCAACATGGA-ATAACTTCGTATAGCATAACATT-3'		51.6
Forward	5'-CTGCAAGTCCCCGCTCATTCTTCCCTCAACCCACGGA AGGACTTGCCTTACTTGT-TCGAGTTTACCACTCCCT-3'	To add homology sequences of 60 bp upstream and downstream of insertion site C4 to the two ends of the <i>TRE-LoxP-Neo-LoxP</i> cassette. Figure 1.9.	57.1
Reverse	5'-AAAGTCCCAATCCAGCAACCCCGCGAGACTCCTGGCACA AAGCTGGATAGTCGCCATA-ATAACTTCGTATAGCATAACATT-3'		51.6
Forward	5'-TTGGCGGGCGGGATGAACGGGAGTGTATATGTCAGATGCTG TAGTGAGGGTAGCTGATGA-TCGAGTTTACCACTCCCT-3'	To add homology sequences of 60 bp upstream and downstream of insertion site C5 to the two ends of the <i>TRE-LoxP-Neo-LoxP</i> cassette. Figure 1.9.	57.1
Reverse	5'-CCCTATATGCTCTACTTTGCAGGTGCATGACAGTGAGGCTCG TCGGTCTAACATCATCA-ATAACTTCGTATAGCATAACATT-3'		51.6

Table M.1c List of PCR primers used (continued)

Direction	Primer sequence	Description	T _m (°C)
Forward	5'-GACCTATCTCAAATAAAGCAAAA-3'	Amplifying 5' junction of <i>TRE-LoxP-Neo-LoxP</i> cassette insertion at C3. Figure 1.11.	62.5
Reverse	5'-CGTCTGCAGTTCATTCA-3'		64.1
Forward	5'-TTCTTTTTGTCAAGACCGAC-3'	Amplifying 3' junction of <i>TRE-LoxP-Neo-LoxP</i> cassette insertion at C3. Figure 1.11.	59.3
Reverse	5'-TGAAAGGTTGCAAGTGTAAGT-3'		62.4
Forward	5'-TAGCTGGATAGGAAAGAGCA-3'	Amplifying 5' junction of <i>TRE-LoxP-Neo-LoxP</i> cassette insertion at C4. Figure 1.11.	59.2
Reverse	5'-CGTCTGCAGTTCATTCA-3'		64.1
Forward	5'-TTCTTTTTGTCAAGACCGAC-3'	Amplifying 3' junction of <i>TRE-LoxP-Neo-LoxP</i> cassette insertion at C4. Figure 1.11.	59.3
Reverse	5'-GTTTTATGGATGCAAACGGA-3'		62.2
Forward	5'-GGTAGCGACTACAGTTAGGG-3'	Amplifying 5' junction of <i>TRE-LoxP-Neo-LoxP</i> cassette insertion at C5. Figure 1.11.	57.9
Reverse	5'-CGTCTGCAGTTCATTCA-3'		64.1
Forward	5'-TTCTTTTTGTCAAGACCGAC-3'	Amplifying 3' junction of <i>TRE-LoxP-Neo-LoxP</i> cassette insertion at C5. Figure 1.11.	59.3
Reverse	5'-ATCTCATCCAGGAACGGAA-3'		62.1
Forward	5'-GAATTCGATATCAAGCTTATCGATACCG TCGAC-ATCAGCCATCTCTAAACCGG-3'	To amplify the first fragment of the <i>TRE-LoxP-Neo-LoxP</i> cassette-inserted DTA3 vector for Gibson assemble. Section 1.3.	62.3
Reverse	5'-TCGTCCTGCAGTTCATTCA-3'		64.1
Forward	5'-CGTCTCTTTTTGTCAAGACC-3'	To amplify the second fragment of the <i>TRE-LoxP-Neo-LoxP</i> cassette-inserted DTA3 vector for Gibson assemble. Section 1.3.	64.1
Reverse	5'-CCCTACTAAAGGGAACAAAAGCTGGG TACC-ATTGCTTTAGGTTCTGGCTTA-3'		60.3
Forward	5'-GAATTCGATATCAAGCTTATCGATACCGT CGAC-ATATGCATTTGCACACTGCC-3'	To amplify the first fragment of the <i>TRE-LoxP-Neo-LoxP</i> cassette-inserted DTA4 vector for Gibson assemble. Section 1.3.	63.5
Reverse	5'-TCGTCCTGCAGTTCATTCA-3'		64.1
Forward	5'-CGTCTCTTTTTGTCAAGACC-3'	To amplify the second fragment of the <i>TRE-LoxP-Neo-LoxP</i> cassette-inserted DTA4 vector for Gibson assemble. Section 1.3.	61.1
Reverse	5'-CCCTACTAAAGGGAACAAAAGCTGGGT ACC-CTTTCTCTAAGGAACCATCG-3'		58
Forward	5'-GAATTCGATATCAAGCTTATCGATACCGTC GAC-CACAGTTTTCACTTGACAGGG-3'	To amplify the first fragment of the <i>TRE-LoxP-Neo-LoxP</i> cassette-inserted DTA5 vector for Gibson assemble. Section 1.3.	63.3
Reverse	5'-TCGTCCTGCAGTTCATTCA-3'		64.1
Forward	5'-CGTCTCTTTTTGTCAAGACC-3'	To amplify the second fragment of the <i>TRE-LoxP-Neo-LoxP</i> cassette-inserted DTA5 vector for Gibson assemble. Section 1.3.	61.1
Reverse	5'-CCCTACTAAAGGGAACAAAAGCTGGGTA CC-GCGCTACTCAGTGTGATAA-3'		61.5
Forward	5'-GGAACACAAAGGTCCTTG-3'	To clone DNA probe 3.3 for southern blot from wildtype mouse genomic DNA.	62
Reverse	5'-GTCTGGCCTTATCTTGGTCA-3'		61.7

Table M.1c List of PCR primers used (continued)

Direction	Primer sequence	Description	T _m (°C)
Forward	5'-GACCACAGTGTCCAGACCAT-3'	To clone DNA probe 7.8 for southern blot from wildtype mouse genomic DNA.	62.6
Reverse	5'-AAAGGATTGCGAAAAAGGAC-3'		61.9
Forward	5'-GACCCTATCTCAAATAAAGCAAAA-3'	Amplifying across the whole insertion at C3; also used for PCR genotyping for <i>TRE3</i> -inserted mice. Figure 1.17, Figure 1.22, Figure 2.1.	62.5
Reverse	5'-TGAAAGGTTGCAAGTGGTAAGT-3'		62.4
Forward	5'-TAGCTGGATAGGAAAGAGCA-3'	Amplifying across the whole insertion at C4; also used for PCR genotyping for <i>TRE4</i> -inserted mice. Figure 1.17, Figure 1.22, Figure 2.1.	59.2
Reverse	5'-GTTTTATGGATGCAAACGGA-3'		62.2
Forward	5'-GGTAGCGACTACAGTTAGGG-3'	Amplifying across the whole insertion at C5; also used for PCR genotyping for <i>TRE5</i> -inserted mice. Figure 1.17, Figure 1.22, Figure 2.1.	57.9
Reverse	5'-ATCTCATCCAGGAACGGAA-3'		62.1

Restriction enzyme digestions were carried out following the manufacturer's instructions (NEB). The general reaction composition and conditions are summarised in **Table M.2**.

Table M.2 General reaction conditions for restriction enzyme digestion

Reagent	Volume
DNA to be digested	x µl (0.5 - 1 µg) *
10x NEBuffer	5 µl (which one to use depends on enzyme)
Restriction enzyme	1 - 4 µl (depending on enzyme)
Sterilized water	To 50 µl
Total reaction volume	50 µl
Incubation temperature	37°C (25°C for <i>Apal</i>)
Incubation Time	1 hour

* value of x depends of DNA concentration

DNA ligation reactions were carried out following the manufacturer's instructions (NEB) as summarised in **Table M.3** below.

Table M.3 Composition and condition of ligation reaction

Reagent	
DNA vector backbone	50 ng
Insert (wildtype or mutant <i>c-myc</i> genes)	3x backbone (molar ratio)
10x T4 DNA Ligase buffer (NEB)	2 μ l
T4 DNA Ligase (NEB)	1 μ l
MiliQ Water	To 20 μ l
Total reaction mixture volume	20 μ l
Incubation temperature	25°C
Incubation time	15 minutes

M.1.2 BAC preparation and verification

The BAC preparation and verification methods used were modified from the online protocol provided by Dr. Douglas Mortlock (<http://kingsley.stanford.edu/Lab%20Protocols-WEB%202003/Molecular%20Biology/BAC%20modification%20protocol.htm>). A 2ml overnight culture was collected in an eppendorf tube and pelleted by centrifugation for 1 minute at 20000 x g. The pellet was resuspended in 250 μ l of resuspension buffer (1x TE buffer pH8, 10mM Tris-HCl containing 1mM EDTA added with 100 μ g/mL RNase A). 250 μ l of lysis buffer (200 mM NaOH, 1%SDS) was added to lyse the cells for 2-3 mins. 350 μ l of neutralisation buffer (3 M potassium acetate, pH5.5) was added followed by vigorous mixing. The mix was then centrifuged for 10 min at 20000 x g. The supernatant was transferred to a tube containing 550 μ l of isopropanol and centrifuged for 15min at 20000 x g. The supernatant was discarded and the pellet washed with 70% ethanol. After briefly air drying, the pellet was resuspended in 30 μ l of water.

PCRs that amplify four short regions across the p53 promoter and intron sequence in the BAC were used to verify the BAC. The four pairs of primers are listed in **Table M.1c**.

M.1.3 Preparing electro-competent EL350, electroporation and recombineering of DNA in EL350

The protocol used was modified from the online protocol provided by Dr. Douglas Mortlock (<http://kingsley.stanford.edu/Lab%20Protocols-WEB%202003/Molecular%20Biology/BAC%20modification%20protocol.htm>).

EL350, a strain of bacteria that harbour heat-inducible expression of recombinase (at 42°C), was grown in 2 mL overnight in Luria-Bertani (LB) broth with appropriate antibiotics at 32°C. A 50 mL culture was inoculated using 1 mL of the overnight culture until the OD at 600 nm reaches 0.4-0.6. Recombinase activity was induced by incubation with constant swirling at 42°C for 10-15 mins and then chilled on ice for 15 mins. A negative control for recombineering that was not incubated at 42°C was also included. The bacteria were collected by centrifugation for 10 mins at 2680 x g. The supernatant was discarded and 30 ml cold water (pre-chilled overnight at 4°C fridge) was added to re-suspend the pellet by mixing the tube on ice. The bacterial pellet was washed twice more and the final bacterial pellet re-suspended in 1 mL of water and transferred to a pre-chilled eppendorf tube. The bacteria were collected by centrifuge for 5 mins at 2680 x g at 4°C. The supernatant was discarded and the bacteria re-suspended in 200 µl of cold sterilised water, which was used for 4 transformations.

DNA diluted in water was added to a pre-chilled eppendorf tube containing 50 µL of electro-competent bacteria and mixed by gentle pipetting up and down. The mixture was transferred to a pre-chilled 1mm cuvette and an electric pulse delivered (volts = 1.8, capacitance = 25µFD and resistance = 200 Ohms). The electroporation mixture was removed by adding 500 µL of LB to the cuvette and transferred to an eppendorf tube. The tube was shaken at 32°C for 1 hour and the bacteria plated onto LB agar plates containing appropriate antibiotics.

M.1.4 Gibson Assembly

Gibson Assembly reactions were carried out following the manufacturer's instructions (NEB), summarised in **Table M.4** below.

Table M.4 Composition and condition of Gibson Assembly

DNA fragment 1	0.02 - 0.5 pmols
DNA fragment 2	0.02 - 0.5 pmols
Gibson Assembly Master Mix (2X)	10 μ l
Deionised H ₂ O	To 20 μ l
Total reaction mixture volume	20 μ l
Incubation at 50°C	Up to 60 minutes

The DNA vector to be recombineered was suspended in water and electroporated into electro-competent EL350 *E. coli* that carried the heat-inducible recombinase gene. Following recovery, the bacteria were then plated on LB agar plates containing appropriate antibiotics for selection.

M.1.5 Antibiotics used in molecular cloning

Antibiotics used to select positive clones were detailed in **Table M.5** below.

Table M.5 List of antibiotics

Name	Working concentration
Ampicillin	100 μ g/mL
Chloramphenicol	10 μ g/mL (in ethanol)
Kanamycin	50 μ g/mL

M.2. Mouse embryonic stem cells (mESCs) culture and targeting

M.2.1 Culture of mESCs

Wild-type mouse embryonic stem cells (mESCs) were cultured on gelatin-coated tissue culture dishes in 2I/LIF medium in a 37°C, 5% CO₂ and 0.1% oxygen environment as described (Silva et al. 2008). For maintenance, cells were normally passaged every two days by trypsinization. When necessary, doxycycline was added to the growth medium to a final concentration of 1 mg/mL for various durations as indicated in the results.

For transfection with DTA targeting vectors, mESCs were cultured on an extra layer of mitomycin C-treated, i.e. mitotically inactivated feeder cells (mouse embryonic fibroblasts) grown on the gelatin-coated plate (mitomycin C concentration = 10 µg/mL; 2 hours at 37°C).

M.2.2 DNA electroporation into mESCs

E14 mESCs were grown to 60% confluence in a 6-well plate, recovered by trypsinization and resuspended in 800 µL of DMEM containing 40 µg of the DTA targeting vector linearised by NotI restriction enzyme digestion (NEB). The cells were then electroporated using a BioRad GenePulser Xcell electroporation machine (0.96 kV, 10 µF) and transferred to 9.2 mL of pre-warmed 2I/LIF medium followed by seeding onto ten 10-cm gelatin-coated dishes with a layer of the inactivated feeder cells mentioned in **M.2.1** (1 mL per dish). Antibiotic selection was added one day after seeding and continued until resistant colonies arose (or non-transfected cells all died).

M.2.3 Isolation of antibiotic-resistant clones of mESCs

Antibiotic-resistant colonies (in the form of embryoid bodies) were picked with a 10 µL pipette tip, dissociated into single cells by treatment with trypsin (0.05% with 0.02% EDTA, 37 °C, 5 minutes) and then seeded into gelatin-coated 96-well plates. 96 colonies were picked for each transfection. Medium was changed one day later and the cells passaged by 1:4 dilution

into four 96-well plates. When confluent, the medium of three of the four duplicate 96-well plates was changed to freezing medium (70% Glasgow Minimum Essential Medium (GMEM), 20% serum, 10% DMSO) and the plates frozen and stored in a -80 °C freezer for later thawing after verification of correct targeting. The remaining plate was used to prepare genomic DNA (gDNA) for southern blot verification of correct targeting.

M.2.4 Preparation of mESCs for blastocyst injection

Correctly targeted clones of mouse embryonic stem cells were thawed and expanded into 6-well plates. The cells were trypsinized and resuspended in 200 µL of injection medium (N2B27 medium with 0.1M HEPES). Blastocyst injection was carried by the core facility of the Cambridge Stem Cell Institute.

M.2.5 Lipofectamine transfection of mESCs

Lipofectamine 2000 transfection reagent (ThermoFisher Scientific Cat. no.: 11668030) was used to introduce the Cre-expressing DNA vector pCAG-Cre (a gift from Connie Cepko; Addgene plasmid #13775; <http://n2t.net/addgene:13775>; RRID:Addgene_13775; (Matsuda & Cepko 2007)) and rtTS-expressing DNA vector following the manufacturer's instructions. While the expression of Cre from pCAG-Cre was only transiently required and hence no permanent integration of the plasmid into the mESCs genome, persistent rtTS expression was required in the mESCs and so the cells were selected with puromycin (working concentration = 1 µg/mL) for stable integration of the linearised pPCAGIPCAG plasmid into the genome.

M.2.6 mESCs culture media composition

N2B27 (base for 2i/LIF)		mESCs freezing medium		
		2x	1x	
DMEM/F12	500 mL	GMEM w/ serum	40%	70%
Neurobasal medium	500 mL	Extra Serum (FBS)	40%	20%
N2 (need to match batch with B27)	5 mL	DMSO	20%	10%
B27 (need to match batch with N2)	10 mL			
Glutamine	10 mL			
2-Mercaptoethanol	1.1 mL			

2i/LIF	
N2B27	200 mL
PD03 (to 1 μ M)	20 μ L (10 μ L of stock/100 mL)
Chiron (to 3 μ M)	60 μ L (30 μ L of stock/100 mL)
Mouse LIF (for mESC)	200 μ L (stock = 1000x)

M.3 Primary mouse embryonic fibroblasts (MEFs) culture

Mouse embryonic fibroblasts (MEFs) of various desired genotypes were prepared from 13 d.p.c. (day post-coitum) embryos as described (Jozefczuk et al. 2012). Cells were passaged and maintained in Dulbecco's minimal essential medium supplemented with 10% BGS, 5% glucose and 2 mM Glutamine (DMEM; Sigma-Aldrich) at 37°C and 5% CO₂. For maintenance, cells were normally passaged every two days by standard trypsinization. When necessary, doxycycline was added to the growth medium to a final concentration of 1 mg/mL for different periods of time as indicated in the results.

M.4 Southern blot

Genomic DNA (gDNA) was harvested from cells grown in culture or mouse tissues extracted using tail lysis buffer (50 mM TRIS, 50 mM EDTA, 0.5% SDS) followed by ethanol precipitation. 4 µg of gDNA was digested overnight at 37 °C with the desired restriction enzymes, separated by agarose gel (0.8% agarose) electrophoresis (70 volt, 8 hours) and transferred onto Hybond C membranes. 50 ng of DNA probes 3.3 or 7.8 prepared by PCR and radioactively labelled with ³²P using the Random Primed DNA Labelling Kit (Roche, Cat. No. 11 004 760 001) were used to anneal to the 5' and 3' ends of the targeted inserted DNA. **Table M.5** shows the sequences of the DNA probes 3.3 and 7.8.

The radioactively hybridised membranes were sequentially washed with a series of buffers with increasing stringency (2x to 0.2x saline-sodium citrate buffer plus 0.1% SDS; 1x saline-sodium citrate buffer = 150 mM sodium chloride, 15 mM trisodium citrate, pH7) and then exposed to X-ray film for 10 days in -80°C freezer and then developed with an AFP Mini-Med 90 automated developer.

The radioactively hybridised membranes were washed with a series of washing buffers of decreasing concentrations (saline-sodium citrate buffer 1x = 150 mM sodium chloride, 15 mM trisodium citrate, pH7; 0.1% SDS) and then visualised by X-ray film exposure in a light-sealed cassette. The X-ray films were exposed to the membrane for 10 days in -80°C freezer (the low temperature intensified the signals) and then developed.

Table M.5 Sequences of southern blot probes

Probe 3.3	5'- <u>GGAACACAAAGGTCCTTGTGTCTACAGGTAAAAACCTATTCTTCCATCCAGAAAGCTAGG</u> AATTGAAGTGATTAATAGTCCTGTGATCTGTTATCTGCTGGGCTAAGCCATACCAAGTTCCTTC AACCAGGGCCAGAGGTGGCTAGTACTCTAAATGAGCCTTACAGACAGGGGCTCCCAAGCT CCCACAGCCAGGACCTGAGATACCTAATAGTCTAAATGACCTTACATCATCTGTATGGCCAGG GGCTTCCCAGGCTCCCACAACCAGGACTACAAGTGGCTAATATCCCAAACGACCTCTATAGC ATCTGTATGACCAAGATAAGGCCAGAC-3'
Probe 7.8	5'- <u>GACCACAGTGTCCAGACCATACATAGAGGGAGTTCAAGGTCATCCTTCCCTGGGTAGTTGT</u> AAGCTGACTTGAGATAAATGAGAGTGTCTTCAAAAACAGAGAAAGAGTACAAAAGTTAACAT TGGCAAACCAGAGCCTACTGGCCTTCTCCTGATGGGTAAATGAGGACGTCTCGATGGCCCG TGCCTTAAATGCTAACACTCTTGGGATGCTGAGGTAAGTGGGCTACTTAGCAAGACCTTGTC TCAGAAAGGCCAAACAGCTGGAGATATGGCTTGGAGTAGATTATTTACCTGGCAAACATGAT ACCCTTGTTTAAATCCTGAGACCACAAAAACAGGTAAACCCAGCTTGACCAAGTGCCAT TGGTCCATGGATTGCTGTATTGGAATCAAACAGAAATCTATGTCATTACAGCAGTAACCTCCT GGGAATACTCAAGAGACGGAGAAAGGGCGACTGACTGTGCCCTCC <u>GTCCTTTTTTCGCAATC</u> <u>CTTT</u> -3'

Underlined are the annealing sequences to which the primers used to amplified the probes from wildtype mouse gDNA by PCRs.

M.5 RNA extraction and qPCR analysis

Messenger RNA was extracted from cells or frozen mouse tissues using Trizol reagent following the manufacturer's protocol (ThermoFisher Scientific, Cat no. 15596018). Complementary DNA (cDNA) was synthesized from the extracted mRNA (1 mg of mRNA used per reaction) by reverse transcription using the High-Capacity cDNA Reverse Transcription Kit following the manufacturer's protocol (Applied Biosystem™, Cat no. 4368814). The synthesized cDNA was diluted 1:5 and then analysed by real time PCR (qPCR) using SYBR™ Green Master Mix (Applied Biosystem, Cat no. 4367659) and the QuantStudio™ 5 Real-Time PCR System (Applied Biosystem, Cat no. A28140). **Table M.6a** outlines the general conditions of the qPCRs and **Table M.6b** lists the details of the qPCR primers used in this thesis.

Table M.6a General qPCR reaction cycle

Step	Temperature	Duration	
1	50°C	2 minutes	
2	95°C	10 minutes	
3	95°C	15 seconds	Repeats 39 times
4*	61 °C	30 seconds	
5	95°C	15 seconds	
4	60°C	1 minute	Melt curve stage
5	95°C	15 seconds	

*Annealing plus amplification step, primers are designed to have an annealing temperature of 60°C.

Table M.6b List of qPCR primers used

Direction	Primer sequence*	Target
Forward	5'-ATGCCCATGCTACAGAGGAG-3'	Mouse endogenous <i>Trp53</i>
Reverse	5'-AGACTGGCCCTTCTTGGTCT-3'	
Forward	5'-ACTTCGTGCAAGAAATGCTGAAT-3'	Mouse endogenous <i>Tbp</i>
Reverse	5'-CAGTTGTCCGTGGCTCTTATT-3'	
Forward	5'-GGCCTGGAACATAATCATATGTG-3'	Mouse <i>Rosa26^{tr5}</i> knockin allele
Reverse	5'-CGAGTAAAGAGCACAGCCAC-3'	
Forward	5'-TAGCAAACGGTGCTCAAGG-3'	Mouse endogenous <i>Bax</i>
Reverse	5'-TCTTGGATCCAGACAAGCAG-3'	
Forward	5'-GACGACCTCAACGCACAGTA-3'	Mouse endogenous <i>Puma</i>
Reverse	5'-CTAATTGGGCTCCATCTCG-3'	
Forward	5'-CCTGGTGATGTCCACCTG-3'	Mouse endogenous <i>Cdkn1a</i>
Reverse	5'-CATGAGCGCATCGCAATC-3'	
Forward	5'-CTCCAGTGAGTTGAGTCCT-3'	Mouse endogenous <i>Wrap53α</i>
Reverse	5'-TTGCAACCTTCAAGAAGTT-3'	
Forward	5'-GATGATGGTTCGCCTCTT-3'	Mouse endogenous <i>Wrap53β</i>
Reverse	5'-AGTAGATGCGCTGATTAGTGGT-3'	

*All primers were designed to have a uniform annealing temperature of 60°C at which the PCR programme was run.

M.6 Protein extraction and Western blot

Cell lysates were prepared either from cultured cells or frozen mouse tissues using RIPA buffer (50 mM Tris-HCl pH 8.0, 150 mM NaCl, 5 mM EDTA, 1% Triton X-100, 1% sodium deoxycholate, 0.1% SDS) supplemented with protease inhibitors (Roche, Cat. no. 11836153001; 1 tablet/10 mL of 1x RIPA). Following sonication and centrifugation to remove genomic DNA, total protein concentration was determined using the BCA protein assay following the manufacturer's protocol (Thermo Scientific™ Pierce™ BCA™, Cat. no. 10678484).

Lysates were supplemented with 0.01% bromophenol blue as a loading dye and 1 mM DTT, heated to 95°C for 3 minutes and 10 - 30 µg of total protein loaded onto SDS-12% polyacrylamide denaturing gels. Proteins were separated by electrophoresis (120 volt, 120 minutes) and then transferred to PVDF membranes by electroblotting in NuPAGE transfer buffer (Invitrogen) at 30v for 60 minutes. Non-specific protein binding to the membranes was blocked by incubation in 5% (w/v) bovine serum albumin in TBS-T (20 mM Tris and 150 mM NaCl, pH7.6, 0.1% Tween 20) for 1 hour at room temperature. The membrane was then incubated for 1 hour each in primary and secondary antibodies with washing three times in TBST in between. Primary antibodies used in the Western blots in this thesis are listed in **Table M.7**. After blotting with secondary antibody the membranes were treated with ECL chemiluminescent substrate (Thermo Scientific) followed by exposure to X-ray. Films were developed and fixed using an AFP Mini-Med 90 automated developer.

Table M.7 Antibodies used in Western blots

Antibody	Source	Target	Primary/ Secondary	Host species	Clone	Concentration used
1C12	Cell Signaling	Mouse p53 protein	1 ^o	Mouse	Monoclonal	1: 1000
AC15	Santa Cruz Biotech.	Mouse β-Actin protein	1 ^o	Mouse	Monoclonal	1:5000
D16H11	Cell Signaling	Mouse Gapdh protein	1 ^o	Rabbit	Monoclonal	1:1000
A4416	Sigma	Mouse IgG	2 ^o -HRP	Goat	Polyclonal	1:10000
A0545	Sigma	Rabbit IgG	2 ^o -HRP	Goat	Polyclonal	1:10000

M.7 Mice

M.7.1 Genetic backgrounds and strains of mice

All mice used in this project were of a mixed genetic background of C57BL/6 and FVB. The strains of genetically altered mice are listed in **Table M.8** below.

Table M.8 Strains of genetically modified mice used

Strain (allele altered)	Source	Purpose	Background
<i>Trp53^{TRE/TRE}</i>	Created in this project	Reversible repression of endogenous <i>Trp53</i>	C57BL/6, 129/SvJ
<i>R26^{CAG-rTS/+}</i>	Dr. Ivonne Gamper, Evan group	Reversible repression of endogenous <i>Trp53</i>	C57BL/6, 129/SvJ
<i>PGK-Cre^{Tg/+}</i>	Evan group	Cre-mediated removal of <i>NeoR</i> from the targeted allele	C57BL/6, 129/SvJ
<i>Trp53^{fllox/fllox};K14-CreER^{Tg/+}</i>	Dr. Michaela Frye	Deletion of endogenous <i>Trp53</i> gene in chemically induced skin cancer experiment	C57BL/6, 129/SvJ

M.7.2 Maintenance of mice

All breeding and experimental mice were housed in a Home Office approved facility at the CRUK Cambridge Institute under licence 70/7586. Day-to-day husbandry and breeding as well as most of the experimental treatments such as intraperitoneal injection, topical treatment of skin, and diet intake of doxycycline were carried out by trained facility staff. Substances administered to mice are shown in **Table M.9**.

Ear biopsies were taken from 3 week old pups at weaning. gDNA was extracted from the biopsies using Chelex 100 following the manufacturer's protocol (BioRad, Cat. no. 1421253). The genotype was determined by PCR as described in **Section M.1**.

M.7.3 Chemical induction of skin cancer

Following the published protocol of chemical induction of skin cancer (Abel et al. 2009), the shaved dorsal skin of 6 week old mice was topically treated with DMBA once and then topically treated with TPA from the age of 7 weeks for up to 20 weeks (three treatments with TPA per week) (**Table M.9**). Mice were shaved weekly at the application site to assist in monitoring the development of skin tumours.

Table M.9 Substances administered to mice

Substances	Route of administration	Concentration	Amount/treatment
Sucrose water	Drinking water	1% (w/v) in water	Continuous
Doxycycline	Drinking water	2 mg/mL in 1% sucrose water	Continuous
Tamoxifen	Intraperitoneal injection	10 mg/mL in oil	1 mg per injection
7,12-dimethyl-benz[a]anthracene (DMBA)	Topical application on skin	666.7 µg/mL in acetone	100 µg per treatment
12-O-tetradecanoyl-phorbol-13-acetate (TPA)	Topical application on skin	33.4 µg/mL in acetone	5 µg per treatment

M.7.4 Collection and preparation of mouse tissues

Experimental mice were culled by cervical dislocation. Small pieces of lung, intestine, liver, pancreas, spleen, thymus and skin were collected in an eppendorf tube and snap-frozen in liquid nitrogen and stored at -80°C or fixed in 10% formalin for 24 hours prior to storage in 70% ethanol. Formalin fixed tissues were embedded in paraffin blocks and 4 µm sections prepared on glass slides.

M.8 Immunofluorescence staining of mouse tissues

Paraffin embedded sections of mouse tissues were de-paraffinized using xylene and ethanol (3 x 5 minute wash in xylene; 2 x 5 minutes wash in 100%, 95% and 70% ethanol respectively; 1 x 5 minutes wash in 50% ethanol and water). The de-paraffinized sections were processed for antigen retrieval using citric buffer (10 mM Sodium citrate, 0.05% Tween 20, pH 6.0): the slides were heated in boiling citric buffer in a microwave for 10 minutes. after cooling by equilibrating in 1x PBS-T (8 mM Na₂HPO₄, 150 mM NaCl, 2 mM KH₂PO₄, 3 mM KCl, 0.05% Tween 20, pH7.4) for 5 minutes, the slides were blocked with blocking solution (2% NGS in 1x PBS-T) for 60 minutes. The sections were then blotted with primary and secondary antibody (in blocking solution) overnight at 4 °C and 1 hour at room temperature respectively. Finally, the sections were stained with DAPI (4',6-diamidino-2-phenylindole, ThermoFisher Scientific Cat. no. 62248) for nuclei and mounted with cover slides. The sections were then examined under a fluorescent microscope.

Table M.10 Antibodies used in immunofluorescence staining of mouse tissues

Antibody	Source	Target	Primary/ Secondary	Host species	Clone	Concentration used
CM5	Leica	Mouse p53 protein	1 ^o	Rabbit	Polyclonal	1:200
A11008	Alexa Fluor 488	Rabbit IgG (H+L)	2 ^o	Goat	Monoclonal	1:500

**BLANK
PAGE**

Chapter 1:

A model for reversible repression of endogenous *Trp53* expression

1.1 Why is a new switchable p53 model needed?

The elucidation of p53 function in animals has relied heavily on comparing phenotypes between *p53* wild type (WT) mice versus mice with germline deletion of *Trp53* (*p53* knockout mice). Although such knockout mice are viable and fertile, they exhibit (with variable penetrance) certain developmental abnormalities such as neural tube closure defects (Armstrong et al. 1995; Sah et al. 1995). Moreover, as with all germline knockout mice, it is unclear to what extent their adult phenotype (or the lack thereof) is a consequence not of the direct absence of the targeted gene, but instead of adaptive developmental compensation or functional redundancy - in the case of p53 deletion, from the functionally overlapping *p63* and *p73* genes (Yang & McKeon 2000). For these reasons, genetic analysis of p53 function in adult tissues clearly benefits from more sophisticated mouse models in which WT p53 function is retained during development but which may then be switched off (and back on) in adults, either systemically or tissue-by-tissue. For example, such models allow for a more discriminating study of p53's physiological functions whilst mitigating the confounding susceptibility towards spontaneous lymphomas in early adult life. Although previous switchable p53 mouse models have been developed, they all suffer from various practical limitations that restrict their use in investigating p53 physiological and tumour suppressing functions. Thus, the well-documented Cre recombinase-dependent *p53^{fllox}* mouse model was developed to model the acute loss of p53 function that occurs in tumours. In these animals, *LoxP* sites are inserted to flank exon 2 - 10 of the endogenous *Trp53* alleles (Jonkers et al. 2001). When combined with a *CreERT²* background, in which Cre-mediated recombination may be acutely triggered by administration of the 4-hydroxytamoxifen (4OHT) ligand, this may be used to inactivate endogenous *Trp53* at will, either systemically or in a tissue-specific manner (Littlewood et al. 1995; Metzger & Chambon 2001). However, this model has profound limitations. First, the *Trp53* deletion is irreversible, precluding study of subsequent restoration of p53 function in tumours that have evolved after p53 loss. Second, Cre-dependent recombination is not completely penetrant and often varies

according to conditions and contexts, making interpretation of results difficult (Bao et al. 2013). Finally, Cre recombinase triggers a profound DNA damage response that, in the case of p53, a pivotal DNA damage sensor, is an unhelpfully confounding complication (Janbandhu et al. 2014). The other well-characterised switchable p53 *in vivo* model is the *p53ER^{KI}* mouse, in which endogenous *Trp53* is modified to encode a 4OHT-dependent p53ER^{TAM} fusion protein (Christophorou et al. 2005). In the absence of 4OHT ligand, p53ER^{TAM} is completely inactive and mice are effectively null for p53 functions. However, systemic administration of the 4OHT ligand rapidly restores p53ER^{TAM} functions to the WT state, together with all the same level and temporal dynamics as the WT p53 protein that it replaces. Importantly, p53 activity in 4OHT-treated *p53ER^{KI}* mice remains completely dependent upon upstream activating signals such as DNA damage (Christophorou et al. 2005). The *p53ER^{KI}* model allows for rapid, reversible switching of p53 in adult mice without the confounding DNA damage of the *p53^{fllox}* models, while its ability to rapidly and reversibly toggle between p53 null and WT state uniquely allows for establishing direct cause and effect relationships in p53 activation (Christophorou et al. 2005; Martins et al. 2006; Christophorou et al. 2006; Junttila et al. 2010). Nonetheless, due to the potent abortigenic activity of Tamoxifen (Nakamura et al. 2006), p53ER^{TAM} must be maintained in its inactivate state throughout embryonic development, raising the same problems of adaptive compensation as in conventional *p53* knockout mice.

To address the inherent limitations of the above existing current models, I have constructed a novel, reversibly switchable p53 model that allows for precise temporal and spatial analysis of the roles of p53 in normal physiology and in tumourigenesis. Importantly, this model allows embryogenesis and neonatal development to proceed in the presence of normal p53 functions yet retains the key capacity to toggle acutely, reversibly and rapidly p53 status from *WT* to *null* and back, either systemically or tissue-by-tissue. This new model relies on tetracycline (Tet, or its derivative ligand doxycycline, Dox) ligand-dependent repression of endogenous *Trp53* expression. A heptad tetracycline response element (*TRE*) is inserted into the

transcriptional control region of *Trp53* that allows tetracycline-dependent binding of a transcriptional repressor to the *TRE* (**Fig. 1.1, right panels**). This system is very flexible and can also be configured as a Tet-off version, as illustrated in **left panels of Figure 1.1** (Gossen & Bujard 1992). The Tet-on model of *Trp53* described below is hereafter referred to as *TRE-p53* throughout this thesis.

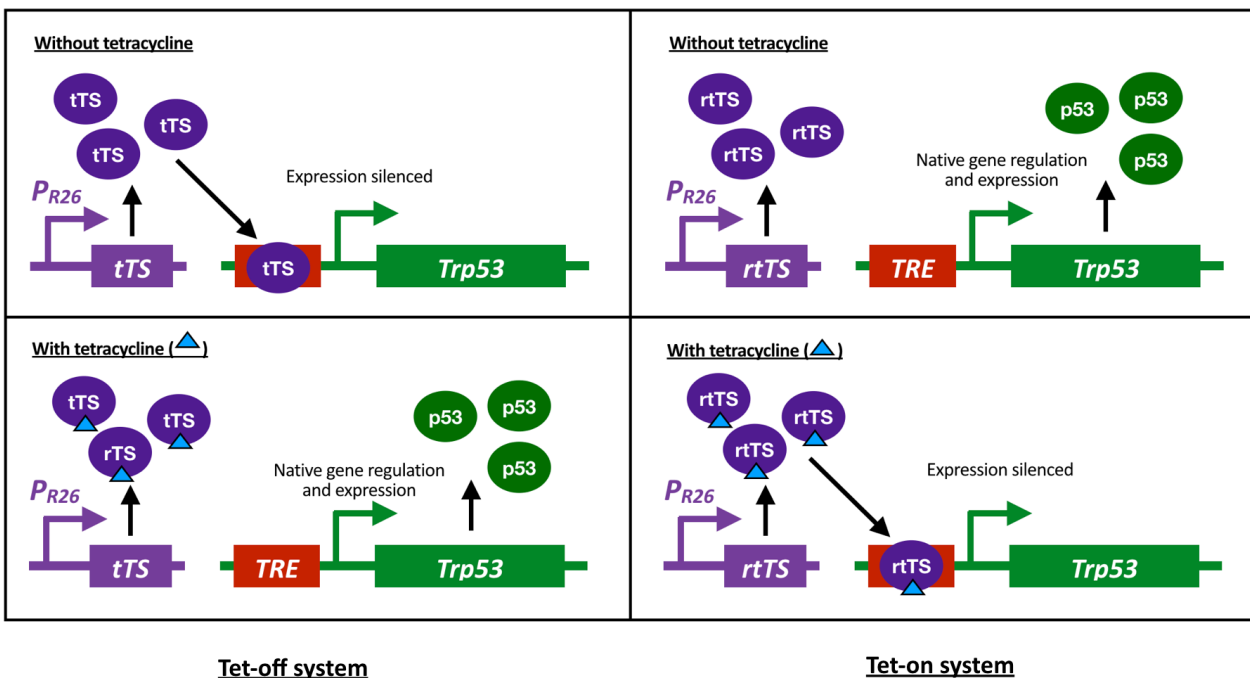


Figure 1.1. Tet-off and Tet-on *TRE* systems. In a Tet-off system (left panel), the modulator protein - be it either a transcription repressor (*tTS*) or activator (not shown here) - will be constitutively active in function in the absence of tetracycline (or its derivatives, e.g. doxycycline) but inactivated otherwise. By contrast, in the reverse Tet-on system (right panel) the modulator protein, *rtTS* the transcription repressor, will only be active and functional in the presence of tetracycline (or its derivatives).

1.2 Designing and optimising the *TRE-p53* repression system

The first step in generating the new switchable p53 model was to decide where to insert the *TRE* cis-regulatory motif – specifically, in the promoter or in the first intronic region of the endogenous *Trp53* gene. Previous work in the Evan group indicated that the careful positioning of *TRE* is critical in such models since it can greatly influence the efficacy of repression of the target gene and any surrounding genes. For example, insertion of a *TRE* in the *E2F3* promoter mediated almost complete Tet-dependent silencing of the target gene (Gamper et al. 2017); by contrast, *TRE* insertion in the second intron of *c-Myc* resulted in only partial repression of expression *Myc* (unpublished). However, the optimal *TRE* insertion site allowing for the most definitive Tet-dependent repression of the target gene without disrupting that gene's normal regulation (or that of nearby genes) is probably highly dependent on subtleties in the local DNA landscape and has to be determined empirically. To this end, the promoter and first intronic region of the mouse *Trp53* locus (chromosome 11 position 69,580,359-69,591,873 bp; from MGI, updated Jan 2014; <http://www.informatics.jax.org/marker/MGI:98834>) were analysed using several available algorithms based on different matrices to identify transcription and splicing regulatory *cis*-DNA elements. In addition, *Trp53* co-locates with an antisense gene of poorly defined function called *Wrap53*. The coding region of the *Wrap53* gene, which is located upstream of the Transcription start site (TSS) of *Trp53*, was also ruled out for placing potential *TRE* insertion sites. Based on this information, the final regions chosen for *TRE* insertion are shown in **Table 1.1.**: -2161 bp, -57 bp and +356 bp in relation to the TSS of endogenous *Trp53*; these sites are hereafter referred to as C3, C4 and C5 respectively (**Figure 1.2**).

	TFSEARCH	JASPAR	MATCH	PMATCH	ACESCAN2 WEB Server
The algorithm and database	Highly correlated sequence fragments vs TFMATRIX transcription factor binding site (TFBS) profile database GBF-Braunschweig	scans sequences for listed factors binding site	Weight matrix-based, predicts TFBS in DNA sequences. Uses a library of positional weight matrices from TRANSFAC® Public 6.0.	Predicts TFBS in DNA sequences. Combines pattern matching and weight matrix approaches. Uses library of positional weight matrices from TRANSFAC® Public 6.0 with site alignments associated with the matrices.	Comparing sequences to overrepresented <i>cis</i> -elements in aligned exons and introns.
Probing for	Vertebrate factor sites	<i>Mus musculus</i> factor sites	Vertebrate factor sites	Vertebrate factor sites	<i>Mus musculus</i> splicing sites
Region checked	From -5kb to +1kb of TSS of <i>Trp53</i>	From -10kb to +1kb of TSS of <i>Trp53</i>			First intron
<i>Cis</i>-element-free windows	<ol style="list-style-type: none"> -4349 to -4250 bp -3449 to -3250 bp -2199 to -2000 bp -709 to -680 bp -449 to -300 bp -99 to -10 bp +301 to +450 bp 	<ol style="list-style-type: none"> -7987 to -7951 bp -6700 to -6644 bp -4318 to -4243 bp -2188 to -2140 bp -57 to -56 bp +330 to +384 bp 	<ol style="list-style-type: none"> -8035 to -7676 bp -6715 to -6356 bp -3475 to -1916 bp -715 to -116 bp -57 to -1 bp +245 to +484 bp 	<ol style="list-style-type: none"> -8079 to -7480 bp -5079 to -4000 bp -2799 to -1000 bp -759 to -400 bp -159 to -56 bp +81 to +1001bp 	<ol style="list-style-type: none"> +314 to +374 *

* Only one window is listed as others are not transcription *cis*-element-free.

Table 1.1. Five online algorithms were used to analyse the promoter and first intron of endogenous *Trp53*. The online algorithms probe for *cis*-DNA elements based on different databases and matrices. Sequence windows consistently free across the four algorithms were picked. The sequence window in the first intron was then analysed for *cis*-DNA elements that regulate splicing. Three insertion sites were then picked from the consistently *cis*-element-free windows. TFSEARCH: <http://diyhl.us/~bryan/irc/protocol-online/protocol-cache/TFSEARCH.html>, JASPAR: <http://jaspar.cgb.ki.se.>, MATCH: <http://www.gene-regulation.com/pub/programs.html#match>, PMATCH: <http://www.gene-regulation.com/pub/programs.html#match> and splicing analyser ACESCAN2 WEB Server: <http://genes.mit.edu/acescan2/index.html>).

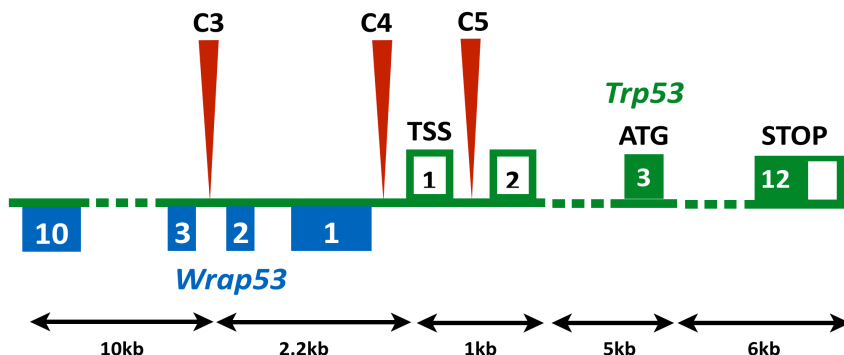


Figure 1.2. (a) A schematic diagram showing the gene structure of *Trp53* and *Wrap53*. The positions of the potential insertion sites C3, C4 and C5 are indicated by the red pointers. The size of the genes are not drawn to scale.

1.3 Generation of *Trp53* targeting vector

1.3.1 Cloning of *TRE-LoxP-Neo-LoxP* cassette into pL452

Cloning of *TRE* into each of the three selected locations required multiple cloning steps. First, the *TRE* sequence and neomycin resistance gene (*NeoR*) flanked by two *LoxP* sites were cloned into the pL452 plasmid to generate the sequence cassette *TRE-LoxP-Neo-LoxP* (**Figure 1.3** shows (a) a schematic of the cassette and (b) a map of pL452 after insertion of the cassette). This initial cloning step had been previously completed by Dr Ivonne Gamper in the Evan group. Inclusion of a *NeoR* sequence allowed for selection of clones targeted with the *TRE* cassette in the subsequent cloning steps, including *E. coli* recombineering and mouse embryonic stem cell (mESC) targeting. The inserted *LoxP* sites allow for later excision of *NeoR* to eliminate any confounding interference the extra 1.6 kb might have on normal *Trp53* expression and function.

1.3.2 Preparation of DTA targeting vector to capture *Trp53* promoter/intron sequence

To accurately target C3, C4 and C5 in the endogenous *Trp53* gene by homologous recombination, the *TRE-LoxP-Neo-LoxP* cassette to be inserted into the sites has to be embedded in 5 kbp of DNA sequence upstream and downstream of the desired insertion sites. This entire sequence has to be cloned into the DTA targeting vector (**Figure 1.4** shows the map of the original DTA vector).

The 5 kbp sequences upstream and downstream of C3, C4 and C5 (10 kbp in total for each) were first captured into the DTA vector. To achieve this, two 200 bp sequences homologous to each end of the 10 kbp fragments were generated by PCRs using the bacterial artificial chromosome (BAC) bMQ358 as template, which carries at least 20 kbp of sequence upstream and downstream of the *Trp53* TSS. The 200 bp sequences were then added to the DTA vector by restriction enzyme digestions and ligation of these PCR products and the original DTA vector. **Figure 1.5** shows a schematic diagram of this cloning process and the resulting DTA vectors with the added homologies.

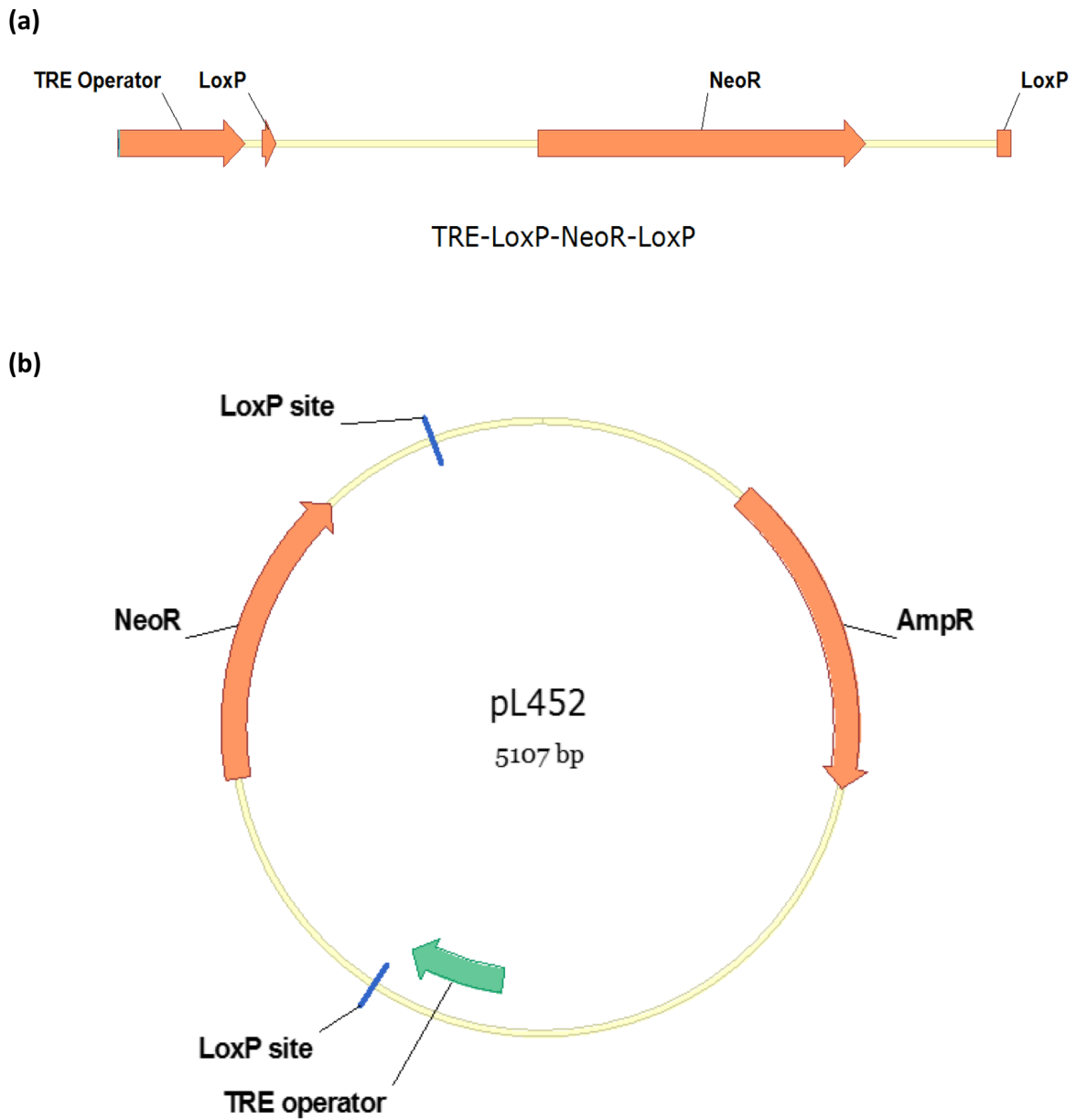


Figure 1.3. (a) A schematic diagram of the *TRE-LoxP-Neo-LoxP* cassette. (b) A map of the DNA plasmid pL452 carrying the *TRE-LoxP-Neo-LoxP* cassette. The plasmid was constructed and kindly provided by Dr. Ivonne Gamper.

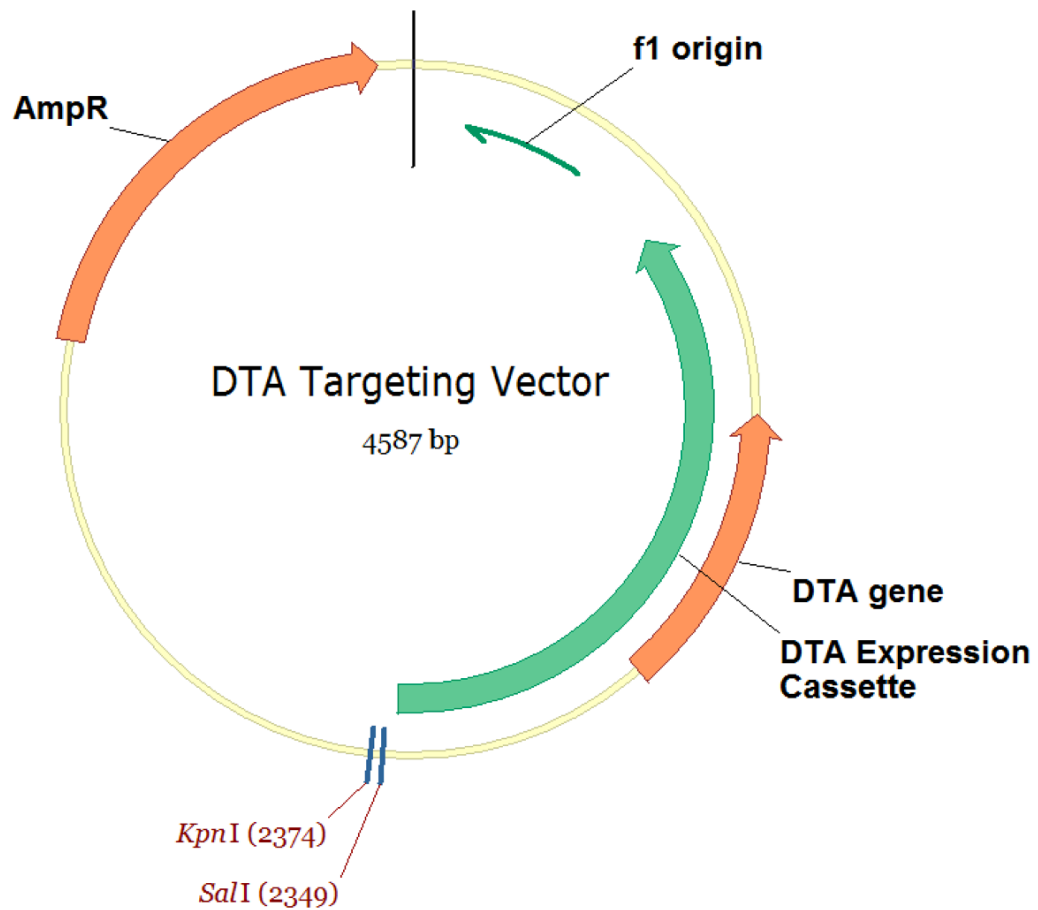


Figure 1.4. The original DTA targeting vector pBSDT-A11. The DTA vector carries the *Diphtheria Toxin A* gene (*DTA*) that encodes the cytotoxic DTA protein. This allowed negative selection of undesired incorporation of the targeting vector backbone into the genome. Restriction enzymes KpnI and SalI were used to linearise the vector for the subsequent cloning step. pBSDT-A11 was a gift from Yoh Wada (Addgene plasmid # 27179 ; <http://n2t.net/addgene:27179> ; RRID:Addgene_27179; Aoyama et al. 2005).

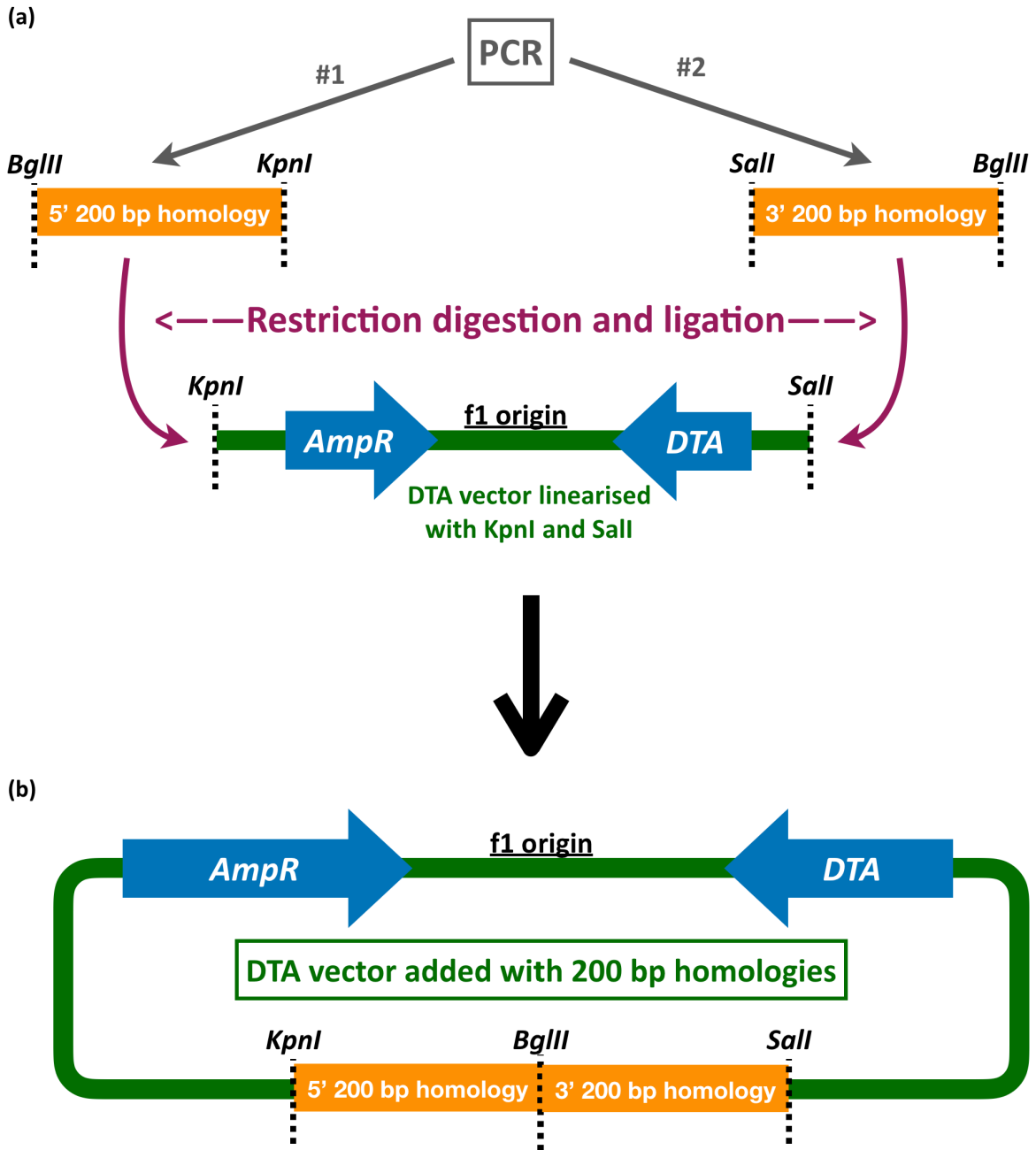


Figure 1.5. Adding the 200 bp homologies to the DTA vector by restriction digestion and ligation. (a) Amplified by PCR using the BAC bMQ358 as template, three sets of 200 bp fragments, one set for each insertion site, were generated with restriction digestion sites at the ends. The 200 bp fragments and the original DTA vector were digested by the respective restriction enzymes, ligated and then transformed into *E. coli* to form the homologies-added DTA vector (b).

1.3.3 Capturing *Trp53* promoter/intron sequence from BAC into DTA vector

The same BAC, bMQ358 was used as a source of the gene promoter and first intron sequence in the cloning process. The BAC DNA was freshly prepared from the carrier bacterial library and its integrity was verified by PCR amplification and sequencing of several short segments across the *Trp53* gene (**Figure 1.6 and data not shown**). The BAC was then transformed by electrophoration into EL350, a specific strain of *E. coli* that expresses heat-inducible recombination protein at 42°C.

The linearised DTA vectors added with the 200 bp homology ends were introduced into the pre-heated (at 42°C) BAC-carrying EL350 cells by electrophoration. Three 10 kbp-fragments carrying the promoter or first intron sequence of *Trp53* were then captured respectively into the DTA vector by recombineering in EL350 cells with the corresponding homologous sequence at the ends of the linearised DTA fragments. **Figure 1.7a** illustrates the recombineering scheme and **Figure 1.7b** is a map of the resulting DTA-10 kbp vectors formed from recombineering. Each of the 10 kbp fragments contained the corresponding *TRE* insertion site positioned in the middle of the 10 kbp sequence so that the *TRE-LoxP-Neo-LoxP* cassette, once inserted, would be flanked on each end by a 5 kbp sequence of the *Trp53* promoter and/or first intron. The three resulting targeting vectors carrying the respective 10 kbp fragments are referred as DTA3, DTA4 and DTA5, containing the *TRE* insertion sites C3, C4 and C5 respectively. The vectors were verified by diagnostic restriction digestion with *KpnI* and *Sall* (**Figure 1.8**).

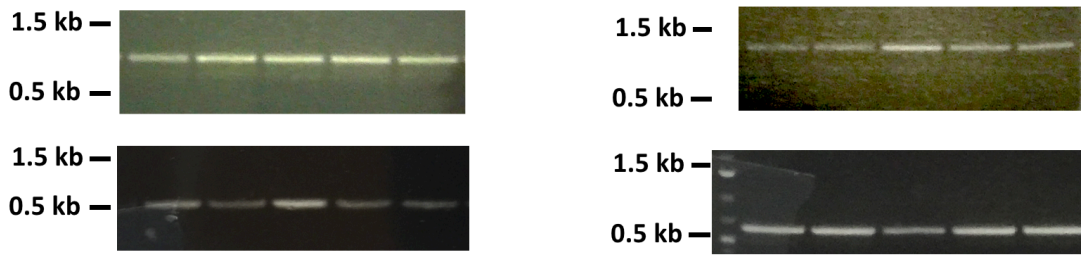


Figure 1.6. PCRs confirmed the BAC bQM368 carried the correct part of mouse chromosome 11. Five colonies were picked from a re-streak plate and four short sequences across the promoter and first intron of the *Trp53* gene were amplified by colony-PCRs to check the integrity of the sequence in the BAC. Top left: a sequence of 900 bp was amplified (-8.3 kb to -7.4 kb from TSS). Top right: a sequence of 1000 bp was amplified (-5.4 kb to -4.4 kb from TSS). Bottom left: a sequence of 500 bp was amplified (-2.5 kb to -2 kb from TSS). Bottom right: a sequence of 600 bp was amplified (+0.8 kb to +1.4 kb from TSS). Sequence of primers used are detailed in **Table M.1c** in the **Methods and Materials** chapter. GeneRuler 1 kb Plus ladder from Thermo Scientific was used in these gel electrophoresis.

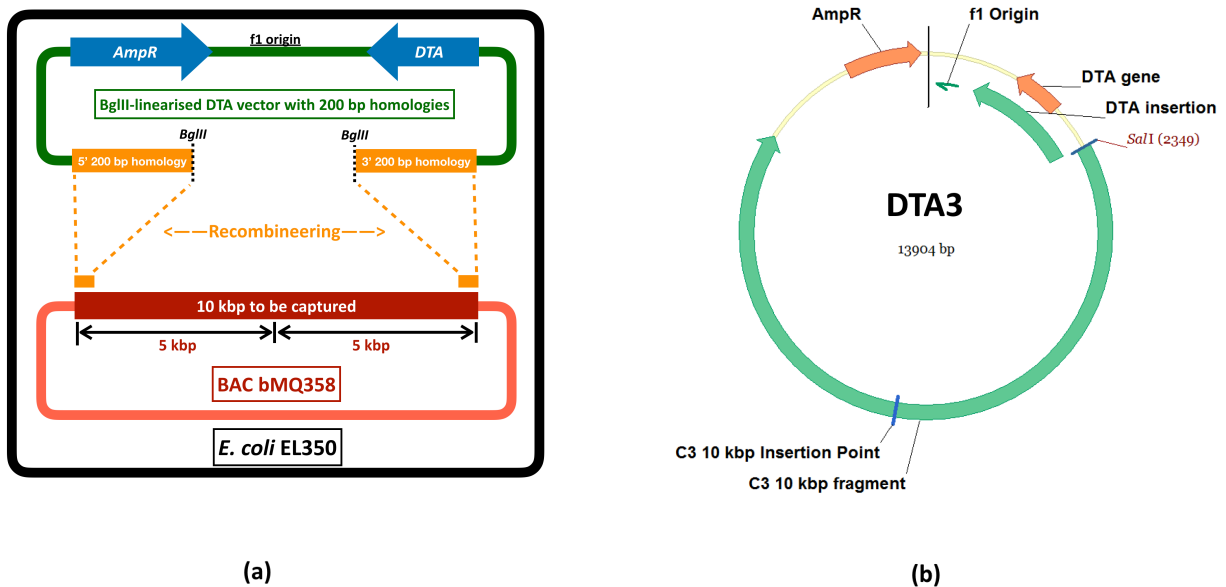


Figure 1.7. Capturing of the 10 kbp homology sequence surrounding the insertion sites into the DTA vector. (a) The 200 bp-homologies-added DTA vectors were linearised with *Bgl*III and electroporated into 42°C pre-heat-shocked EL350 cells carrying the BAC bMQ358. The 10 kbp sequences from the BAC were then captured respectively by recombineering to form the DTA-10kbp vectors DTA3, DTA4 and DTA5. (b) A map of DTA3 resulting from the recombineering process is shown as an example.

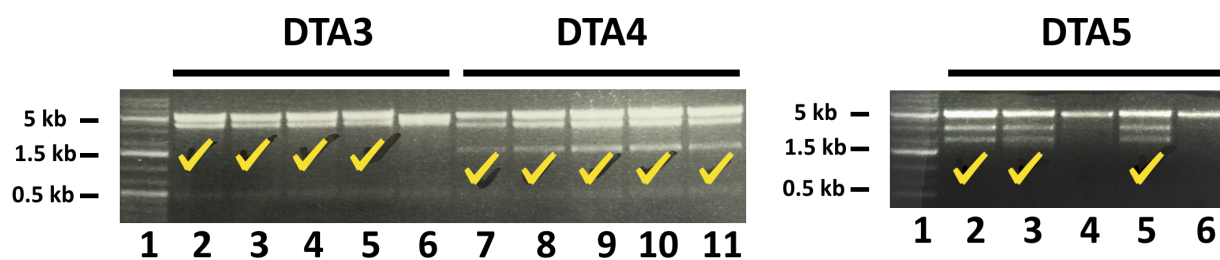


Figure 1.8. Diagnostic digestions by KpnI-HK and Sall-HF of the three targeting vectors that carried the corresponding 10 kb fragment. Five colonies were picked and cultured overnight, from which plasmids were prepared by miniprep. The plasmids were then digested by KpnI-HK and Sall-HF and the products were run on an agarose gel. The expected restriction fragments size for DTA3 are 5.3 kbp, 4.6 kbp, 3.6 kbp and 0.46 kbp; DTA4 are 5.0 kbp, 4.6 kbp, 3.2 kbp, 1.5 kbp and 0.46 kbp; DTA5 are 5.0 kbp, 4.6 kbp, 2.8 kbp, 1.9 kbp and 0.46 kbp. The lanes marked with a tick indicate clones that gave a correct digestion profile. GeneRuler 1 kb Plus ladder from Thermo Scientific was used in these electrophoresis (first lane of both panel).

1.3.4 Insertion of *TRE-LoxP-Neo-LoxP* cassette into DTA3/4/5

To introduce the *TRE-LoxP-Neo-LoxP* cassette into DTA3/4/5 vectors at the selected sites, 60 bp sequences homologous to the region adjacent to the desired *TRE* insertion sites were added to both ends of the cassette by PCR (**Figure 1.9**). The PCR products generated with each of the site-specific homologous 60 bp primers were column-purified and verified by DNA sequencing (data not shown). Then, the *TRE-LoxP-Neo-LoxP* cassettes with the homology arms for C3, C4 and C5 were introduced by electroporation into the pre-heat-shocked EL350 bacteria carrying DTA3, DTA4 and DTA5. This generated DTA-TRE3-NeoR, DTA-TRE4-NeoR and DTA-TRE5-NeoR respectively (**Figure 1.10**). Five individual colonies were selected from each transformation plate and the presence of the insertion was confirmed by PCR amplification of the junctions where the *TRE-LoxP-Neo-LoxP* sequence was inserted into the middle of the 10 kbp genomic fragments in the vectors (**Figure 1.11**). Vectors generating the correct PCR fragments were amplified, column purified and analysed by diagnostic restriction enzyme digestion (**Figure 1.12**). All the digestions generated profiles that included all the expected bands, but with the addition of one or two unexpected fragments. This suggested that the vectors prepared were probably a mixture of *TRE*-inserted and non-*TRE*-inserted vectors, possibly due to incomplete and/or non-specific recombineering in EL350 cells.

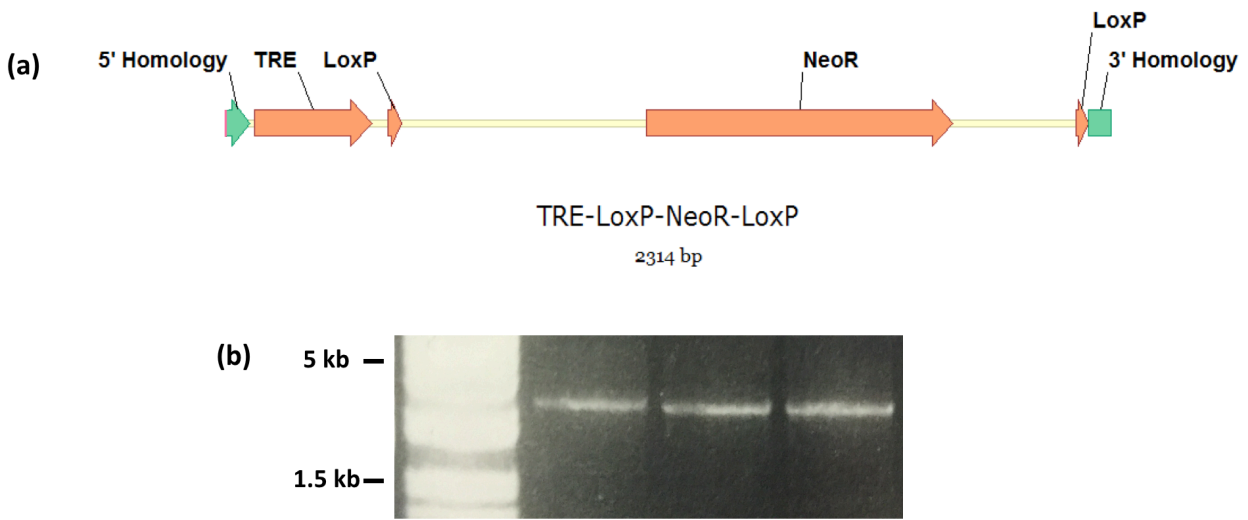


Figure 1.9. Adding homologies to both ends of the *TRE-LoxP-Neo-LoxP* cassette by PCR. (a) A schematic diagram of the 60 bp homologies-added cassette. (b) Three sets of primers were used to add the three different sets of homologies to the *TRE-LoxP-Neo-LoxP* cassettes. Sequence of primers used are detailed in **Table M.1c** in the Methods and Materials. The expected size of the amplicons were around 2.3 kbp (the size of the cassette was nearly 2.2 kb while each homologous sequence was 60 bp). From left to right: 1 Kb Plus DNA Ladder from Invitrogen, homologies-added *TRE-LoxP-Neo-LoxP* cassettes for DTA3, DTA4 and DTA5 respectively.

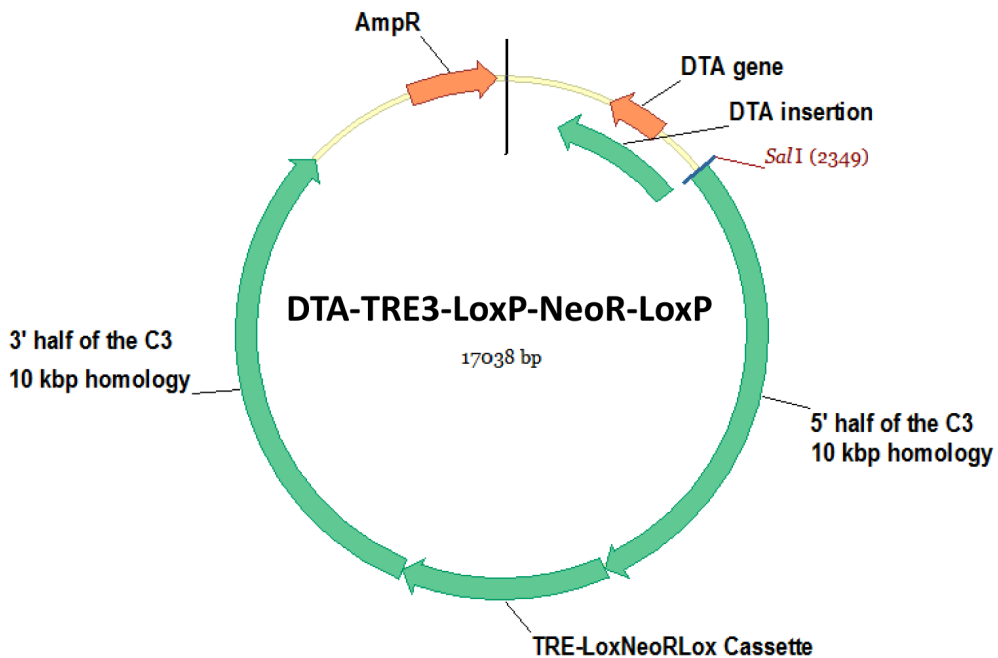


Figure 1.10. A map of the cassette-added DTA3 vector, i.e. DTA-TRE3-LoxP-NeoR-LoxP. The *TRE-LoxP-Neo-LoxP* cassette was added to the insertion points of DTA3/4/5 respectively by recombineering in EL350 cells.

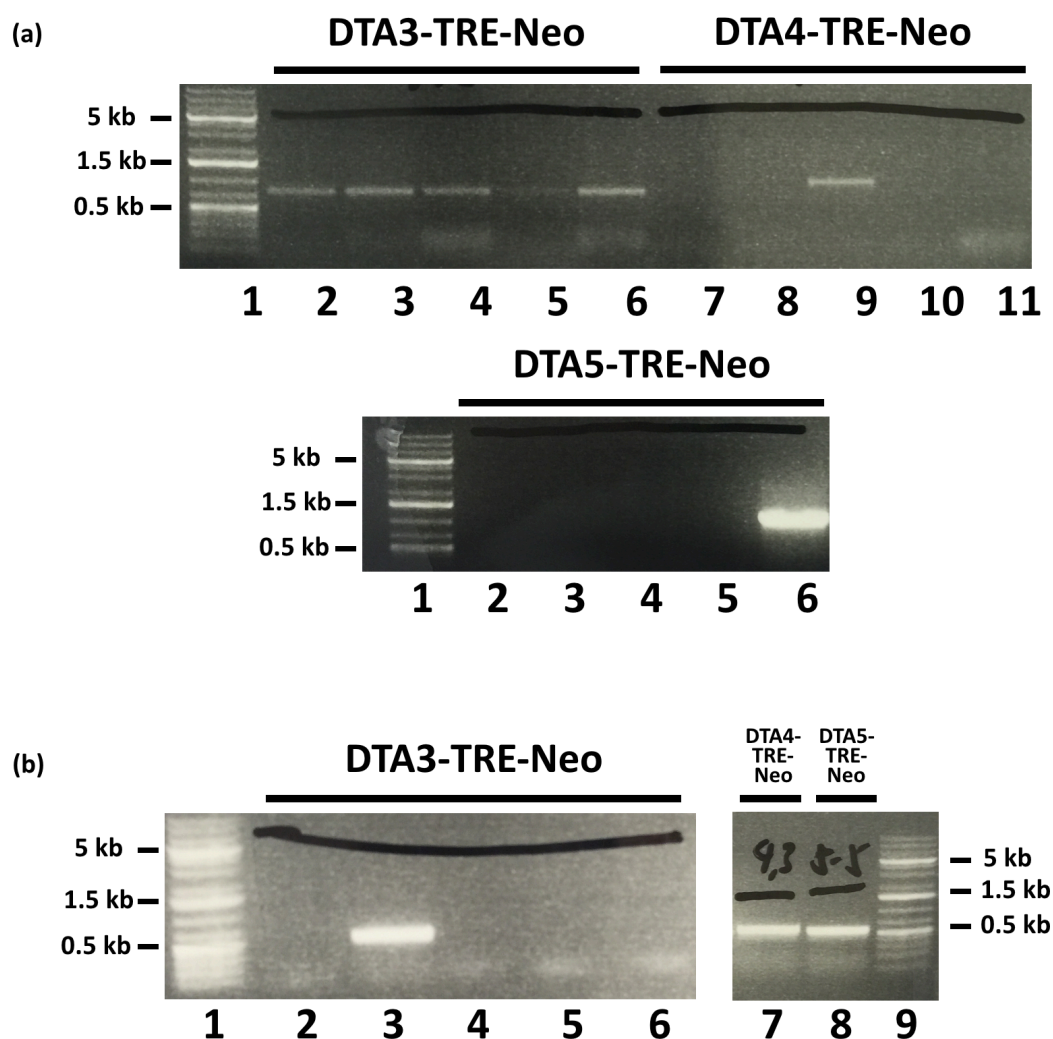


Figure 1.11. Confirmation of *TRE* insertion by PCR across the insertion junctions. Five colonies were picked from each of the transformation plates and tested with colony-PCR using construct-specific primers amplifying the junctions of the insertion. (a) PCR amplifying the 5' junction of the insertion in the plasmid. The expected amplicon sizes for DTA-TRE3-NeoR, DTA-TRE4-NeoR and DTA-TRE5-NeoR are 600 bp, 700 bp and 700 bp respectively. (b) The colonies that gave a positive result in the first PCR was then checked further with the PCR amplifying the corresponding 3' junctions. The expected amplicon sizes for DTA-TRE3-NeoR, DTA-TRE4-NeoR and DTA-TRE5-NeoR were all 500 bp. Sequence of primers used are detailed in **Table M.1c** in Methods and Materials. GeneRuler 1 kb Plus ladder from Thermo Scientific was used in all these gel electrophoreses.

	DTA-TRE3-NeoR	DTA-TRE4-NeoR	DTA-TRE5-NeoR
Restriction enzyme	EcoRI	BstXI	DrdI
Expected band sizes	7.1 kbp 4.6 kbp 2.1 kbp 1.7 kbp 0.6 kbp	7.6 kbp 3.4 kbp 3.0 kbp 2.0 kbp 1.0 kbp	5.4 kbp 3.9 kbp 2.9 kbp 1.9 kbp 1.6 kbp 1.4 kbp

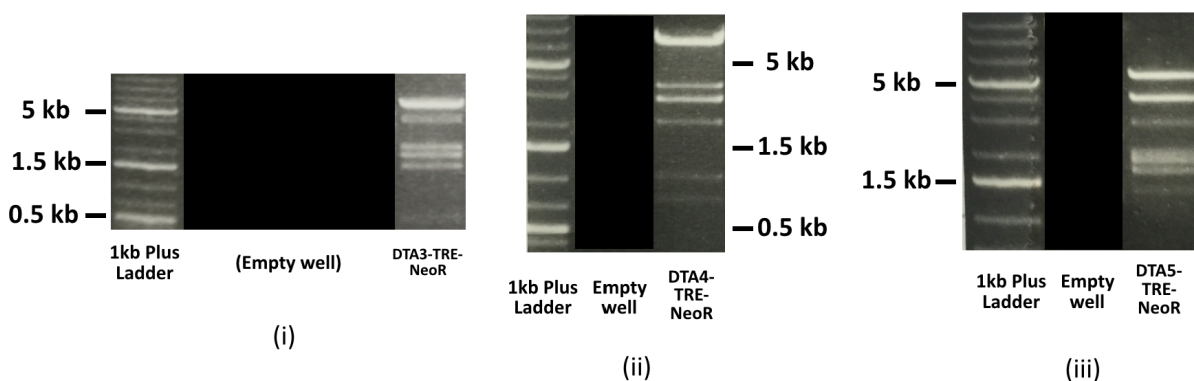


Figure 1.12. First round of *TRE-LoxP-Neo-LoxP* cassette recombineering didn't yield the expected DTA-TRE3/4/5-NeoR constructs. Top panel: A table summarising the enzymes used in the diagnostic digestions and the expected results. Bottom: Images of digestion reactions after electrophoresis by agarose gel. (i) The digestion of DTA-TRE3-NeoR gave two unexpected bands with a size of 5 kbp and 2.5 kbp respectively. (ii) A digestion profile with an unexpected band sized around 700 bp was observed for DTA-TRE4-NeoR. (iii) An unexpected band sized around 2 kb was observed for digestion of DTA-TRE5-NeoR. GeneRuler 1 kb Plus ladder from Thermo Scientific was used in all these gel electrophoreses.

1.3.5 Isolation of DTA-TRE3/4/5-NeoR vectors

Based on the hypothesis that the prepared vectors were a mixture of *TRE* cassette-inserted and non-inserted vectors, several approaches were used to isolate the DTA-TRE3/4/5-NeoR vectors. First, competent *E. coli* were transformed with the mixed DTA plasmids (with and without *TRE*) and plasmid DNAs were prepared from the picked colonies. However, subsequent screening revealed that all individual clones selected still retained a mixture of plasmids (results not shown). It is possible that the mixed plasmids were supercoiled together and therefore not taken up separately into cells. Second, the mixed products were digested with two different restriction enzymes, both of which only cut at a single site, and the fragment carrying the *TRE-LoxP-NeoR-LoxP* cassette purified and ligated with the DTA3/4/5 plasmids cut with the same restriction enzymes. The products of these ligations were then transformed into competent *E. coli*. However, no colonies were observed, possibly due to a failed ligation as a result of insufficient *TRE-LoxP-NeoR-LoxP*-carrying DNA fragment (results not shown). Third, Gibson Assembly of PCR products was attempted (Gibson et al. 2009). Using the mixed products as templates, the two halves of the *TRE-LoxP-NeoR-LoxP* cassette were amplified along with the respective adjacent sequences of the *Trp53* gene (up to 2.5 kb). Each half of the *TRE-LoxP-NeoR-LoxP* cassette carried half of the *NeoR* gene, with 30 bp of overlapping sequence at that end of the fragment, which was required for Gibson Assembly. Sequences identical to the ends of the cut empty DTA vector backbone were introduced by PCR to the other end of the fragments respectively. Gibson Assembly was then used to assemble the three fragments into complete DTA-TRE3/4/5-NeoR constructs. However, following transformation of *E. coli*, selection with ampicillin and neomycin yielded no colonies. This failure was likely due to the low efficiency of Gibson Assembly for large plasmids (12 kb in this case). A final attempt to isolate pure *TRE*-containing plasmids was to digest the mixed plasmids with a restriction enzyme that cut at multiple sites, ligate all the cut fragments, and transform the ligated products directly into competent *E. coli*. The rationale for this approach was to free any supercoiled DTA3/4/5-TRE-

NeoR and non-*TRE*-inserted vectors by cutting them into specific fragments, which would then be ligated into separate plasmids and taken up individually by bacteria. All DTA-TRE3/4/5-NeoR vectors were successfully isolated with this approach, as indicated by the diagnostic digestion with the corresponding restriction enzymes (**Figure 1.13**). The verified DTA-TRE3/4/5-NeoR vectors were then used to target the endogenous *Trp53* gene in mESC as described below.

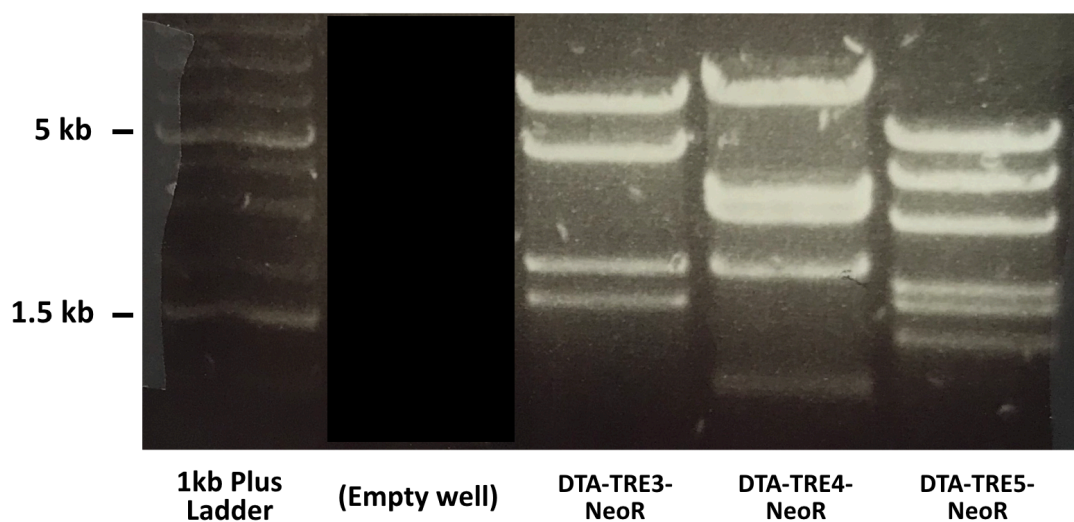


Figure 1.13. The final approach to separate the correctly targeted DTA-TRE constructs from the mixture was successful. The constructs were verified by digestion with corresponding restriction enzymes. DTA-TRE3-NeoR, DTA-TRE4-NeoR and DTA-TRE5-NeoR were digested by *EcoRI*, *BstXI* and *DrdI* respectively. The lane between DTA-TRE3-NeoR and ladder was not shown as it was irrelevant. The expected band sizes are listed in the table in **Figure 1.12**. GeneRuler 1 kb Plus ladder from Thermo Scientific was used as size marker.

1.4 Targeting *Trp53* gene in mESC

To insert the *TRE* element into the desired locations in the endogenous mouse *Trp53* locus, two different targeting approaches were used - the CRISPR/Cas9 gene editing system and the mESC homologous recombination targeting method. CRISPR/Cas9 gene editing has been shown to be highly efficient in modifying the mouse genome, especially when deleting or truncating target genes. In addition, it can be used directly on early stage embryos (e.g. single-cell stage) without having to first target and select the embryonic stem cells. I attempted to insert the *TRE* using the CRISPR/Cas9 system but no successfully targeted pups were generated after multiple attempts. I then tried the second approach of mESC homologous recombination. The E14 line of mESC, kindly provided by Ken Jones from the Cambridge Stem Cell Institute, was cultured in 2i/LIF medium with the established conditions and procedures (Silva et al. 2008) detailed in the **Methods and Materials** chapter. The three DTA-TRE3/4/5-NeoR vectors were linearised using the restriction enzyme *Sall* and introduced into cultured mESC by electroporation. These mESC were then subject to neomycin selection for the stable expression of *NeoR* from the cassette, which supposedly indicated integration of the whole cassette into the genome. 96 Neo-resistant clones were picked for each insertion site, expanded and screened for correct insertion of the cassette by Southern blots, as detailed below.

Correct insertions of the cassette were verified by Southern blotting rather than PCR analysis (because the latter can only confirm the presence of the *TRE-LoxP-NeoR-LoxP* cassette in the genome but not the insertion location, nor the orientation of the insertion). The cassette embedded in the 10 kbp homology region could be integrated randomly at undesired positions in the genome, disrupting gene functions at those loci, information about which a PCR analysis would not provide.

Two DNA probes (7.8 and 3.3, sequence shown in **Methods and Materials**), each approximately 300 - 500 bp, were designed to anneal to within 5 kbp of 5' and 3' sides of the insertion sites respectively. Annealing of these two probes to restriction enzyme-digested

genomic DNA (gDNA) from targeted mESC clones would indicate whether the *TRE-Lox-NeoR-Lox* cassette (embedded in the 10 kbp homology) had been integrated correctly into the desired positions. To digest the gDNA, two restriction enzymes were used - one cutting outside of the 5 kbp homology on one side while the other inside the 5 kbp homology at the other side proximal to the insertion of the cassette. In the cases of the 3' Southern of C4 and C5, XbaI cuts in the *TRE-LoxP-NeoR-LoxP* cassette in addition to cutting inside the 5 kbp homology. As such, a digestion fragment of the expected size would result only from the correct incorporation of the *TRE-LoxP-NeoR-LoxP*-embedded 10 kbp homologies into the desired loci of the genome where the correct restriction digestion sites were present. **Figure 1.14** illustrates the design of the Southern blots while **Table 1.2** gives details of the probes, restriction enzyme cutting sites and the expected results of correct insertion.

gDNA of Neo-resistant mESC clones (96 each for C3, C4 and C5) was prepared from the cells, restriction digested (**Table 1.2**) and then fractionated by electrophoresis. **Figure 1.15** shows the restriction digestion of the C4-targeted clones by EcoRV and HindIII. Presence of a smear instead of visibly discrete bands indicated the gDNA was completely digested. The digested gDNA on the gels were then transferred to Hybond C membranes and incubated with the radioactively labelled probes. The target fragments hybridised with the probes were visualised on X-ray films (**Figure 1.16**). Positive mESC clones (**Figure 1.16, coloured boxes**), hereafter referred to as *Trp53^{TRE3/4/5-NeoR}*, were thawed and expanded in tissue culture for further analyses (see below). Note that some positive clones displayed significantly different band intensities in comparison with the wild type band, suggesting an increased copy number of the targeted allele or a mosaic of targeted and non-targeted cells in the picked colonies. These clones were not selected.

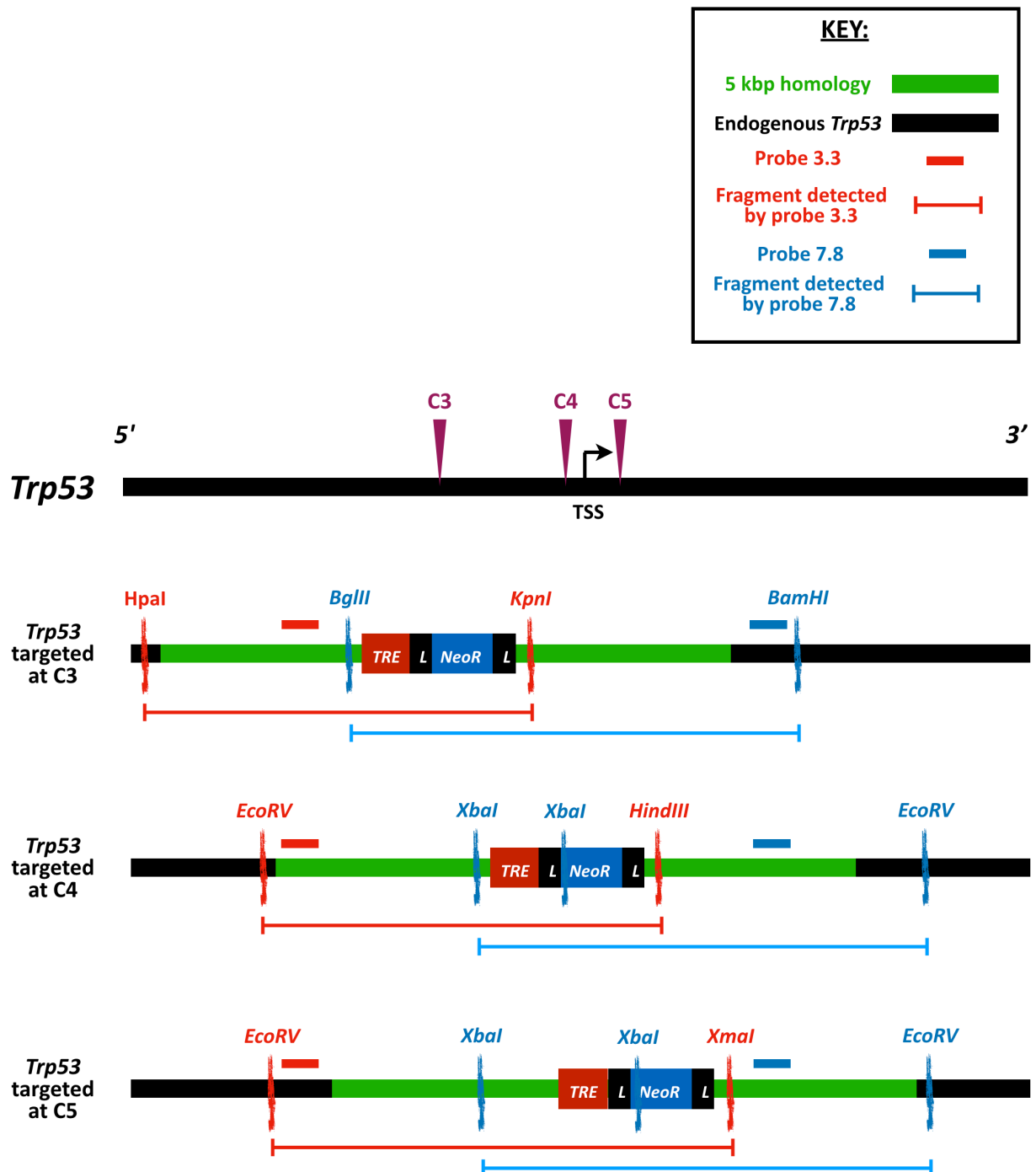


Figure 1.14. Southern blots were designed to assess whether the endogenous *Trp53* allele was correctly targeted with the DTA-TRE3/4/5-NeoR cassettes at the desired sites respectively. Labels: TSS: *Trp53* transcription start site; Green line: 5 kbps homologies; black line: *Trp53*/adjacent genomic sequence; red short line: probe 3.3; blue short line: probe 7.8; : fragment resulting from the restriction digestion detectable by probe 3.3; : fragment resulting from the restriction digestion detectable by probe 7.8; C3, C4, C5: corresponding TRE insertion sites.

	Southern on the 5' side			Southern on the 3' side		
Insertion site	C3	C4	C5	C3	C4	C5
Probe	3.3			7.8		
Restriction Enzyme	HpaI, KpnI	EcoRV, HindIII	EcoRV, XmaI	BglII, BamHI	XbaI, EcoRV	XbaI, EcoRV
Cutting sites	1. 5' of 5 kbp homology 2. 3' of inserted cassette	1. 5' of 5 kbp homology 2. 3' of inserted cassette	1. 5' of 5 kbp homology 2. 3' of inserted cassette	1. 5' of inserted cassette 2. 3' of 5 kbp homology	1. 5' of inserted cassette 2. 3' of 5 kbp homology 3. inside cassette	1. 5' of inserted cassette 2. 3' of 5 kbp homology 3. inside cassette
Detectable +ve band	8.4 kbp	7.5 kbp	8.4 kbp	8.2 kbp	7.0 kbp	6.6 kbp
Detectable -ve band	6.3 kbp	5.4 kbp	6.3 kbp	6.1 kbp	8.8 kbp	8.8 kbp

Table 1.2. Details of the Southern blots - probes, restriction digestions and expected results.

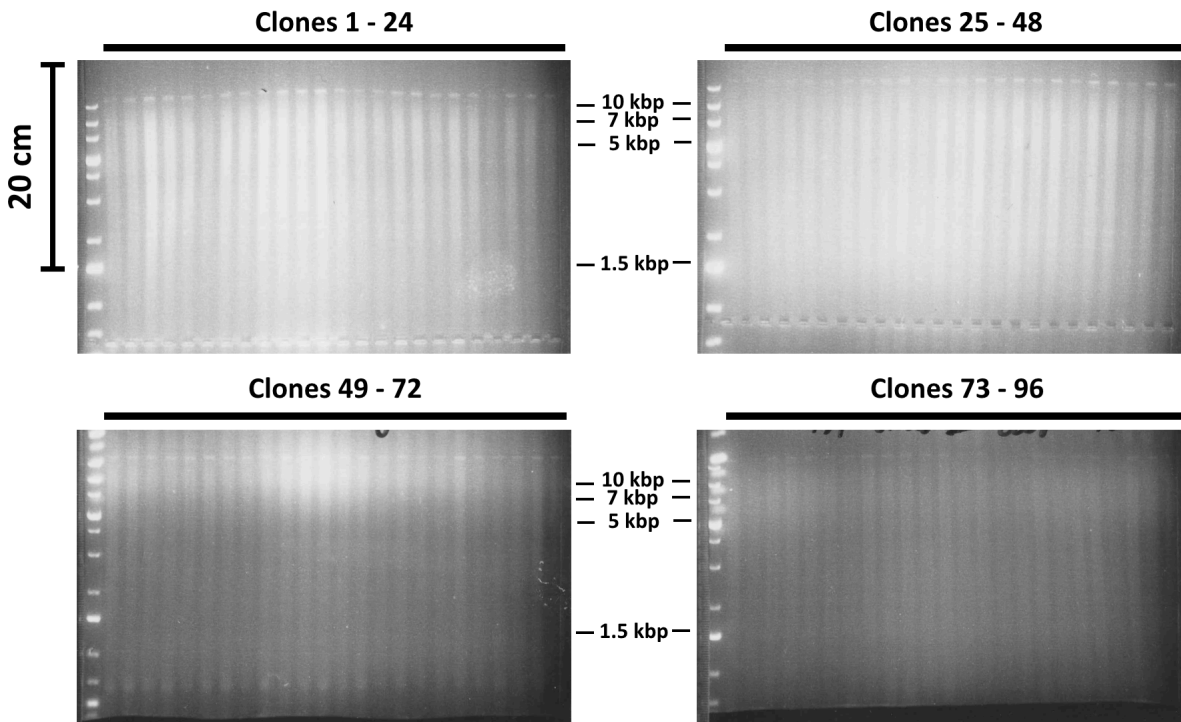


Figure 1.15. Agarose gel of separated gDNA of the picked Neo-resistant C4-targeted mESC clones digested by EcoRV and HindIII. GeneRuler 1 kb Plus ladder from Thermo Scientific was loaded to the first lane from the left as a size marker.

1.5 Analyses of positional effect of *TRE* insertion

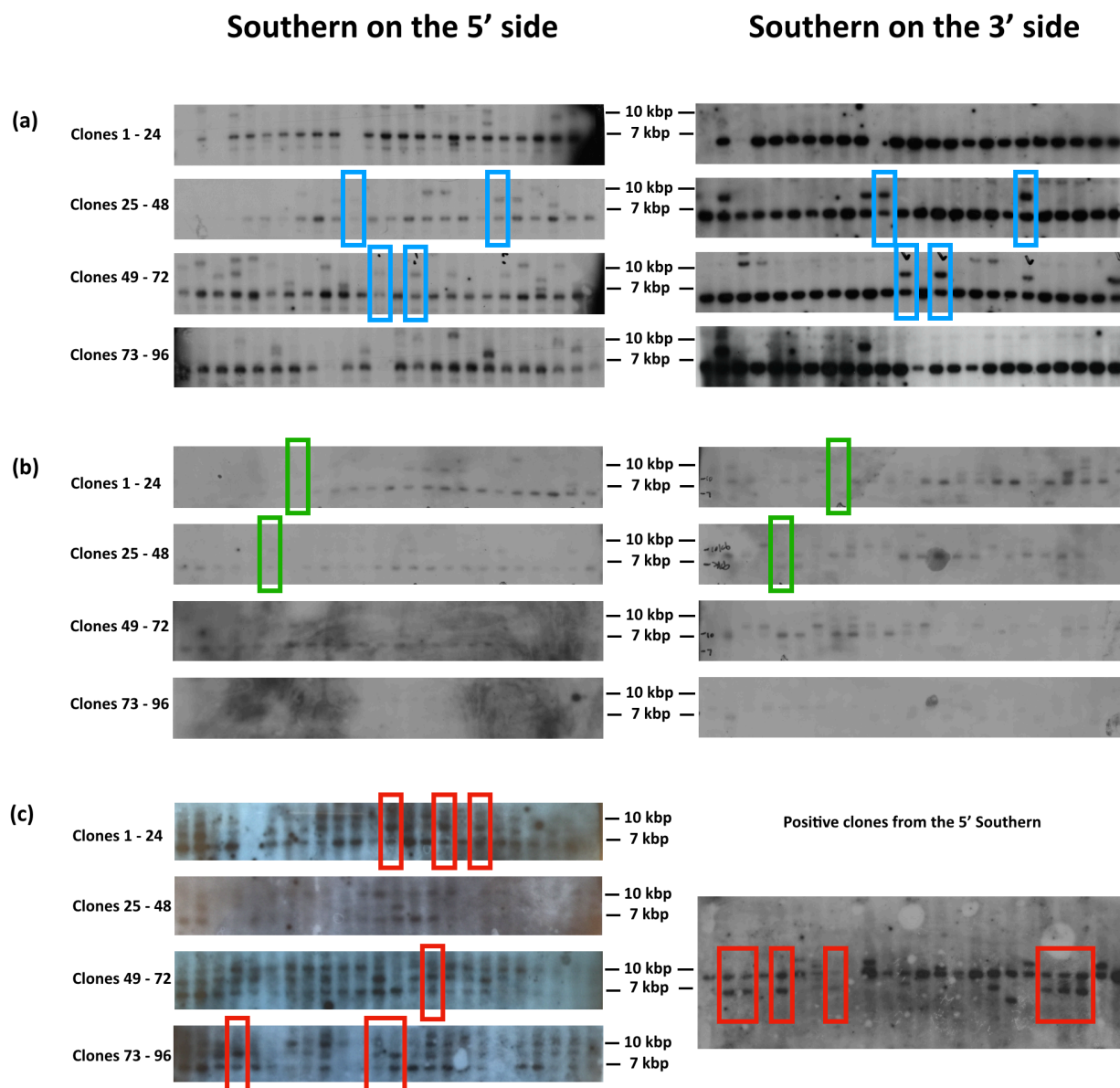


Figure 1.16. Southern blots of correspondingly digested gDNA of the picked Neo-resistant mESC clones targeted at (a) C3, (b) C4 and (c) C5. Digested gDNA of each clone was loaded onto one lane of the agarose gel in each Southern blot. Details of the digestions, probes used and expected target fragment sizes are outlined in **Table 1.2**. Southern blots of both sides were run for all 96 of the C3- and C4-targeted clones, while for the C5-targeted clones the 3' Southern blot was only run on the ones that were positive in the 5' Southern blot. Blue (C3-targeted), green (C4-targeted) and red (C5-targeted) boxes indicate the clones that gave positive results in both Southern blots.

To determine which of the *TRE* insertion sites allow for the most efficient and tight repression of *Trp53* by the system yet with a minimal impact on normal *Trp53* expression in the absence of rtTS repressor activity, representative targeted mESC clones verified by the Southern

blots were expanded in culture and had the *TRE* repression system implemented by addition of an rtTS-expressing gene into the mESC genome. Prior to addition of the rtTS-expressing gene, each expanded clone was transiently infected by Lipofectamine with the DNA plasmid pCAG-Cre (a gift from Connie Cepko; Addgene plasmid #13775; <http://n2t.net/addgene:13775>; RRID:Addgene_13775; (Matsuda & Cepko 2007)), which drives constitutive expression of Cre recombinase activity inside the cells. This efficiently excised the *NeoR* sequence (flanked by the *loxP* sites) previously used for selecting the targeted mESC. The infected cells were sparsely plated on a dish until discrete embryoid bodies (a three-dimension aggregates of cells arisen from a single cell; here referred to as colonies) were evident. Twelve such colonies were selected, expanded and excision of the *NeoR* sequence confirmed by PCR. **Figure 1.17** shows the result of the PCRs; the decrease in band size indicates successful Cre-removal of the *NeoR* sequence. The three targeted *Trp53* alleles with *NeoR* removed were henceforth denoted *Trp53^{TRE3/4/5}* respectively. Successful removal of *NeoR* demonstrated the removability of *NeoR* from the cassette, a prerequisite for utilisation of the system for experiments *in vitro* and *in vivo*. Next, the *Trp53^{TRE3/4/5}* clones were transfected with the linearised DNA plasmid pPCAGIPCAG that expresses the rtTS repressor from a constitutive *CAG* promoter (*CAG-rtTS^{tg}*) and resistance to puromycin (pPCAGIPCAG was kindly provided by Ken Jones from Cambridge Stem Cell Institute). Cells with stable expression of rtTS resulting from successful integration of *CAG-rtTS^{tg}* into the mESC genome were selected in the presence of puromycin. These cells harboured a single copy of the *Trp53^{TRE3/4/5}* allele and multiple copies of the *CAG-rtTS^{tg}* transgene.

Any positional effect of the *TRE* insertions on normal expression of *Trp53* and efficiency

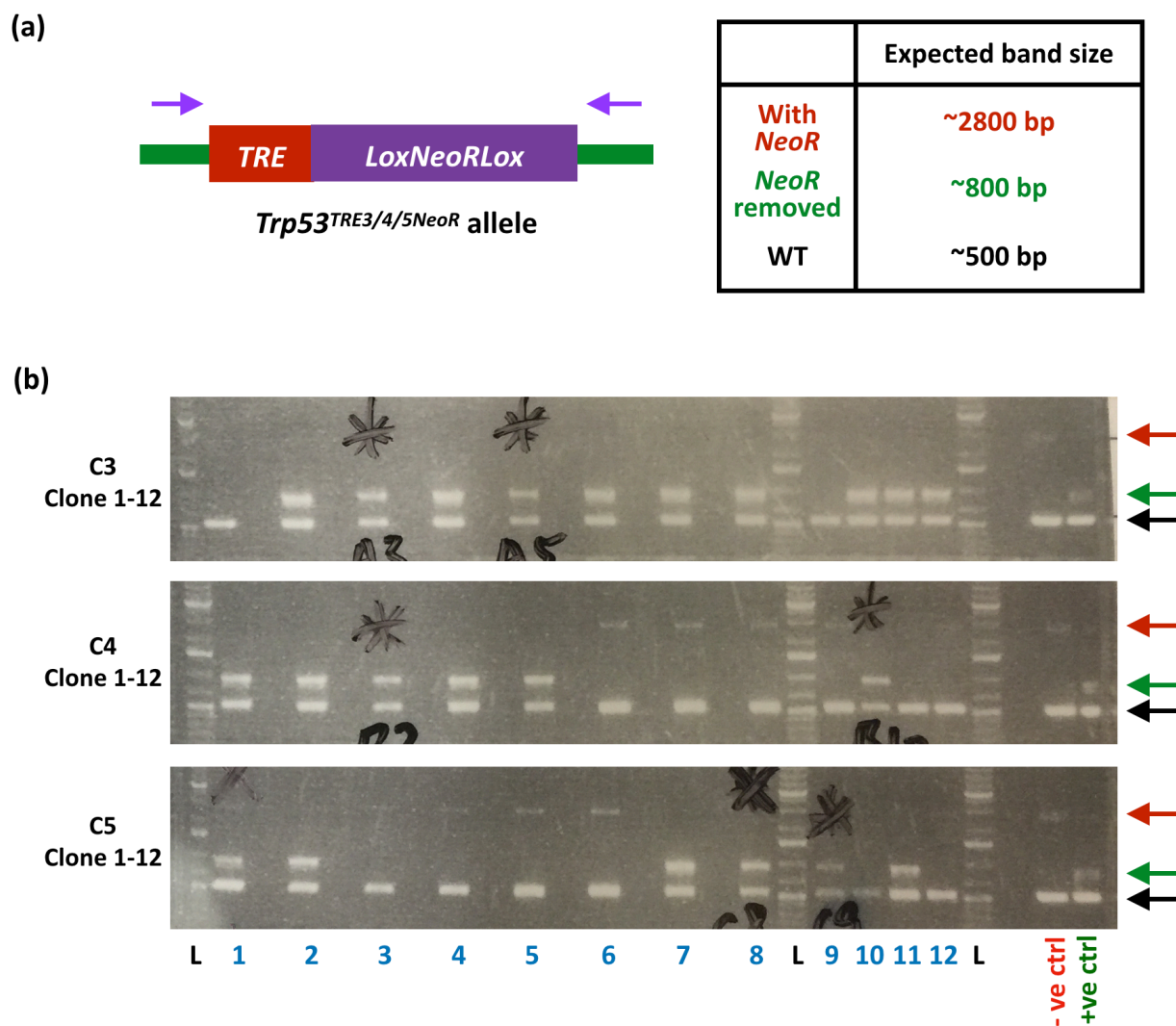


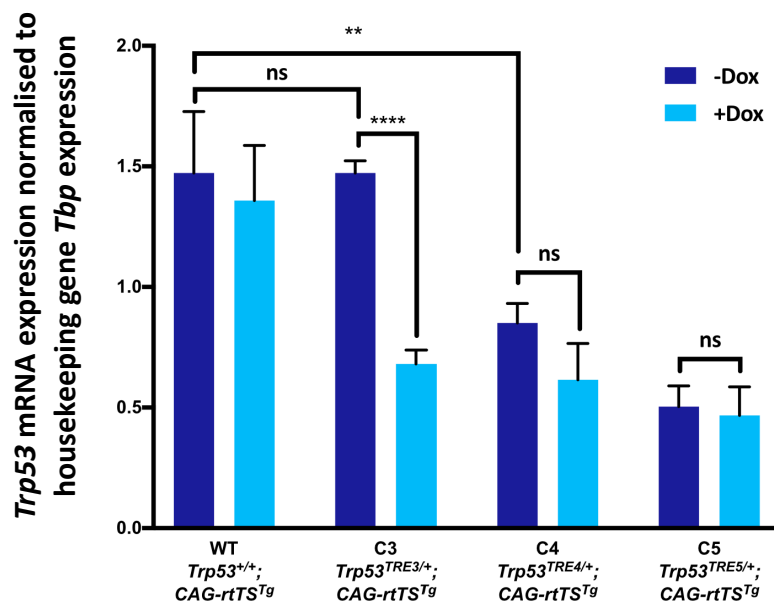
Figure 1.17. Genotyping PCRs to verify removal of *NeoR* by Cre from the inserted cassettes in targeted mESCs. (a) Left: schematic diagram of the cassette inserted in *Trp53*. Primers (the pair of purple arrows) annealing to the sequence just outside the inserted cassettes were used to assess the removal of *NeoR* by Cre from the transient infection of pCAGIPCAG. Right: a summary of the size of expected PCR products. (b) The products of the PCRs on the gDNA of the 12 picked clones of each insertion sites were separated by gel electrophoresis. Red arrow: position of band with *NeoR*; green arrow: position of band that had *NeoR* removed; black arrow: position of WT band. Negative control: PCR on plasmid carrying the full cassette inserted in WT sequence (plus one with WT sequence). Positive: PCR on plasmid carrying the *NeoR*-removed cassette embedded in WT sequence (plus one with WT sequence). GeneRuler 1 kb Plus ladder from Thermo Scientific was used in these gel electrophoresis. Sequence of primers used are detailed in **Table M.1c** in Methods and Materials.

of the repression system was assessed by determining the expression of *Trp53* RNA in the

absence and presence of doxycycline (Dox) in the re-constituted mESC (**Figure 1.18**). Cells were seeded, cultured for 24 hours and then treated with Dox at 1000 $\mu\text{g}/\text{mL}$ for 48 hours. This concentration of Dox was found to give the maximum response *in vitro* and was used for all *in vitro* experiments in this thesis (Gamper et al. 2017). mRNA was prepared by Trizol extraction and complementary DNA (cDNA) synthesised by reverse transcription. Quantitative PCR (qPCR) was used to quantify *Trp53* mRNA levels with *Tbp* (TATA box binding protein) mRNA as reference. Unless otherwise specified, mRNA from *in vitro* experiments was prepared and quantified as such. The results of the qPCR of this experiment are plotted in **Figure 1.18a**. Comparing WT with the three *TRE*-targeted lines of mESC in the absence of Dox, it is clear that *TRE* insertion at C4 and C5 significantly affects *Trp53* mRNA expression ($p = 0.0035$ and < 0.0001 , respectively) and addition of Dox fails to reduce expression further. This is most probably due to the proximity of the *TRE* insertion to the *Trp53* TSS in C4 and C5, such that it disrupts the recruitment of core transcriptional factors. It is also possible that the computational analyses I undertook in **Section 1.2** failed to provide a comprehensive list of all local *cis*-elements necessary for *Trp53* expression. By contrast, normal *Trp53* mRNA expression appeared unaffected by *TRE* insertion at the C3 position in the absence of Dox ($p > 0.9999$), and this was reduced by about 50% within 48 hours of Dox addition. As these cells harbour only a single copy of the *TRE*-modified p53 locus – the other being *WT* - this is consistent with complete repression of the single *TRE*-targeted *Trp53* allele. This is, of course, assuming there is no negative impact on expression from the WT *Trp53* allele, which is suggested by the lack of impact of rtTS (with Dox) in WT mESC with no *TRE* insertion (**Figure 1.18a**). **Figure 1.18b** shows that the *CAG-rtTS^{Tg}* transgene expresses the *rtTS* mRNA regardless of whether or not Dox is present. Also, while the mRNA level expressed did vary across the various cell lines, this did not appear to affect the functionality of the repression system. Hence, in conclusion, these data indicate that *TRE* targeted at C3 has minimal impact on the normal expression of *Trp53* mRNA

but confers effective repressibility of *Trp53* expression in the presence of both rtTS expression and Dox.

(a) Positional effect of *TRE* insertion on endogenous *Trp53* mRNA expression and Dox-regulated repression in mESC



(b) *rtTS* expression in WT and reconstituted *TRE*-targeted mESC

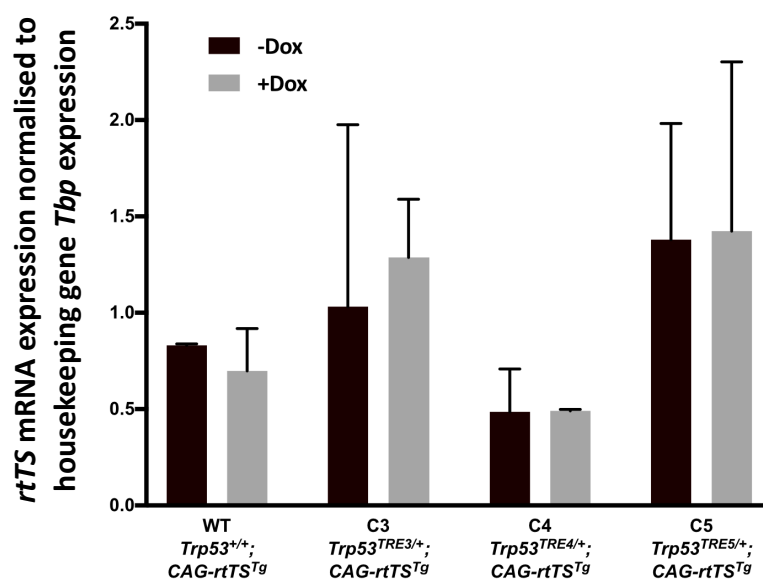


Figure 1.18. (a) *TRE* insertion at C4 and C5 hampered normal *Trp53* expression. (b) Dox-independent *rtTS* expression from the transgene. Pairs of primers specific to *Trp53*, *rtTS* and *Tbp* mRNA were used in the qPCR analysis. Plotted were the mean values of samples from cells of 3 or 4 different passages and the error bars denote the respective standard deviations. The *p*-values indicated are results of a Two-way ANOVA test (a). Primers used here are listed in Table M.6b in the Methods and Materials chapter).

Next, I determined whether p53 protein expression followed that of *Trp53* mRNA expression in the C3 targeted mESC cells. Protein lysates were prepared from cells treated as described above and analysed by western immunoblotting with anti-p53 antibody (**Figure 1.19**). Indeed, the p53 protein level was significantly reduced after 48 hours of Dox treatment in *Trp53^{TRE3/+};CAG-rtTS^{Tg}* cells, with the residual expression again attributed to the WT allele. By contrast, p53 protein levels were unchanged in WT cells whether Dox was present or not. This is consistent with the *TRE* repression system implemented at C3 effectively regulating *Trp53* at the transcriptional level effectively leading to a rapid consequential effect on p53 protein level with a rapid 48-hour time frame.

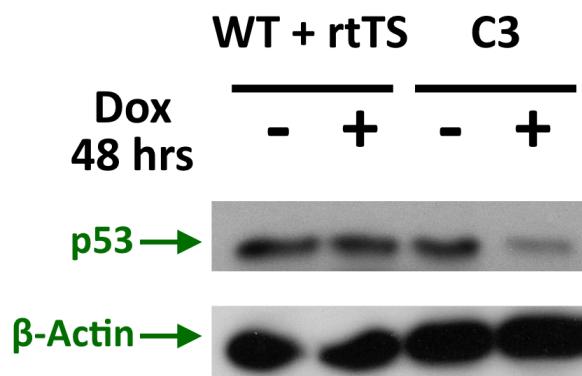


Figure 1.19. A western blot showing p53 protein level from WT mESCs expressing rtTS and the reconstituted targeted mESCs with or without Dox treatment (48 hours). 12 µg of proteins were loaded per lane and separated on the 12% acrylamine gel. p53 was detected with the primary antibody 1C12 while β-Actin with AC15 (details of antibodies are described in **Section M.6** in the **Methods and Materials** chapter).

Finally, I assessed whether regulation of *Trp53* mRNA and protein expression following DNA damage are compromised by the *TRE* insertion at C3. C3-targeted and WT mESC cells harbouring *CAG-rtTS^{Tg}* were cultured with or without Dox for 48 hrs and then exposed to the DNA damage-inducing agent doxorubicin for 8 hours (Doxo; concentration used = 1 µg/mL, (Cho et al. 2012)). mRNA was harvested from these cells and the relative *Trp53* mRNA level was determined by qPCR (**Figure 1.20**). In both WT and C3-targeted cells, levels of *Trp53* mRNA expression were not measurably altered by Doxo treatment. Importantly, in the presence of Dox the *TRE* repression system was equally efficient in repressing *Trp53* mRNA expression with or without DNA damage. Consistent with the notion of DNA damage inducing p53 protein stabilisation, both WT and C3-targeted mESC demonstrated a significant increase in p53 protein level in response to Doxo-induced DNA damage (**Figure 1.21**). However, this increase was significantly repressed in C3-targeted cells in the presence of Dox, consistent with the repression of *Trp53* mRNA under the same condition (**Figure 1.20**). In conclusion, the *TRE* insertion at position C3 in the presence of rtTS and Dox mediates effective repression of both *Trp53* mRNA and p53 protein expression even in the presence of DNA damage.

The above series of experiments clearly demonstrated that, at least in mESC, *TRE* insertion at certain locations (C4 and C5) in the endogenous *Trp53* gene has a significant negative impact on both normal *Trp53* expression and capacity for Dox-dependent repression of *Trp53* expression. However, insertion of *TRE* at C3 allows for wild type expression of *Trp53* mRNA and protein under physiological conditions and for Dox-dependent repression of both *Trp53* mRNA and protein, even when subjected to the potent pro-stabilising actions of DNA damage. Accordingly, *TRE* insertion at C3 was chosen for all subsequent *in vivo* experiments.

Repression of *Trp53* mRNA expression by Dox upon DNA damage in mESCs

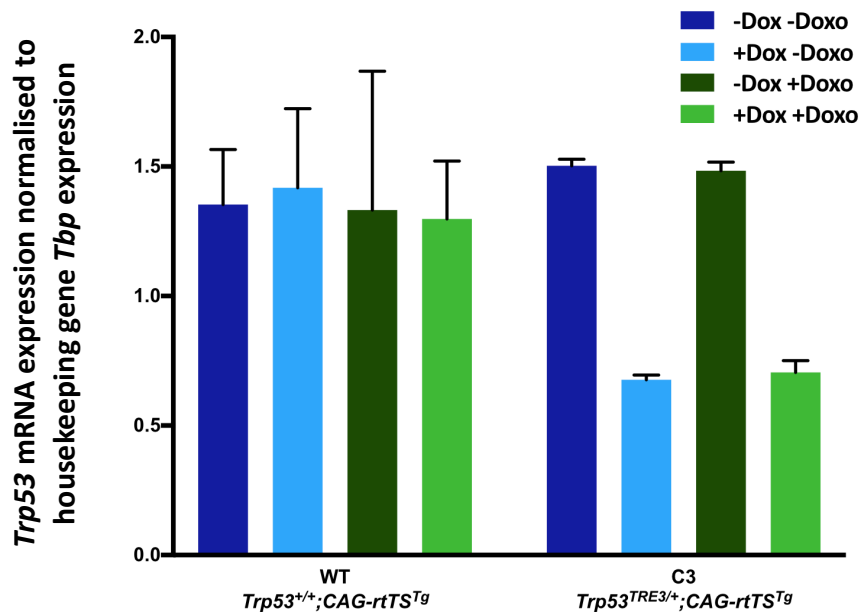


Figure 1.20. The *TRE* repression system represses *Trp53* mRNA expression in the presence of DNA damage inflicted by doxorubicin treatment. Pairs of primers specific to *Trp53*, *rtTS* and *Tbp* mRNA were used in the qPCR analysis and their details are listed in **Table M.6b** in the **Methods and Materials** chapter). Plotted are the mean values of samples from cells of 2 different passages and the error bars denote the respective standard deviations.

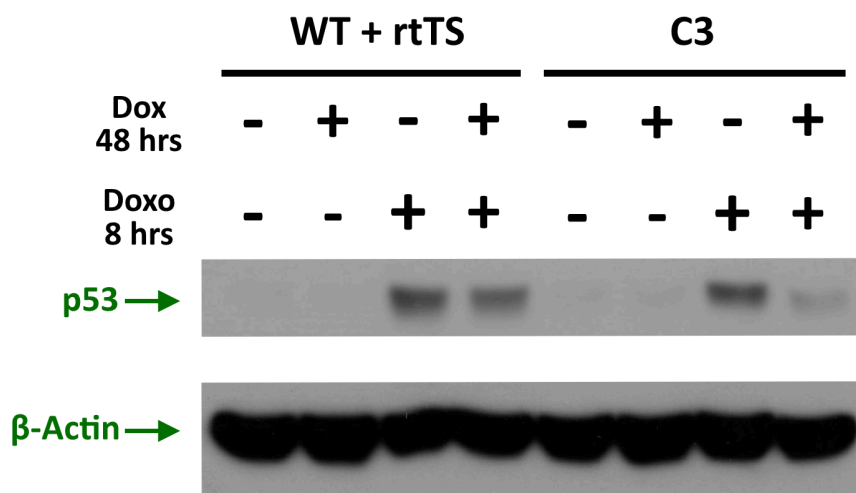


Figure 1.21. A western blot showing p53 protein level from wild type mESCs expressing *rtTS* and the reconstituted C3-targeted mESCs in combinations of Dox and Doxo treatment. 12 μ g of protein was loaded per lane and separated on a 12% acrylamine gel. p53 was detected with the primary antibody 1C12 while β -Actin with AC15 (details of antibodies described in **Section M.6** in **Methods and Materials**).

1.6 Generation of TRE-p53 animals

Trp53^{TRE3-Neor/+} mESC were injected into mouse blastocysts by the Transgenic Unit of the Cambridge Stem Cell Institute. The injected blastocysts were then implanted into surrogate mothers to produce F0 animals - chimaeric mice comprising mixtures of WT cells from the recipient blastocyst and injected *Trp53^{TRE3-Neor/+}* mESC. Germline transmission of the *Trp53^{TRE3-Neor/+}* allele requires at least one of the *Trp53^{TRE3-Neor/+}* mESC to contribute to the resultant embryo's germ cells, an eventuality assessed by examination of the resulting progeny. Male chimaeric mice (not female mice because the mESC used were generated from a male embryo) with a predominantly E14 mouse chinchilla coat colour were mated with black coat colour C57/Bl6 female mice. Production of F1 mice of chinchilla coat colour indicates germline-transmission of the chimaera and of these F1 mice 50% should inherit the *Trp53^{TRE3-Neor}* allele.

Although several F0 male chimaeras were produced, unfortunately none of them was germline-transmitted. The reason for this is unclear. While it is formally possible that the *TRE-LoxP-Neor-LoxP* cassette insertion in one *Trp53* allele caused embryonic lethality, this was considered unlikely as mice with a single WT *Trp53* allele are viable and exhibited no deleterious phenotypes. Moreover, mice with a germline knockout of *Trp53* were viable and fertile. It is possible that the targeted mESC were compromised during the targeting process, although karyotyping did not reveal any major defects of chromosome number (data not shown). To expedite generation of these mice, gene targeting and the generation and breeding of chimaeras was outsourced to the Transgenic Unit of the Babraham Institute. This resulted in the production of germline-transmitted chimaeras after 6 months. The resulting F1 was biopsied and genotyped using PCR to amplify the whole inserted *TRE-LoxP-Neor-LoxP* cassette and the junctions respectively (**Figure 1.22**). Correct insertion of *TRE* at C3 of the PCR-positive F1 mice was confirmed by Southern blot (**Figure 1.23**) using the strategy illustrated in **Figure 1.13** and **Table 1.2**. The F1 mice confirmed by the Southern blots were used as founder animals.

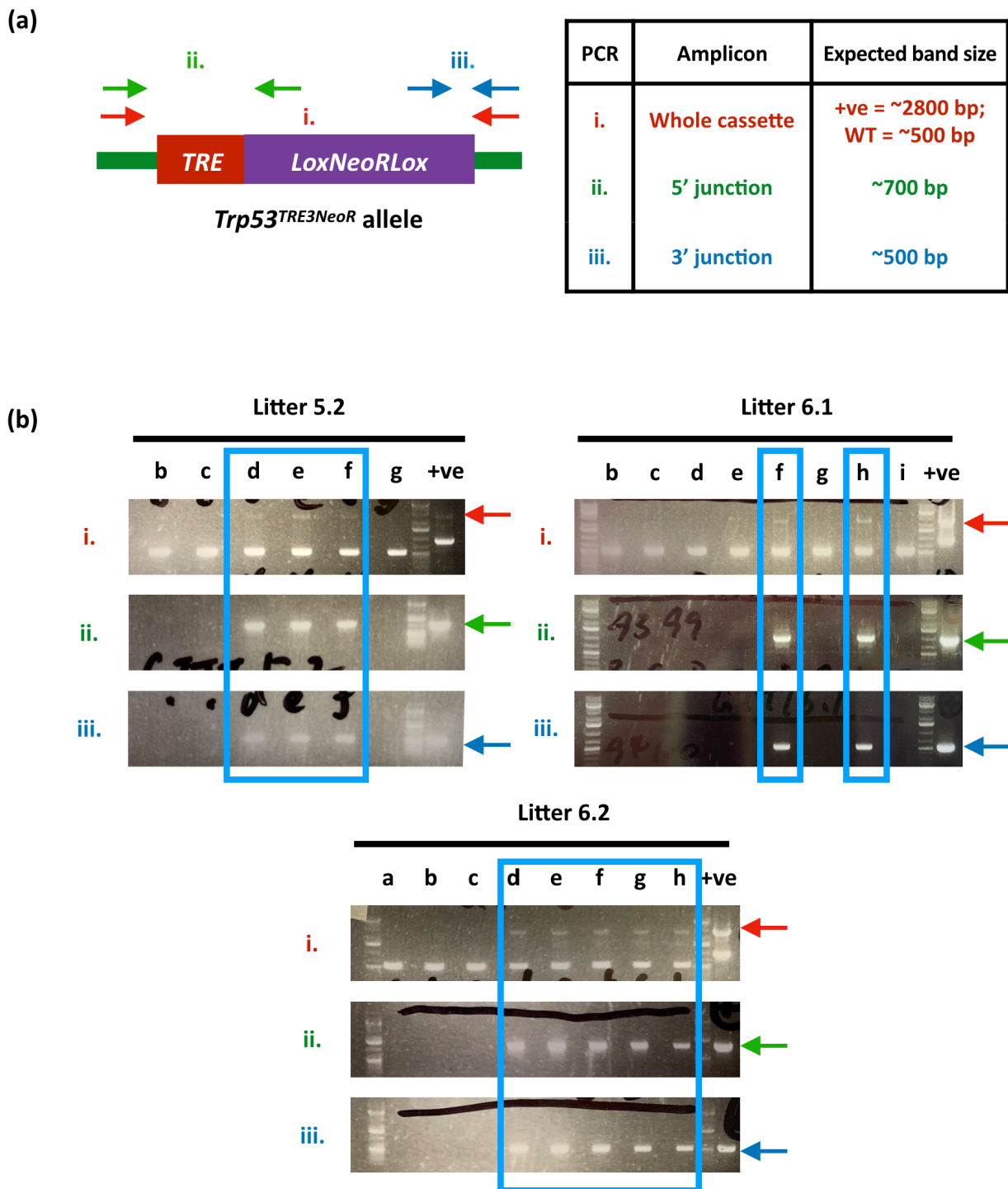


Figure 1.22. Genotyping PCRs to screen for F1 pups that inherited the *Trp53*^{TRE3NeoR} allele from the chimaeras. (a) Left: schematic diagram of the *Trp53*^{TRE3NeoR} allele and the primers (arrows of colours) used in the PCRs. Right: details of the PCRs and expected results. (b) PCR products on agarose gel after electrophoresis. gDNA from each F1 pup was analysed with the three PCRs and only the ones that were positive in all three (indicated by light blue boxes) were further analysed with Southern blots. Arrows indicate the expected band size of the respective PCR. GeneRuler 1 kb Plus ladder from Thermo Scientific was used in these gel electrophoresis. Sequences of primers used are detailed in **Table M.1c** in **Methods and Materials**.

1.7 Reconstituting the repression system *in vivo*

Removal of the embedded *NeoR* sequence, to avoid any chance that it interfered with native *Trp53* expression and regulation, was achieved by breeding the male founders with *Pgk-Cre* female mice that express Cre recombinase activity from the diploid phase of oogenesis onwards. Pups born from these breedings were genotyped by PCR to confirm *NeoR* removal. *NeoR*-excised mice, carrying the *Trp53^{TRE3}* allele, were mated with mice carrying the *R26^{CAG-rtTS}* allele that drives expression of rtTS (allele generated by Dr Ivonne Gamper in Evan group). Pups from these crosses were genotyped and further bred to generate mice homozygous for *Trp53^{TRE3}* with *R26^{CAG-rtTS}* (*Trp53^{TRE/TRE};R26^{CAG-rtTS/+}*). The system was further verified in these animals and cells derived from them, as described in **Chapter 2**.

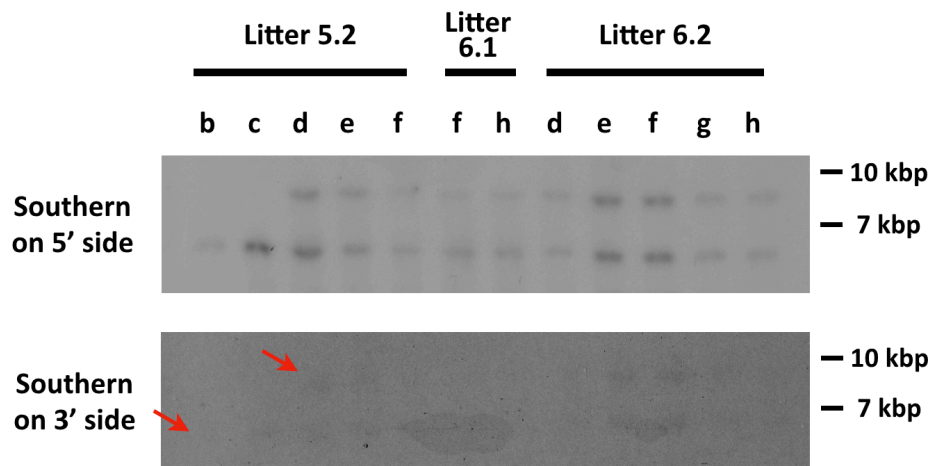


Figure 1.23. Southern blots of correspondingly digested gDNA of F1 pups that gave positive results in the genotyping PCR (see Figure 1.22). Top: Southern blot on the 5' side of the insertion site; bottom: Southern blot on the 3' side of the insertion site. Digested gDNA of each F1 pup was loaded onto one lane of the agarose gel in each blot. Details of the digestions, probe used and expected target fragment sizes are outlined in **Table 1.2**. All pups, barring 5.2 b and c which were shown to be WT, gave positive results in the Southern blots. The bands on the film of the 3' Southern blot appeared very faint on the scanned image but were visible on the actual film to be indicative of the results. The red arrows indicate the positions of the faint bands.

**BLANK
PAGE**

Chapter 2:

Validation of the TRE-p53 model

The results reported in **Chapter 1** indicate efficient repression of *Trp53* in the heterozygous *Trp53^{TRE3/+}* mESCs in which the *TRE* was targeted to position C3 of the endogenous *Trp53* allele. In order to further confirm the functionality of the *TRE* system, similar experiments were conducted in homozygous *Trp53^{TRE3/TRE3}* mESCs and targeted mouse embryonic fibroblasts (MEFs) as well as in the targeted animals.

2.1 Validating the repression system in mESCs

2.1.1 Creating homozygous *Trp53^{TRE3/TRE3};CAG-rtTStg* mESCs

The preliminary results in **Chapter 1** suggest that *Trp53* expression can be effectively repressed by the Dox-dependent rtTS without interfering with the native expression and regulation of *Trp53* when the *TRE* was inserted into position C3 in *Trp53*'s promoter. However, since these *Trp53^{TRE3/+}* mESCs retained one WT *Trp3* allele, it was impossible to discern how effectively the *Trp53^{TRE3}* allele was repressed. To this end, homozygous *Trp53^{TRE3/TRE3}* mESCs were generated.

Trp53^{TRE3/+} cells were re-infected with the DTA3-TRE-NeoR vector to target the remaining WT allele (same strategy as described in **Chapter 1 Section 1.4**). Of the 43 selected clones, genotyping PCR indicated that 8 had the WT allele successfully targeted with the *TRE-LoxP-NeoR-LoxP* cassette (**Figure 2.1**). These positive clones were further analysed by Southern blots as described in **Figure 1.13** and **Table 1.2** to confirm accurate targeting (**Figure 2.2**). All of the eight clones tested with the genotyping PCR were also positive in the Southern blots. These clones, of the genotype *Trp53^{TRE3/TRE3-NeoR}*, were then used to reconstitute the *TRE* repression system. The *NeoR* sequence from the *Trp53^{TRE3-NeoR}* allele was first excised and the *CAG-rtTStg* transgene was added to the cells, as described in **Chapter 1 section 1.5**.

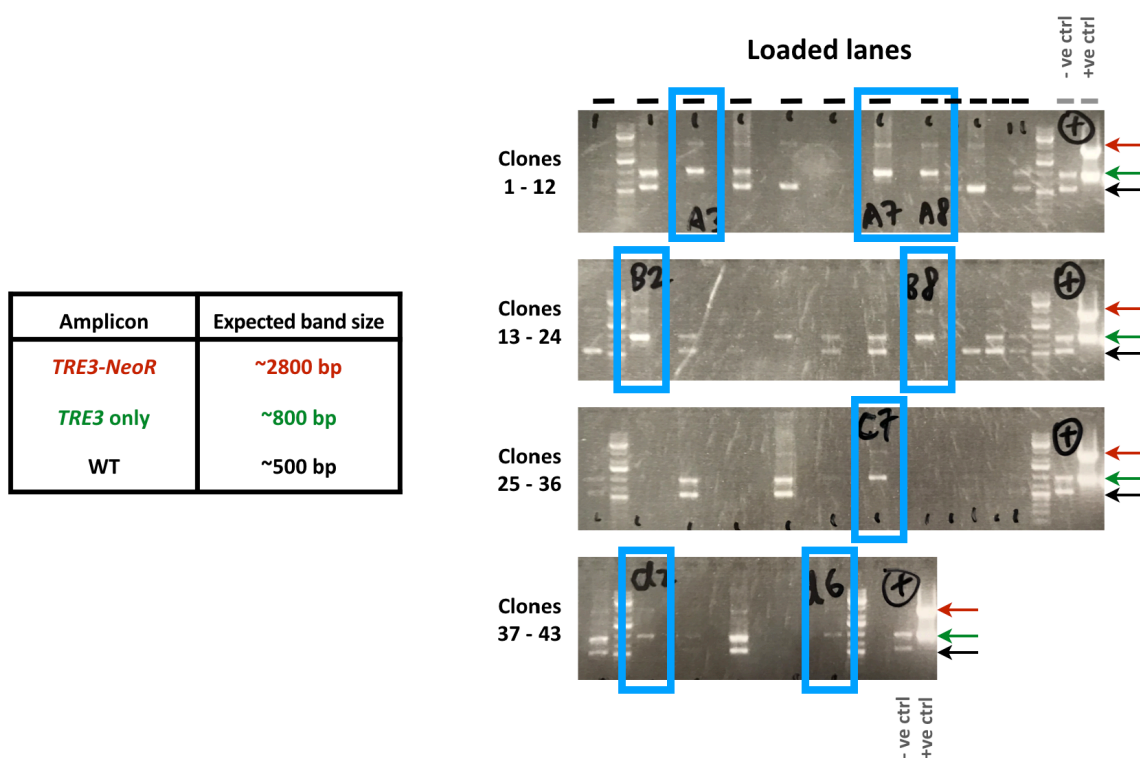


Figure 2.1. Genotyping PCR to preliminarily screen for mESCs that had the second allele targeted at C3 with the *TRE-Lox-NeoR-Lox* cassettes. Left: a summary of the expected size of PCR products. Right: Products of the genotyping PCRs on the gDNA of the 44 picked clones were separated by gel electrophoresis. The red arrow indicates position of the band amplified from the *Trp53^{TRE3-NeoR}* allele on the gel; the green arrow indicates the band amplified from the *Trp53^{TRE3}* allele; the black arrow indicates the WT band. The eight positive clones are indicated by the blue boxes. GeneRuler 1 kb Plus ladder from Thermo Scientific was used in these gel electrophoresis. The sequences of primers used are detailed in **Table M.1c** in the **Methods and Materials** chapter.

(a)

	Southern on the 5' side	Southern on the 3' side
<i>Trp53^{TRE3NeoR}</i> band	8.4 kbp	8.2 kbp
<i>Trp53^{TRE3}</i> band	6.8 kbp	6.6 kbp

(b)

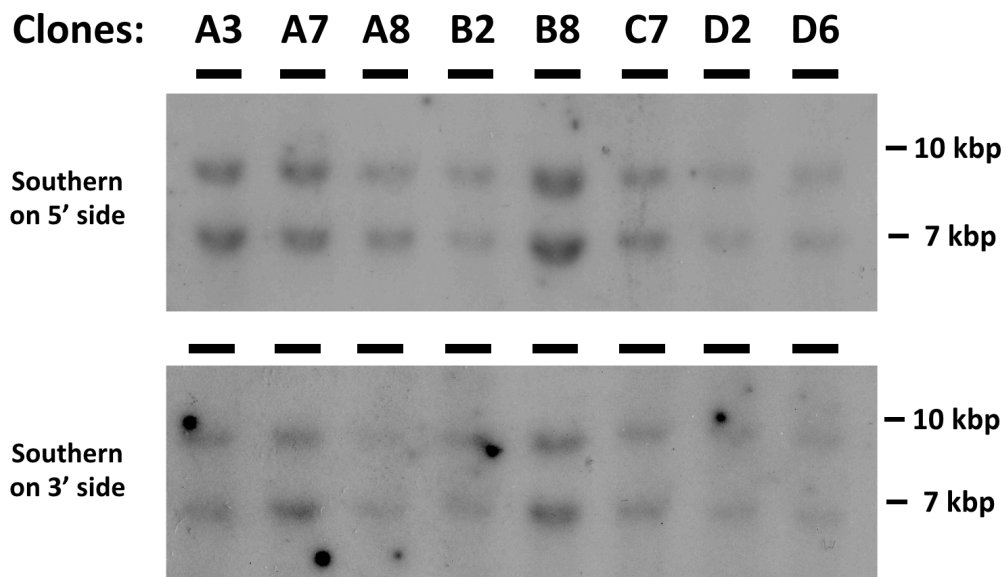


Figure 2.2. Southern blots of the eight PCR-positive clones. (a) A table of expected detectable targeted fragment sizes. Details of the digestions and the probes used were outlined in **Table 1.2**. (b) Digested gDNA of each clone was loaded onto one lane of the agarose gel in each Southern blot. Top blot: Southern blot on the 5' side; bottom blot: Southern blot on the 3' side.

2.1.2 Kinetics of *Trp53* repression and de-repression in mESCs

Both kinetics of *Trp53* mRNA repression by the system upon Dox treatment and its recovery after removal of Dox were assessed. The system in a heterozygous state (*Trp53^{TRE3/+}*) was included to check if the system would function differently than in the homozygous state (*Trp53^{TRE3/TRE3}*) in terms of kinetics due to, for example, the potential influence exerted by the WT allele.

To assess the repression kinetics, *Trp53^{TRE3/+};CAG-rtTStg* and *Trp53^{TRE3/TRE3};CAG-rtTStg* mESCs cultured on petri dishes for 24 hours were treated with Dox for various times and *Trp53* mRNA expression in these cells was assessed by qPCR (**Figure 2.3**). 48 hours of Dox treatment reduced *Trp53* mRNA expression by 50% and 98.5% in *Trp53^{TRE3/+};CAG-rtTStg* and *Trp53^{TRE3/TRE3};CAG-rtTStg* cells respectively. The 50% reduction in the heterozygous *Trp53^{TRE}* cells is consistent with the retention of expression from the WT allele. Interestingly, it was consistently observed that untreated *Trp53* mRNA level slightly decreased as the cells were cultured on the same dish for a longer period of time (e.g. 12 hours vs 96 hours of culturing on the same plate). The exact reason for this is unclear but it may be due to the increase in cell confluence.

To assess the recovery rate of *Trp53* mRNA level after withdrawal of Dox treatment, the mESCs were treated with Dox for 48 hours and then cultured in Dox-free growth medium for different periods of time. mRNA was extracted from the cells and the relative *Trp53* mRNA level was quantified by qPCR (**Figure 2.4**). In both *Trp53^{TRE3/+};CAG-rtTStg* and *Trp53^{TRE3/TRE3};CAG-rtTStg* mESCs, the *Trp53* mRNA level recovered to that seen in untreated cells and control cells with or without Dox treatment within 48 hours after withdrawal of Dox treatment.

These data confirm that *Trp53* mRNA expression from the *Trp53^{TRE3}* allele can be rapidly and reversibly repressed even in the heterozygous state, suggesting that the remaining wild type allele exerts no influence on regulation of the targeted allele by the *TRE* system.

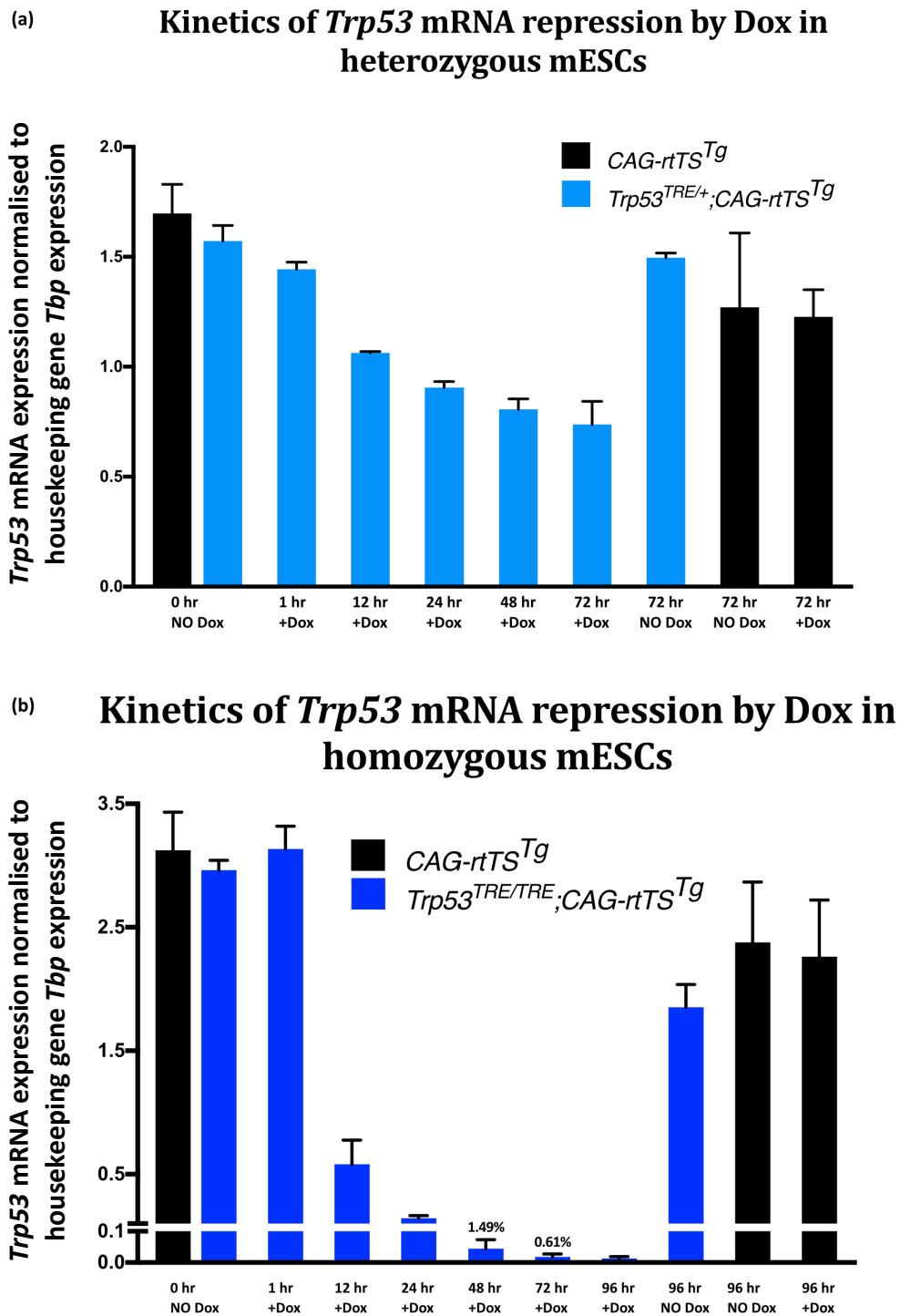


Figure 2.3. Kinetics of Dox repression by the *TRE* system in heterozygous and homozygous mESCs. The relative *Trp53* mRNA level in each sample was quantified with qPCR and then plotted against length of Dox treatment. Plotted are the mean values of samples from cells of 2 different passages and the error bars denote the respective standard deviations. (a) Heterozygous *Trp53^{TRE/+};CAG-rtTS^{Tg}* mESCs. (b) Homozygous *Trp53^{TRE3/TRE3};CAG-rtTS^{Tg}* mESCs. The % mRNA at 48 and 72 hours of Dox treatment was calculated with reference to the level at 0 hour with no treatment. Primers specific to *Trp53* and *Tbp* mRNA were used in the qPCR analysis and their details are listed in **Table M.6b** in the **Methods and Materials** chapter.

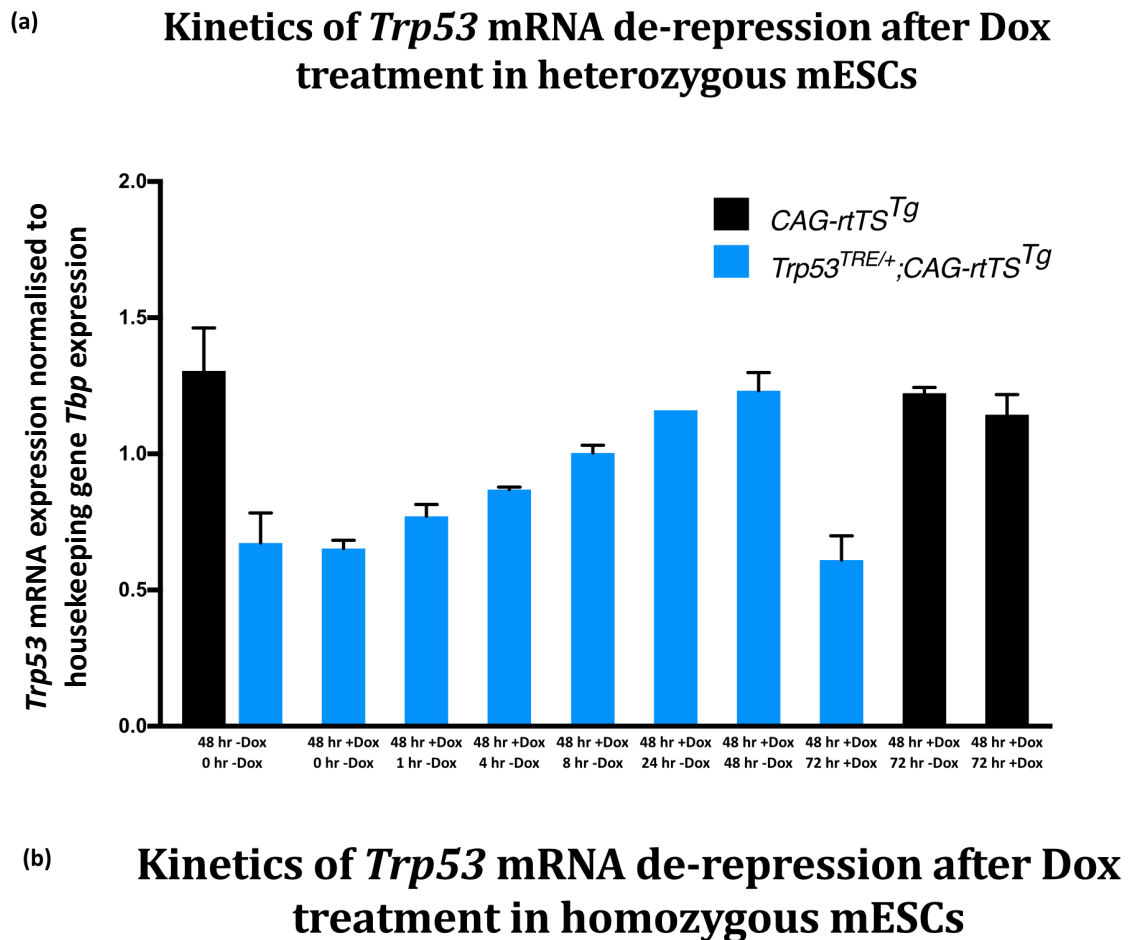


Figure 2.4. Kinetics of de-repression of *Trp53* mRNA following Dox repression by the *TRE* system in heterozygous and homozygous mESCs. Relative *Trp53* mRNA level were quantified by qPCR and plotted correspondingly against the Dox-removal timepoints. Shown are the mean values of samples from cells of 2 different passages and the error bars denote the respective standard deviations. (a) Heterozygous $Trp53^{TRE/+};CAG-rtTS^{Tg}$ mESCs. (b) Homozygous $Trp53^{TRE/TRE};CAG-rtTS^{Tg}$ mESCs. Primers specific to *Trp53* and *Tbp* mRNA were used in the qPCR analysis and their details are listed in **Table M.6b** in the **Methods and Materials** chapter. Plotted were the mean values of samples from cells of 2 different passages and the error bars denote the respective standard deviations.

2.2 Repression of *Trp53* in primary MEFs

To complement the results in mESCs reported above and in **Chapter 1**, I determined the efficiency and kinetics of Dox-dependent repression of p53 in MEFs. Despite also being an *in vitro* cell system, the MEFs resemble the *in vivo* mouse system more than the mESCs in two regards. First, the rtTS repressor in MEFs is expressed from the ubiquitous constitutive *Rosa26* promoter rather than from the potentially multiple insertions of the transgenes in the mESCs. Second, primary MEFs of early passages were used to avoid any compensation or changes that may have occurred during the long-term culture of the mESCs.

Whether the *TRE* insertion affects normal *Trp53* expression in the MEFs system was first assessed. Heterozygous *Trp53^{TRE3/+};R26^{CAG-rtTS/+}* E13.5 embryos were harvested and disaggregated into MEFs, which were then cultured *in vitro*. *Trp53* mRNA expression of these cells in the absence of Dox was compared to WT cells. As shown in **Figure 2.5**, there was no difference in *Trp53* mRNA level between the heterozygous and WT cells after either 24 hours or 120 hours in culture, indicating that the *TRE* insertion itself did not affect *Trp53* mRNA expression. Similar to the mESCs system (**Section 2.1.2** above), a statistically significant reduction of *Trp53* mRNA expression correlating with time in culture was also observed in the MEFs (**Figure 2.5**; statistically tested with One-way ANOVA; *p* values = 0.0352 for WT and 0.0481 for *Trp53^{TRE3/+}* cells).

Then, *rtTS* expression from the endogenous *R26* locus in the *Trp53^{TRE3/+};R26^{CAG-rtTS/+}* MEFs with or without the Dox treatment was quantified with qPCR (**Figure 2.6**). Robust expression of *rtTS* mRNA was detected in these cells both in the absence and presence of Dox. The slight fluctuation of the expression level observed with longer Dox treatment is apparently irrelevant to the efficient repression of *Trp53* expression by the *TRE* system. (**Figure 2.7** below).

TRE insertion exerted no effect on *Trp53* mRNA expression in MEFs

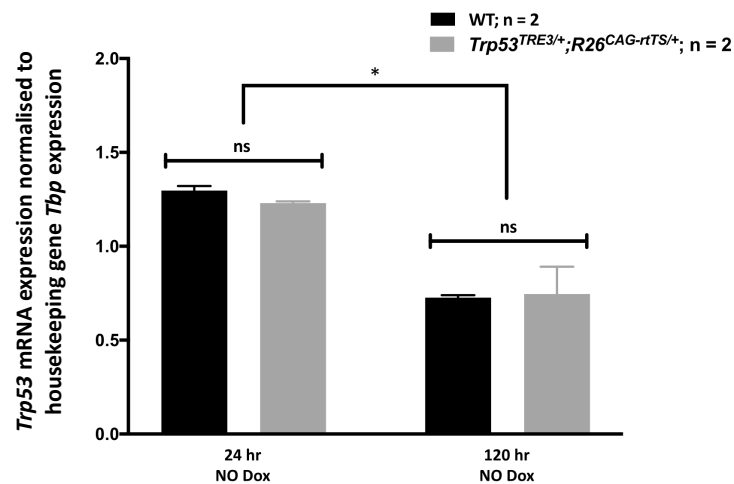


Figure 2.5. TRE insertion did not affect normal *Trp53* mRNA expression in MEFs. Two WT and two *Trp53*^{TRE3/+} MEFs cell lines were grown on culture dishes for 24 and 120 hours with no treatment and harvested for mRNA extraction. Relative *Trp53* mRNA level of the cells were quantified by qPCR and the mean value of 2 cell lines of the same genotype were plotted respectively against the corresponding time point. The error bars denote the respective standard deviations. A One-way ANOVA test was used to test the significance of the apparent decrease of relative mRNA level at 120 hours from 24 hours (WT $p = 0.0352$; *Trp53*^{TRE3/+} $p = 0.0481$). Primers specific to *Trp53* and *Tbp* mRNA were used in the qPCR analysis and their details are listed in **Table M.6b** in the **Methods and Materials** chapter.

***rtTS* expressed from *R26*^{CAG-rtTS} in MEFs treated with Dox for different period of time**

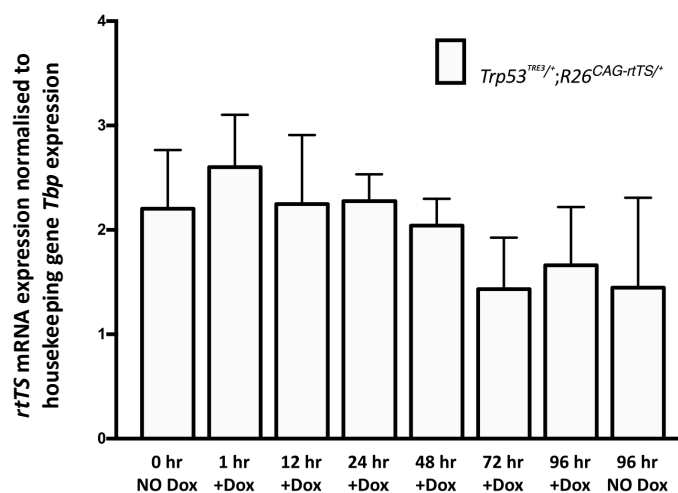


Figure 2.6. *rtTS* expression level from the *Rosa26* locus is independent of Dox treatment. Two *Trp53*^{TRE3/+}; *R26*^{CAG-rtTS/+} MEFs cell lines were grown on culture dishes for 24 hours and then treated accordingly with Dox for the indicated period of time and harvested for mRNA extraction. Relative *rtTS* mRNA levels in the cells were quantified by qPCR and the mean value of the two lines were plotted against the corresponding timepoint. The error bars denote the respective standard deviations. Primers specific to *rtTS* mRNA were used in the qPCR analysis and their details are listed in **Table M.6b** in the **Methods and Materials** chapter.

Next, how quickly the *TRE* system repressed *Trp53* expression was determined. Heterozygous *Trp53^{TRE3/+};R26^{CAG-rtTS/+}* MEFs were treated with Dox for various periods of time and the relative expression level of *Trp53* mRNA quantified by qPCR (**Figure 2.7**). Total *Trp53* mRNA was reduced by approximately 50% within 24 hours of addition of Dox to the culture medium. Given that expression from the WT allele of p53 was unaffected by the system, this result suggests that the *Trp53^{TRE3}* allele was completely repressed within 24 hours of Dox treatment. To further confirm the degree and kinetics of repression of the *Trp53^{TRE3}* allele by the system, homozygous MEFs (*Trp53^{TRE3/TRE3};R26^{CAG-rtTS/+}*) derived from mice were also treated with Dox for different periods of time and the *Trp53* mRNA expression quantified by a qPCR. As shown in **Figure 2.8**, the *Trp53* mRNA level was repressed to 1.15% of the untreated level after 12 hours of Dox treatment. This repression rate, like in the heterozygous MEFs, was substantially faster than in mESCs. For example, it took 48 hours of Dox treatment to reach 98.5% repression of *Trp53* mRNA expression in homozygous mESCs (**Figure 2.4**). Though the exact reasons for such a difference are unknown, it could be a result of the dissimilar cellular contexts. For instance, *Trp53* is found to be expressed at a higher level in embryonic stem cells (Solozobova & Blattner 2011) and it is possible that such a level was more robustly regulated and resilient against repression exerted by the *TRE* system in mESCs than in MEFs.

Lastly, the kinetics of de-repression was determined. *Trp53^{TRE3/TRE3};R26^{CAG-rtTS/+}* cells were first treated with Dox for 48 hours, changed to fresh Dox-free medium and cultured for different periods of time before mRNA was harvested from the cells. *Trp53* mRNA from these cells was then quantified with qPCR (**Figure 2.9**). *Trp53* mRNA level recovered to the untreated level within 24 hours after Dox removal, again with faster kinetics than the corresponding mESCs.

In conclusion, the *TRE* system proved to be capable of reversibly repressing *Trp53* mRNA expression in both mESCs and MEFs, though with slightly different kinetics of repression and de-repression. However, the fast repression and de-repression observed in MEFs likely represents the baseline, probably maximal, rate at which the system could operate because of the absence

of hindrances such as delay by Dox delivery to individual tissues *in vivo* and/or a reduced stability of Dox due to metabolism after intake by the animals. Indeed, the *in vivo* verifications in the following section show the system functioned in a slightly lower rate than *in vitro* at general.

Kinetics of *Trp53* mRNA repression by Dox in heterozygous MEFs

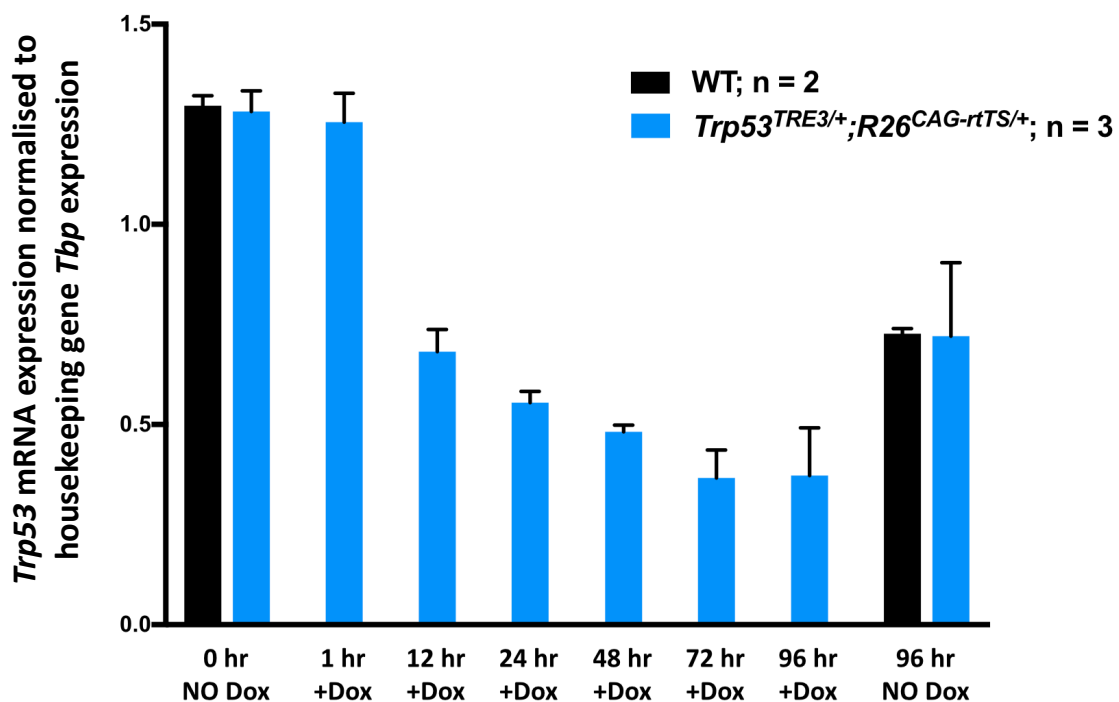


Figure 2.7. Rapid repression of *Trp53* mRNA level by Dox in heterozygous *Trp53*^{TRE3/+};*R26*^{CAG-rtTS/+} MEFs. Three *Trp53*^{TRE3/+};*R26*^{CAG-rtTS/+} MEFs cell lines (and two WT as reference) seeded and cultured for 24 hours were treated with Dox with the indicated periods of time and harvested for mRNA. Relative *Trp53* mRNA level of the cells were quantified by qPCR and the mean value of the cell lines were plotted against the corresponding timepoint. The error bars denote the respective standard deviations. Note that the complete repression of expression from the *Trp53*^{TRE3} allele (i.e. 50% of untreated or WT level) was reached substantially faster than in heterozygous mESCs at 12 - 24 hours. Primers specific to *Trp53* and *Tbp* mRNA were used in the qPCR analysis and their details are listed in **Table M.6b** in the **Methods and Materials** chapter.

Kinetics of *Trp53* mRNA repression by Dox in homozygous MEFs

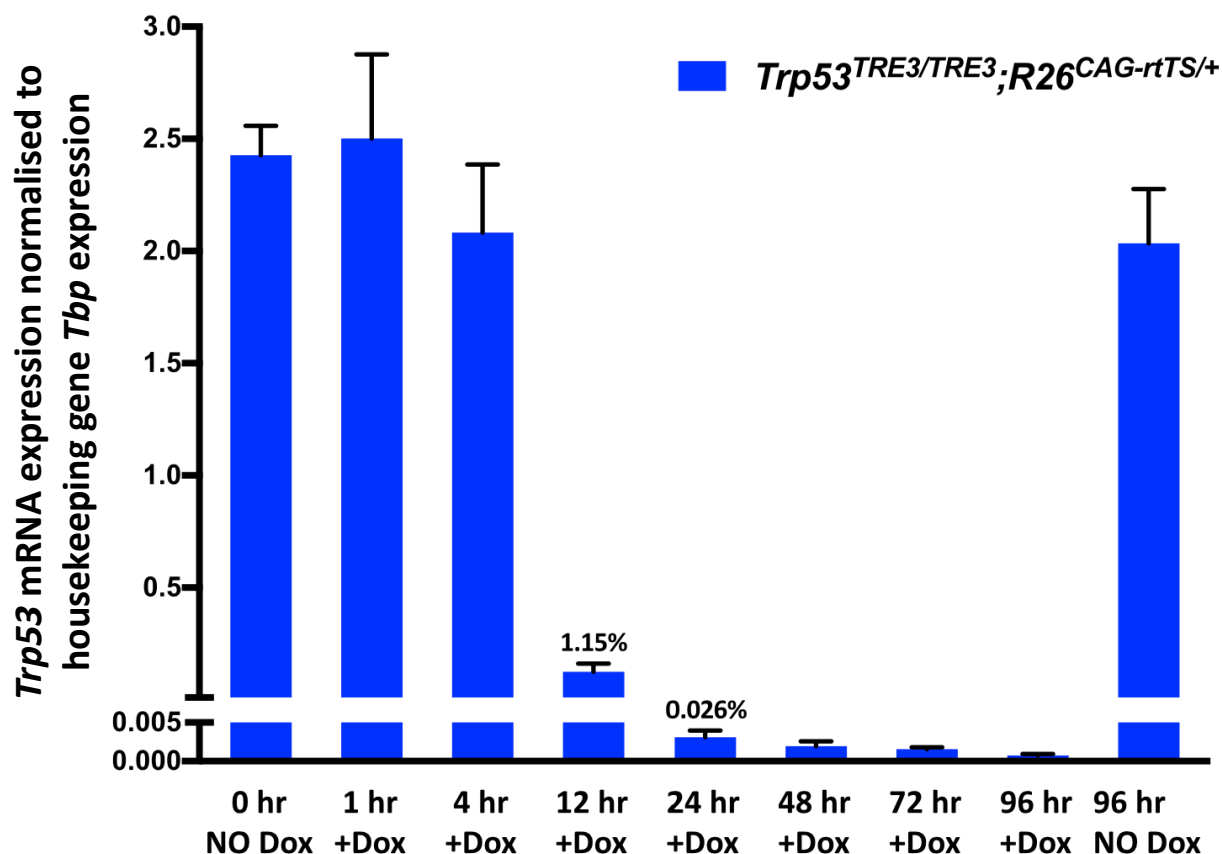


Figure 2.8. Rapid repression of *Trp53* mRNA level by Dox in homozygous *Trp53*^{TRE3/TRE3};*R26*^{CAG-rtS/+} MEFs. Three *Trp53*^{TRE3/TRE3};*R26*^{CAG-rtS/+} MEFs cell lines cultured for 24 hours were treated with Dox according to the indicated periods of time and then harvested for mRNA. Relative *Trp53* mRNA level of the cells were quantified by qPCR and the mean value of the cell lines were plotted against the corresponding timepoint. The error bars denote the respective standard deviations. Note that 98.8% repression of the *Trp53* mRNA level (1.15% of untreated level) was reached substantially faster than in heterozygous mESCs after 12 hours of Dox treatment. Primers specific to *Trp53* and *Tbp* mRNA were used in the qPCR analysis and their details are listed in **Table M.6b** in the **Methods and Materials** chapter.

Kinetics of *Trp53* mRNA de-repression after Dox treatment in homozygous MEFs

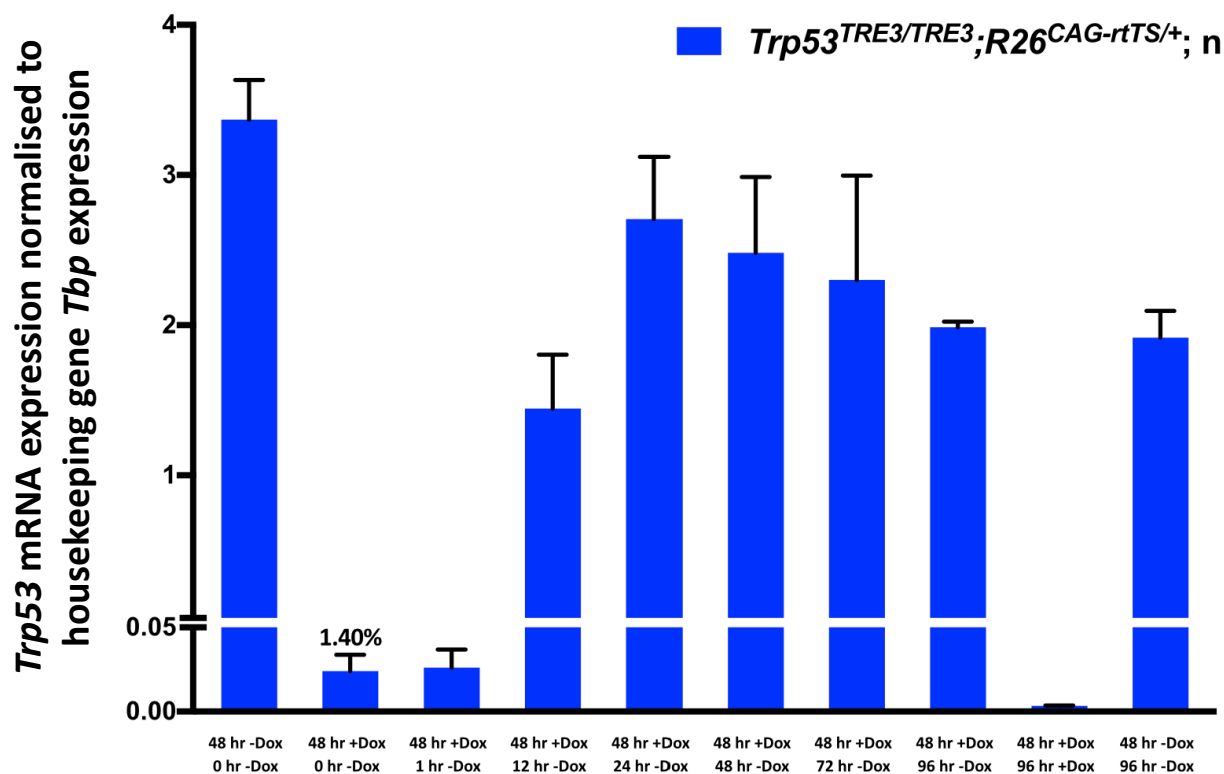


Figure 2.9. Rapid recovery of *Trp53* mRNA level after Dox repression in homozygous $Trp53^{TRE3/TRE3};R26^{CAG-rtTS/+}$ MEFs. Three $Trp53^{TRE3/TRE3};R26^{CAG-rtTS/+}$ MEFs cell lines cultured for 24 hours were treated with Dox for 48 hours and then switched to Dox-free medium for different periods of time as indicated and then harvested for mRNA. Relative *Trp53* mRNA level of the cells were quantified by qPCR and the mean value of the cell lines were plotted against the corresponding timepoint. The error bars denote the respective standard deviations. The relative mRNA level recovered to normal level 24 hours after removal of Dox, significantly faster than in homozygous mESCs. Primers specific to *Trp53* and *Tbp* mRNA were used in the qPCR analysis and their details are listed in **Table M.6b** in the **Methods and Materials** chapter.

2.3 Repression of *Trp53* *in vivo*

2.3.1 Does *TRE* insertion interfere with normal *Trp53* mRNA expression in tissues?

To address whether the implementation of the system exerted any impact on normal *Trp53* expression, various tissues reported to be radio-sensitive (intestine, spleen and thymus) or radio-resistant (lung, liver, pancreas and skin) were harvested from 6-week-old *Trp53^{TRE3/+}* and *Trp53^{TRE3/TRE3}* mice. Both radio-sensitive and radio-resistant tissues were included in all experiments in this thesis despite the radio-sensitive tissue-specific p53 expression and transcription activities speculated by previous reports, because the use of a germline p53-null model in these reports could have missed the subtler functions of p53 (MacCallum et al. 1996; Komarova et al. 1997; Bouvard et al. 2000; Burns et al. 2001; Fei et al. 2002; Fei & El-Deiry 2003). From the collected tissues mRNA was extracted and relative *Trp53* mRNA expression was quantified by qPCR (**Figure 2.10**). From the plot, it is clearly demonstrated that the insertion of *TRE* at position C3 did not affect mRNA expression of the endogenous *Trp53* gene in all the tissues analysed. These data (as are all subsequent mouse qPCR results) are derived from several mice (number denoted as n) and the results plotted as the mean and standard deviations.

TRE insertion did not affect normal *Trp53* mRNA expression in tissues

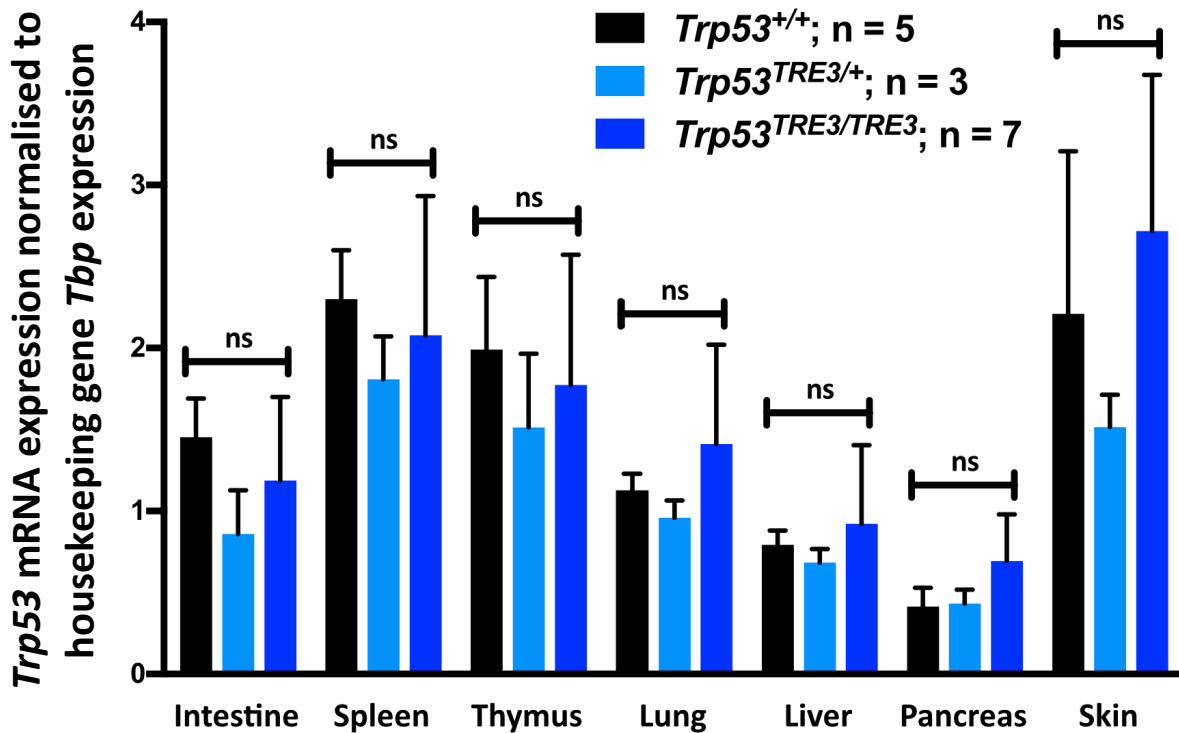


Figure 2.10. *TRE* insertion at one or both alleles of the endogenous *Trp53* gene did not affect normal *Trp53* mRNA expression in different tissues. Plotted are the mean quantified relative *Trp53* mRNA level of the animals in each genotype group (n = number of animals in the group) while error bars denotes the standard deviation. Only results from 3 mice were plotted for skin of the *Trp53*^{+/+} and *Trp53*^{TRE3/TRE3} group respectively because of the poor inefficient mRNA extractions from skin of the other mice. The differences in the relative p53 mRNA level amongst the three genotype groups in all tissues were insignificant, as indicated by a One-way ANOVA test. Primers specific to *Trp53* and *Tbp* mRNA were used in the qPCR analysis and their details are listed in **Table M.6b** in the **Methods and Materials** chapter.

2.3.2 Verifying *rtTS* mRNA expression *in vivo*

The *in vivo* expression of *rtTS* mRNA from the *R26* locus was analysed. Relative mRNA levels of *rtTS* in the tissues collected from 6-week old *Trp53^{TRE3/TRE3};R26^{CAG-rtTS/+}* and *Trp53^{TRE3/TRE3};R26^{CAG-rtTS/CAG-rtTS}* mice was quantified by qPCR and the results are plotted in **Figure 2.11**. A five-fold variation of *rtTS* mRNA expression levels in different tissues was observed with a rough trend of doubled expression level in homozygous compared to *R26^{CAG-rtTS/+}* tissues. Enriching the data set of the homozygous tissues should increase the significance of the data. The varying *rtTS* mRNA expression across the tissues did not appear to correlate with the efficiency or the kinetics of repression and de-repression of *Trp53* mRNA by the *TRE* system, as shown in the following sections.

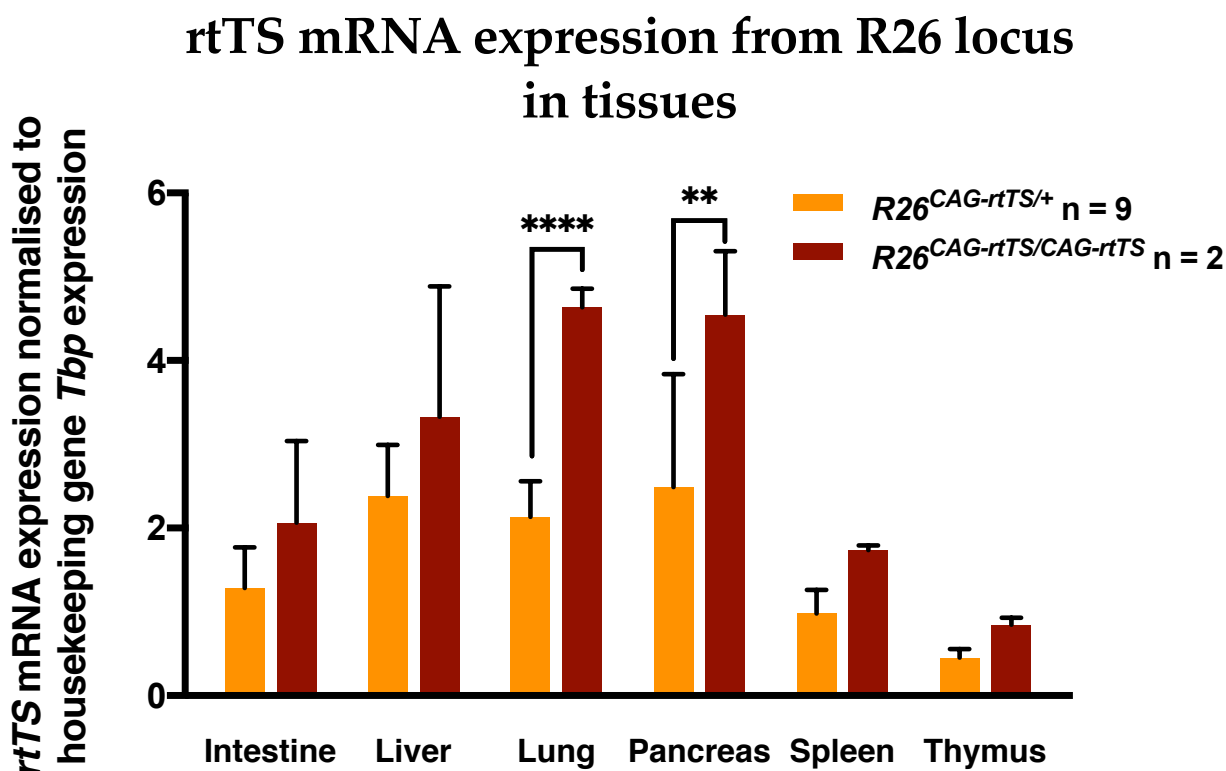


Figure 2.11. *rtTS* mRNA expression from one or two copies of the *R26^{CAG-rtTS}* allele varied across tissues. Plotted are the mean quantified relative *rtTS* mRNA level of the animals in each genotype group (n = number of animals in that group) and the error bars denote the standard deviations (**** : $p < 0.0001$; ** : $p = 0.0019$; unmarked = non significant). Primers specific to *rtTS* mRNA were used in the qPCR analysis and their details are listed in **Table M.6b** in the **Methods and Materials** chapter.

2.3.3 Repression of *Trp53* mRNA expression by Dox *in vivo*

Having verified the components of the system *in vivo*, the *TRE* system's capacity to repress endogenous *Trp53* mRNA expression in tissues upon Dox treatment was assessed. To this end, tissues were collected from *Trp53^{TRE3/TRE3};R26^{CAG-rtTS/+}* mice that had been administered with Dox in sucrose-sweetened water for 7 days, a timepoint at which *E2f3* expression was >95% repressed from the *TRE-Ef3* allele in similar experiments in Gamper *et al.* (Gamper *et al.* 2017). The relative *Trp53* mRNA level in the collected tissues was determined by qPCR (**Figure 2.12**). Consistent with Gamper *et al.*, after 7 days of Dox treatment the *Trp53* mRNA level was almost completely eliminated across the panel of tissues tested. The residual level of *Trp53* mRNA in the pancreas and spleen was 3.39% and 2.56% of the untreated group respectively, while in the other tissues it was less than 1%. The statistical significance of the mRNA levels between the treated and untreated group was affirmed by a One-way ANOVA test and the *p*-values are indicated in the graph.

Note that in all *in vivo* experiments in this thesis, Dox was administered to mice in drinking water at a concentration of 2 mg/1 mL of 1% (w/v) sucrose water while the untreated control groups were treated with the Dox-free 1% sucrose water. Sucrose was added to the drinking water to mask the bitter taste of Dox dissolved in water, which might dissuade the animals from drinking.

2.3.4 Kinetics of *Trp53* mRNA repression by Dox

To utilise the *TRE* repression system in *in vivo* experiments, it is necessary to know how quickly the system responds upon Dox treatment. To this end, I set up a timepoint experiment where *Trp53^{TRE3/TRE3};R26^{CAG-rtTS/+}* mice were treated with Dox for 1, 2 or 3 days. Note that tissues were always harvested from 6-week old mice to minimise any possible age-related effects. Relative *Trp53* mRNA levels in intestine, spleen, thymus, lung, liver, pancreas and skin were quantified by qPCR (**Figure 2.13**). Results from the 7 days Dox treatment was also included as a

timepoint in the plot. The graphs indicate that for all the tested tissues, a Dox treatment of 2 days sufficed to repress *Trp53* mRNA expression to a minimal level, though in the pancreas and skin more variations were observed at the 2 and 3 day timepoints.

Repression of *Trp53* mRNA in tissues by 7 days of Dox treatment

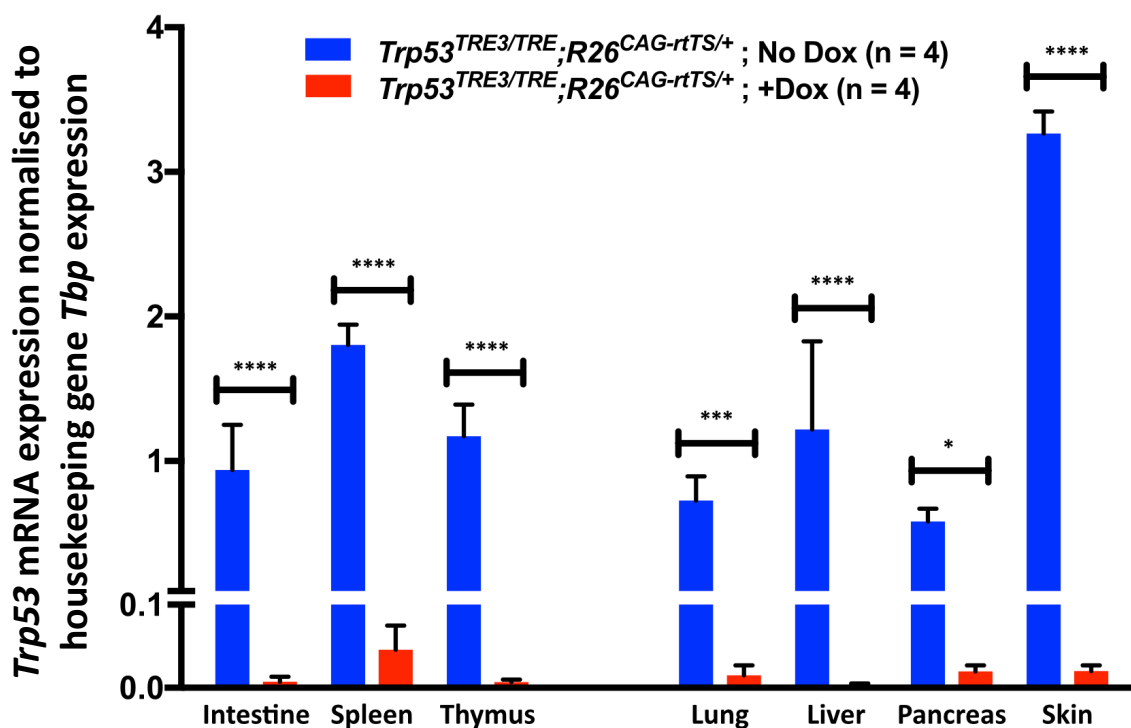


Figure 2.12. *Trp53* mRNA expression was almost completely repressed in various tissues after 7 days of Dox treatment. Plotted are the mean quantified relative *Trp53* mRNA level in the tissues of the animals in each treatment group (n = number of animals in the group) while error bar denotes the standard deviation. The differences between the treated and untreated group in each tissue was tested for significant by a One-way ANOVA test and the *p*-values are indicated by asterisks (*: *p* = 0.0101; ***: *p* = 0.002; ****: *p* < 0.0001). Primers specific to *Trp53* and *Tbp* mRNA were used in the qPCR analysis and their details are listed in **Table M.6b** in the **Methods and Materials** chapter.

Kinetics of *Trp53* mRNA repression by Dox in tissues

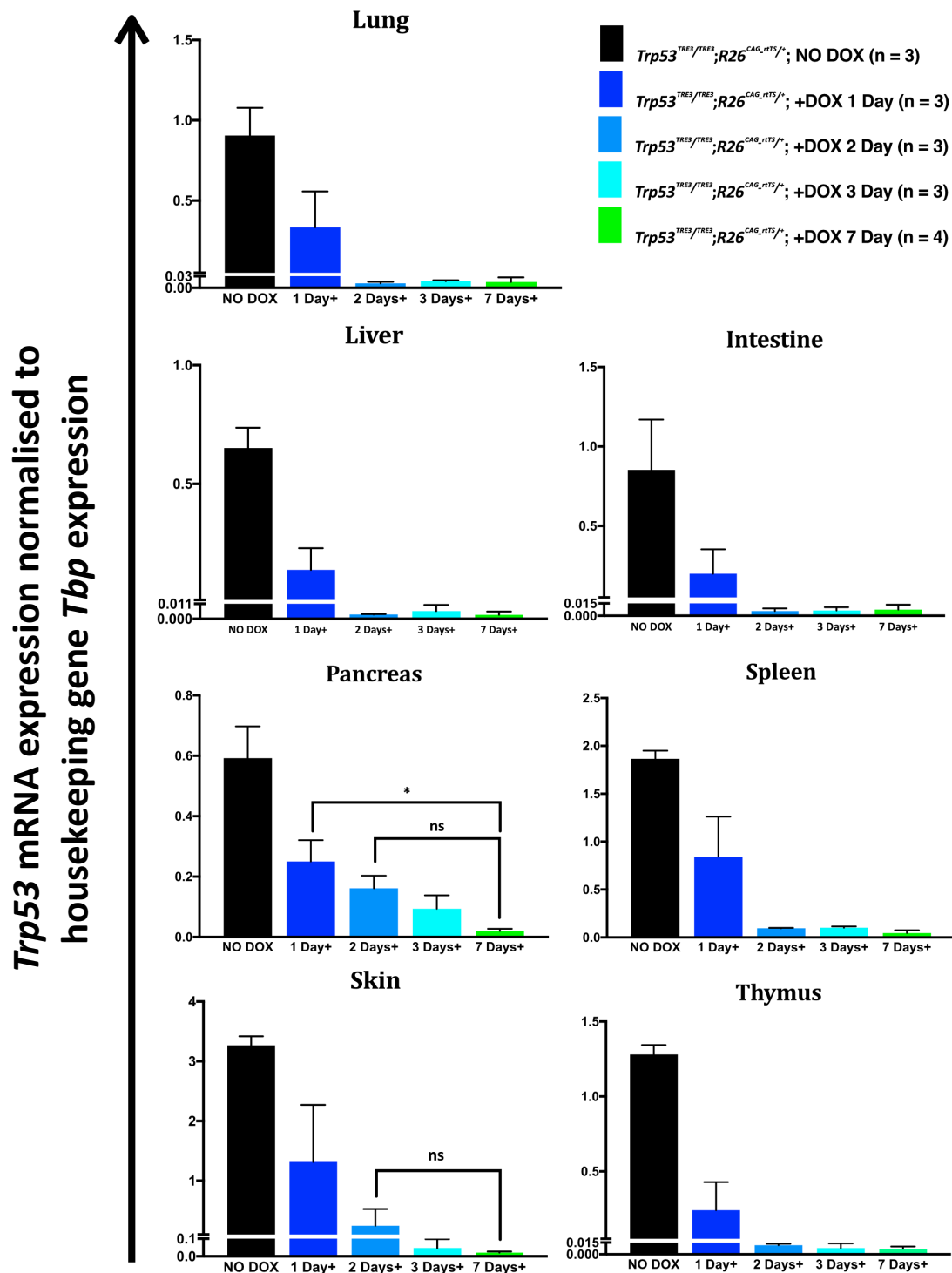


Figure 2.13. Kinetics of Dox repression of *Trp53* mRNA in various tissues. Plotted are the mean quantified relative *Trp53* mRNA level of the indicated tissues from the animals at each timepoint (n = number of animals in that timepoint) while error bar denotes the standard deviation. Note that the scale of the y-axis representing relative *Trp53* mRNA levels is not necessarily the same across the tissues. The statistical significance shown in the pancreas graph resulted from a One-way ANOVA test and the *p*-values are indicated by asterisk (ns = non-significant; *: *p* = 0.0413). Primers specific to *Trp53* and *Tbp* mRNA were used in the qPCR analysis and their details are listed in **Table M.6b** in the **Methods and Materials** chapter.

2.3.5 Kinetics of *Trp53* mRNA de-repression following removal of Dox

The ability to reversibly suppress *Trp53* function is essential to determine *Trp53*'s temporal functionality in different processes, such as tumour evolution and tissue regeneration. Therefore it is necessary to determine the kinetics of *Trp53* mRNA level recovery in tissues after withdrawal of Dox. In this experiment, *Trp53^{TRE3/TRE3};R26^{CAG-rtTS}/+* mice were first administered Dox-added sucrose water for 7 days (where maximum repression was achieved; **Figure 2.13**) and switched to Dox-free fresh water for 1 or 3 days; the animals were euthanised at the timepoints indicated and tissues were collected by snap-freezing. Relative *Trp53* mRNA levels in these tissues were then quantified by qPCR (**Figure 2.14**). With the exception of skin where insufficient mRNA was isolated, *Trp53* mRNA in all tissues returned to the normal, untreated level by 3 days (See **Figure 2.20** below for recovery of p53 protein activities in skin in three days, which is similar to the other tissues). The uniform rate of *Trp53* mRNA recovery across these tissues suggests that inherent *Trp53* transcription is not overly influenced by any tissue-specific *trans*-effects.

Recovery of *Trp53* mRNA expression from repression by Dox in tissues

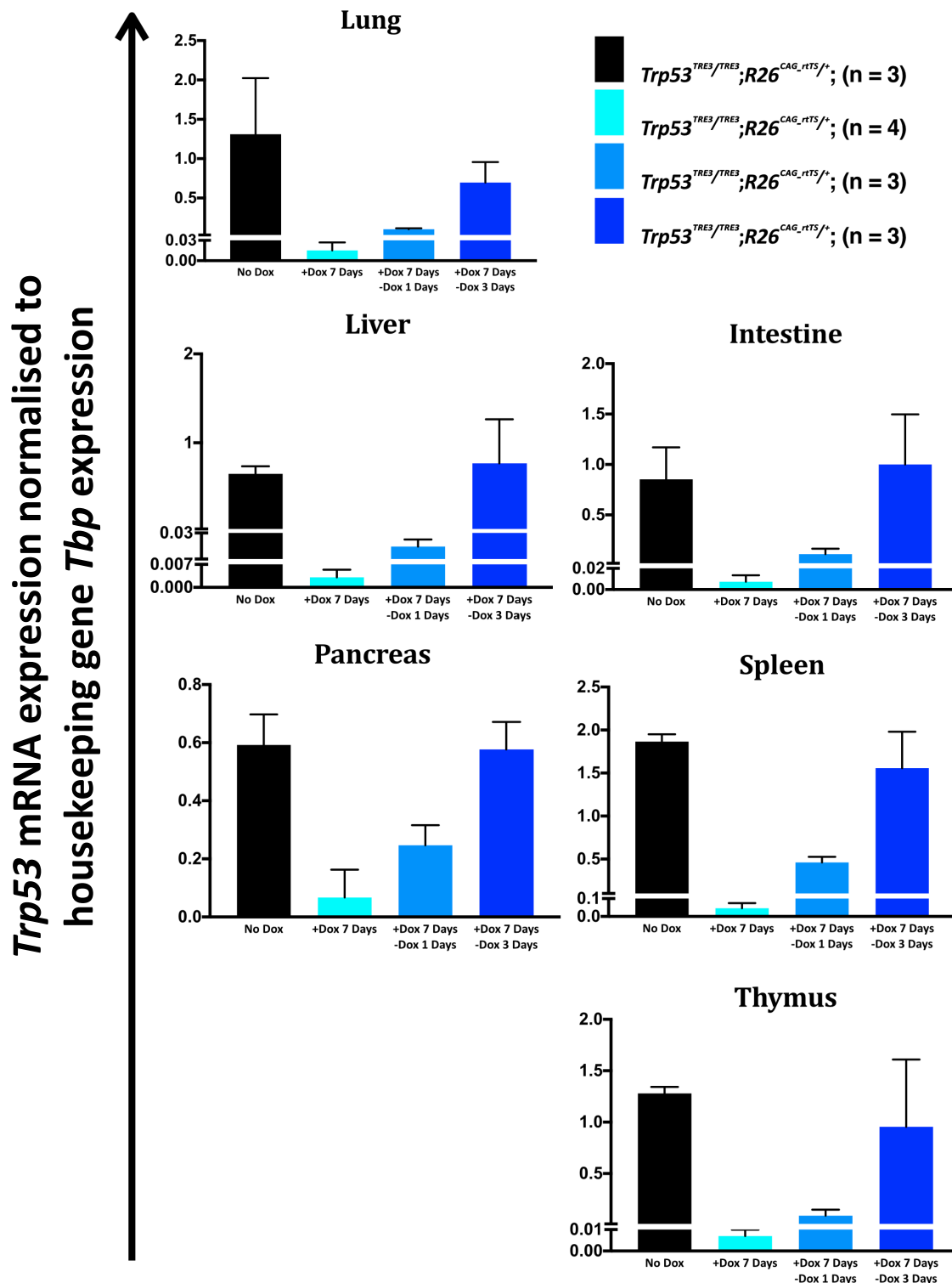


Figure 2.14. De-repression of *Trp53* mRNA following removal of Dox treatment from mice. Plotted were the mean quantified relative *Trp53* mRNA levels in the indicated tissues of the animals at each timepoint (n = number of animals in that timepoint) while error bar denotes the standard deviation. Note that the scale of the y-axis representing relative *Trp53* mRNA level is not necessarily the same across the tissues. Primers specific to *Trp53* and *Tbp* mRNA were used in the qPCR analysis and their details are listed in **Table M.6b** in the **Methods and Materials** chapter.

2.3.6 Repression of p53 protein levels by the *TRE* system

Having established the rate at which the system represses and de-represses *Trp53* mRNA *in vivo*, repression of p53 protein level by the *TRE* system *in vivo* was determined. *Trp53^{TRE3/TRE3};R26^{CAG-rtTS/+}* mice were treated with Dox for 3, 5 and 7 days and proteins prepared from whole cell lysate of frozen tissues of these mice were analysed by western blots (**Figure 2.15**). p53 protein in spleen, thymus and surprisingly pancreas was shown to be expressed under normal conditions at a detectable level in the western blots. It also showed that the presence of *TRE* in the *Trp53* allele or *rtTS* expression from the *R26* locus did not significantly change p53 levels in the three tissues. Upon Dox treatment, p53 was repressed substantially in the three tissues, though with slightly varying rates. In spleen, the level reduced to a minimal level by 5 days whereas it took three days in the thymus and pancreas. Intriguingly, in spite of the remaining p53 level in spleen after 5 days of Dox treatment, the transcription activity of p53 was shown to be repressed by three days (see section **2.3.7** below). The blots also show that a 7-day Dox treatment prevented up-regulation of p53 protein level in spleen upon DNA damage signals (**Figure 2.15a** lanes 11 - 13). Note that in all the pancreas samples a peptide species with slower mobility was detected but it was absent in the positive control (γ -irradiated thymus) and other tissues tested.

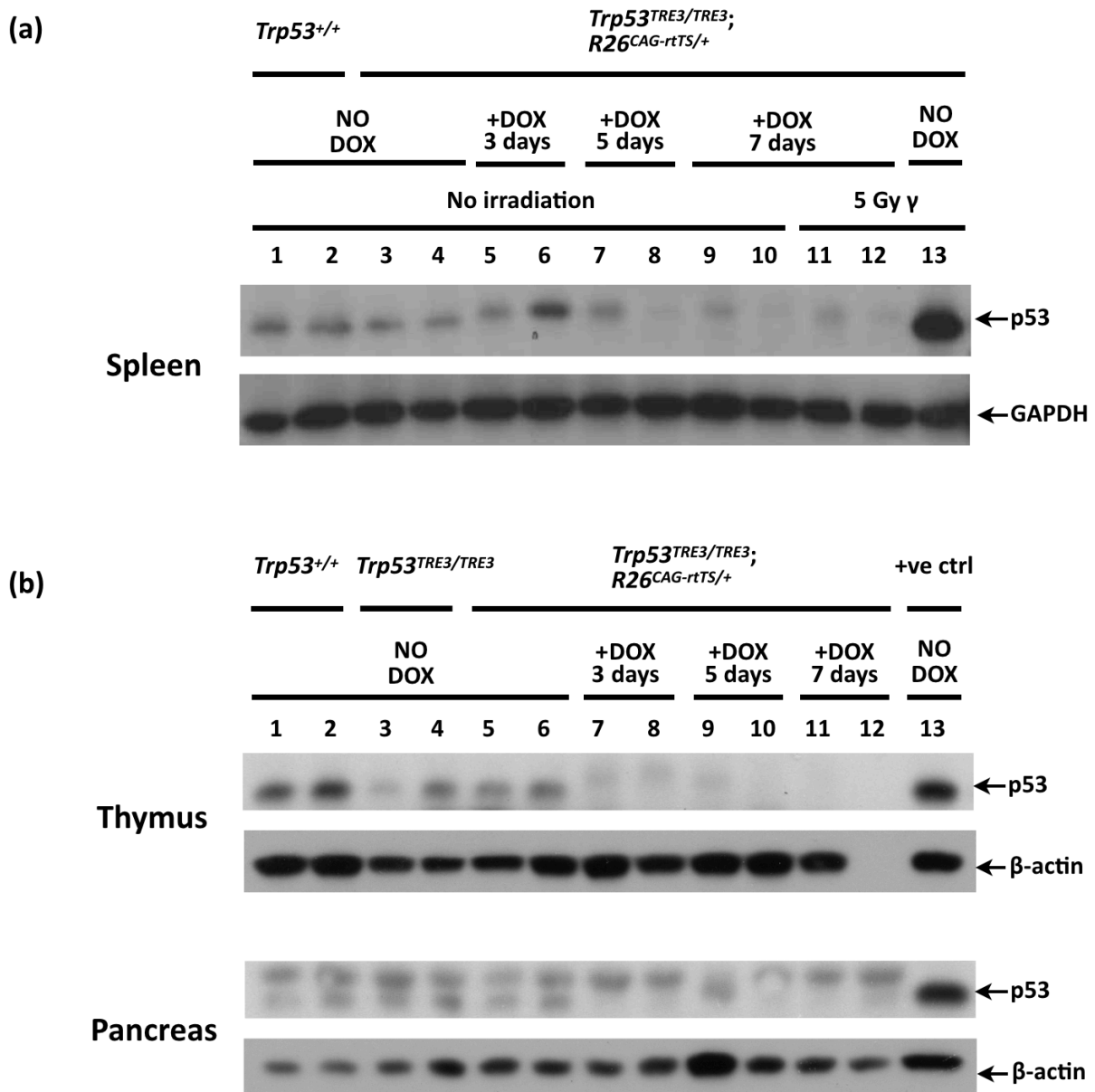


Figure 2.15. Repression of p53 protein level in spleen, thymus and pancreas by Dox treatment. (a) Spleen. A separate gel was run for GAPDH as there was an air bubble blocking the transfer of the original gel to the membrane blot at GAPDH's position of lane 9 - 13. (b) Thymus (top) and pancreas (bottom). Lane 12 is empty in the thymus blot. +ve ctrl: positive control for p53 staining which was lysate from γ -irradiated thymus. For each genotype/treatment group, proteins from two mice were analysed. 20 μ g of proteins were loaded per lane and separated by 12% acrylamine gel. p53 was detected with the primary antibody 1C12 while GAPDH and β -Actin with antibodies D16H11 and AC15 respectively (details of antibodies described in **Section M.6** in the **Methods and Materials** chapter). Note that the spleen Western blot *per se* in (a) was executed by Ms. Maria-Myrsini Tzoni, a rotatory student in the Evan group, under my supervision and used in this thesis with her consent.

2.3.7 Regulation of p53 transcription activity

Although p53 was repressed substantially following Dox treatment, in some cases residual protein level was present after the treatment but the biological relevance was not discernible in the western blots. p53 as a transcription factor has been well characterised for mediating stress-induced responses such as transcriptional regulation of its downstream targets following DNA damage (Lakin & Jackson 1999). The transcriptional activity of p53 upon DNA damage could therefore potentially be used as a parameter to gauge the repression of p53 activities by the *TRE* system.

Firstly the functionality of the *TRE* repression system upon DNA damage *in vivo* was confirmed. In this experiment, 5-week old mice of the genotype *Trp53^{TRE3/TRE3;R26^{CAG-rtTS/+}}* were treated with either Dox-added or Dox-free sucrose-sweetened water for 3, 5 or 7 days followed by whole body 5 Gy γ -radiation to inflict DNA damage such as DNA single- and double-strand breaks in cells of different tissues. Five hours after irradiation, the mice were euthanised, tissues harvested, RNA extracted and *Trp53* mRNA level determined by qPCR (**Figure 2.16**). As shown in the plots, the *TRE* system repressed *Trp53* mRNA expression in the presence of Dox to a similar extent with or without the γ -radiation. On a separate note, *Trp53* mRNA expression in the irradiated mice was up-regulated in pancreas and thymus, but in lung and liver the level decreased comparing to non-irradiated tissues. While an increase in *Trp53* mRNA level would be biologically reasonable considering the stabilisation of *Trp53* mRNA by antisense *Wrap53* mRNA in the presence of a DNA damage signal (Mahmoudi et al. 2009), the observed decreases were unexpected. However, given the rather small extent of the increases and decreases and the nature of variation in animal experiments, the dataset will have to be enlarged to draw any conclusion confidently.

Trp53 mRNA repression by Dox in tissues upon γ -irradiation

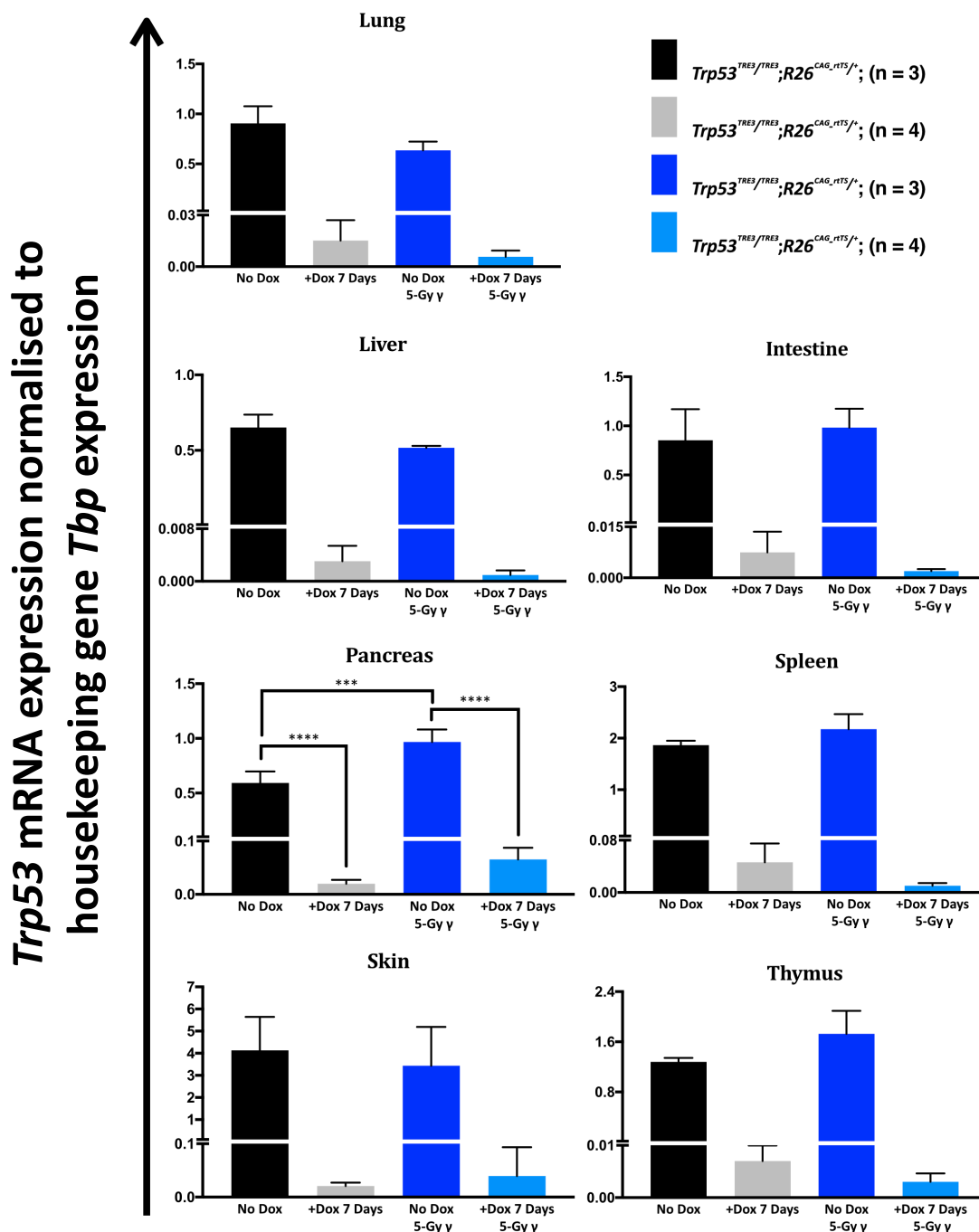


Figure 2.16. Repression of *Trp53* mRNA expression in tissues by Dox after a dose of 5 Gy γ -irradiation. Plotted were the mean quantified relative *Trp53* mRNA level of the animals in each treatment group (n = number of animals in the group) while error bar denotes the standard deviation. Note that the scale of the y-axis representing relative *Trp53* mRNA level is not necessarily the same across the tissues. One-way ANOVA test was used to analyse the statistic significance of the differences between the treatment groups as exemplified on the Pancreas Plot in which the p -values are indicated (ns: non-significant; ***: $p = 0.0006$; ****: $p < 0.0001$). Primers specific to *Trp53* and *Tbp* mRNA were used in the qPCR analysis and their details are listed in **Table M.6b** in the **Methods and Materials** chapter.

Having confirmed that *Trp53* mRNA was still repressed by the system in the presence of DNA damage signals, I next checked whether the p53 transcriptional target gene *Bax* (BCL2-associated X) could be used as a readout for the transcriptional activity of p53. *Bax* encodes the apoptotic activator protein Bax that facilitates apoptosis by permeabilisation of the mitochondrial outer membrane, releasing pro-apoptotic factors including cytochrome c (Oltvai et al. 1993; Finucane et al. 1999) and is up-regulated by p53 upon DNA damage (Miyashita & Reed 1995). To assess whether *Bax* mRNA expression could be used as a reporter of p53 transcriptional activity, relative *Bax* mRNA level in the tissues of the mice irradiated with or without Dox treatment was quantified by qPCR (**Figure 2.17**). From the plots, it is clear that *Bax* mRNA was expressed at a basal level in all the tissues even without irradiation and this expression was not dependent on p53 as it remained unchanged after 7 days of Dox treatment. Upon irradiation, the relative mRNA level of *Bax* was up-regulated in all tissues as expected, though to a different extent. This induction of *Bax* by irradiation was entirely absent in the tissues of mice treated with Dox for 3 days prior to irradiation (except the skin where unfortunately *Bax* induction could not be determined at the 3 and 5 day timepoints due to poor quality of the extracted mRNA) and hence was p53-dependent. These data demonstrate that within 3 days of Dox treatment p53's transcriptional activity was completely repressed.

p53 transcription activity repressed by three days of Dox treatment

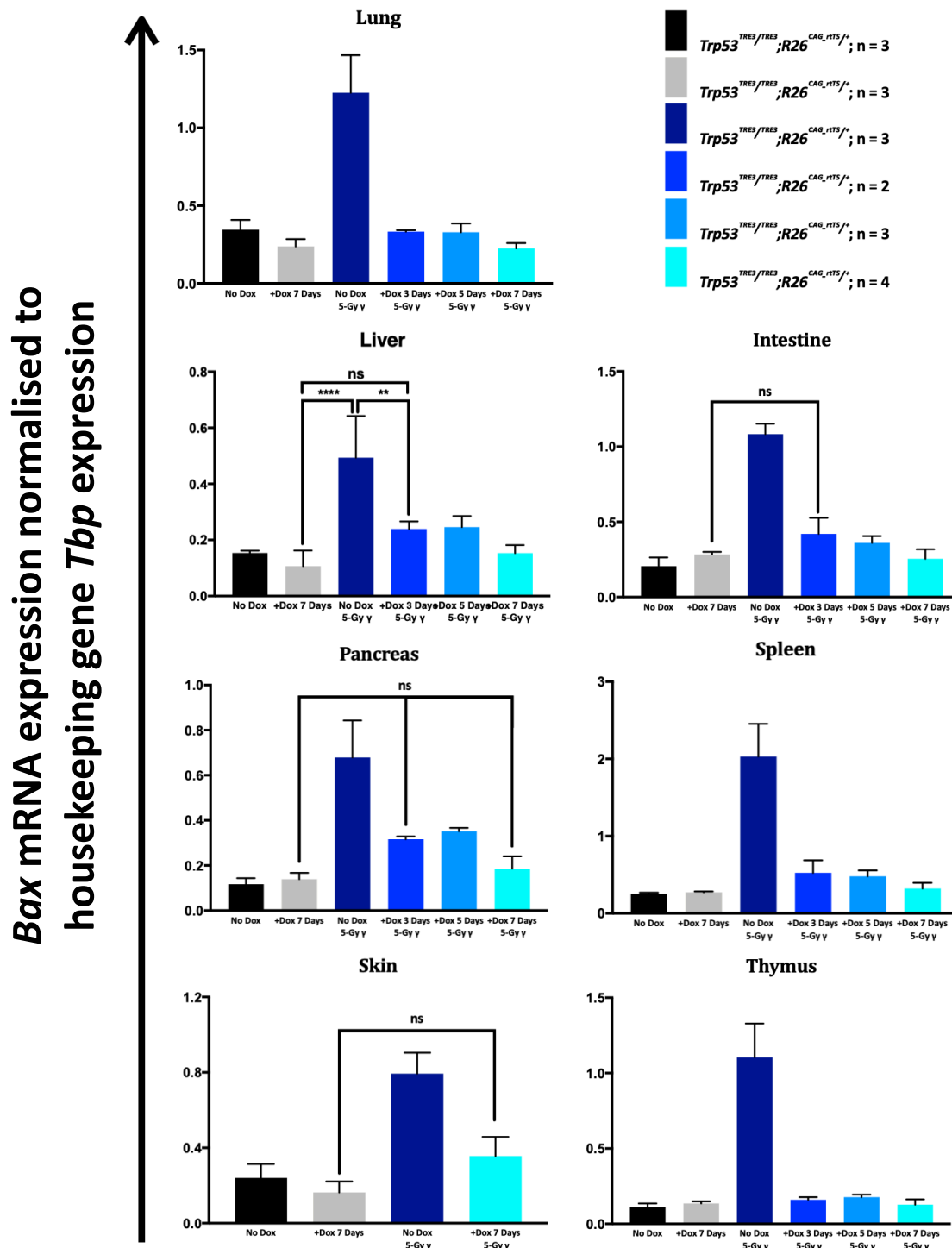


Figure 2.17. p53-dependent γ -irradiation-induced up-regulation of *Bax* expression showed repression of p53 transcription activity by three days of Dox treatment. Plotted were the mean quantified relative *Bax* mRNA level of the animals in each treatment group (n = number of animals in the group) while error bar denotes the standard deviation. Note that the scale of the y-axis representing relative *Trp53* mRNA level is not necessarily the same across the tissues. One-way ANOVA test was used to analyse the statistic significance of the differences between the treatment groups/timepoints (ns = non significant; **: p = 0.0048; ****: p < 0.0001). Primers specific to *Bax* and *Tbp* mRNA were used in the qPCR analysis and their details are listed in **Table M.6b** in the **Methods and Materials** chapter.

To examine whether this induction by p53 in all tissues is specific to *Bax* or general to other p53 target genes as well, the mRNA expression of two other direct p53 targets, namely *Puma* (*p*53 *u*pregulated *m*odulator of *a*poptosis) and *Cdkn1a*, were analysed in the same manner. *Puma*, like *Bax*, encodes a pro-apoptotic protein Puma that is a member of the Bcl-2 apoptotic protein family. It functions to interact with anti-apoptotic Bcl-2 proteins to free Bax and/or Bak to trigger apoptosis via the mitochondrial pathway. Regulated by transcription factors, Puma is expressed upon various signals in both p53-dependent and -independent manners (Nakano & Vousden 2001; Melino et al. 2004; Matallanas et al. 2007; Ming et al. 2008). *Cdkn1a*, on the other hand, connects DNA damage to cell cycle arrest instead of apoptosis. This gene expresses a cyclin-dependent kinase inhibitor protein p21^{Cip1} (alternatively p21^{Waf1}) that limits cell cycle progression by primarily binding and thus inhibiting the activity of CDK2 (cyclin-dependent kinase 2) in response to DNA damage signals channeled through p53 (El-Deiry 1993; Brugarolas et al. 1995). The p21^{Cip1} protein also interacts with PCNA (proliferating cell nuclear antigen) to regulate S-phase DNA synthesis (Waga et al. 1994). The expression of *Puma* and *Cdkn1a* mRNA in the same samples as those in **Figures 2.16 and 2.17** is shown in **Figures 2.18 and 2.19**, respectively. With the exception of *Puma* in the liver where unexpectedly high variations were observed, transcription of both *Puma* and *Cdkn1a* exhibited patterns of mRNA expression similar to that of *Bax*. In conclusion, the p53-dependent induction of *Bax*, *Puma* and *Cdkn1a* upon γ -irradiation occurred in all tested tissues (except *Puma* in liver, the irregularity of the data was likely due to poor RNA quality resulted from compromised extraction) and can all be used as a readout of p53's activities.

Puma mRNA expression induction by γ -irradiation is p53-dependent

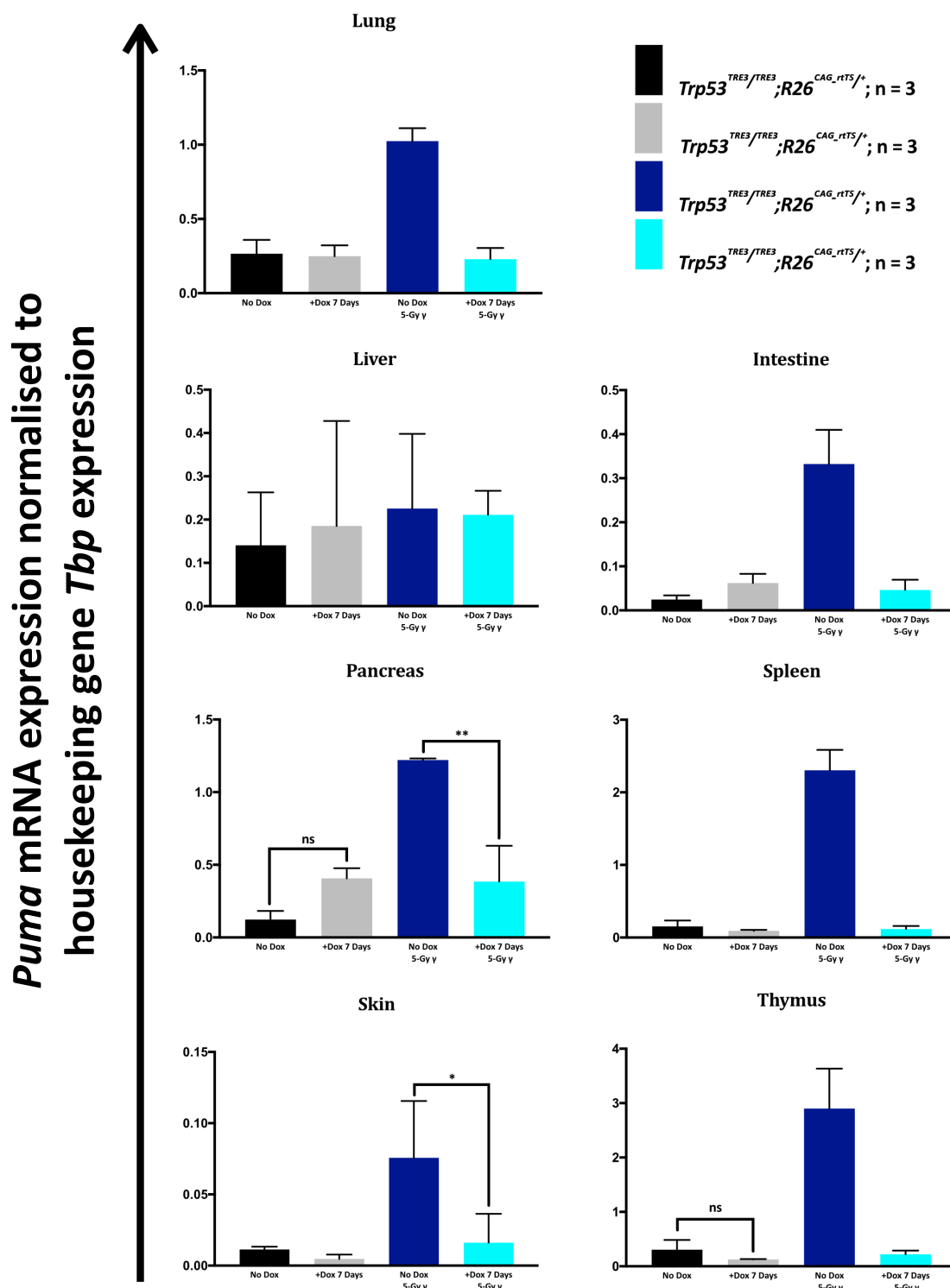


Figure 2.18. γ -irradiation induced *Puma* mRNA up-regulation is dependent on p53. Plotted are the mean quantified relative *Puma* mRNA levels in the indicated tissues of the animals in each treatment group (n = number of animals in the group) while error bar denotes the standard deviation. Note that the scale of the y-axis representing the relative mRNA level is not necessarily the same across the tissues. One-way ANOVA test was used to analyse the statistic significance of the differences between the treatment groups (ns = non significant; *: $p = 0.0470$; **: $p = 0.0034$). Primers specific to *Puma* and *Tbp* mRNA were used in the qPCR analysis and their details are listed in **Table M.6b** in the **Methods and Materials** chapter.

**BLANK
PAGE**

Cdkn1a mRNA expression induction by γ -irradiation is p53-dependent

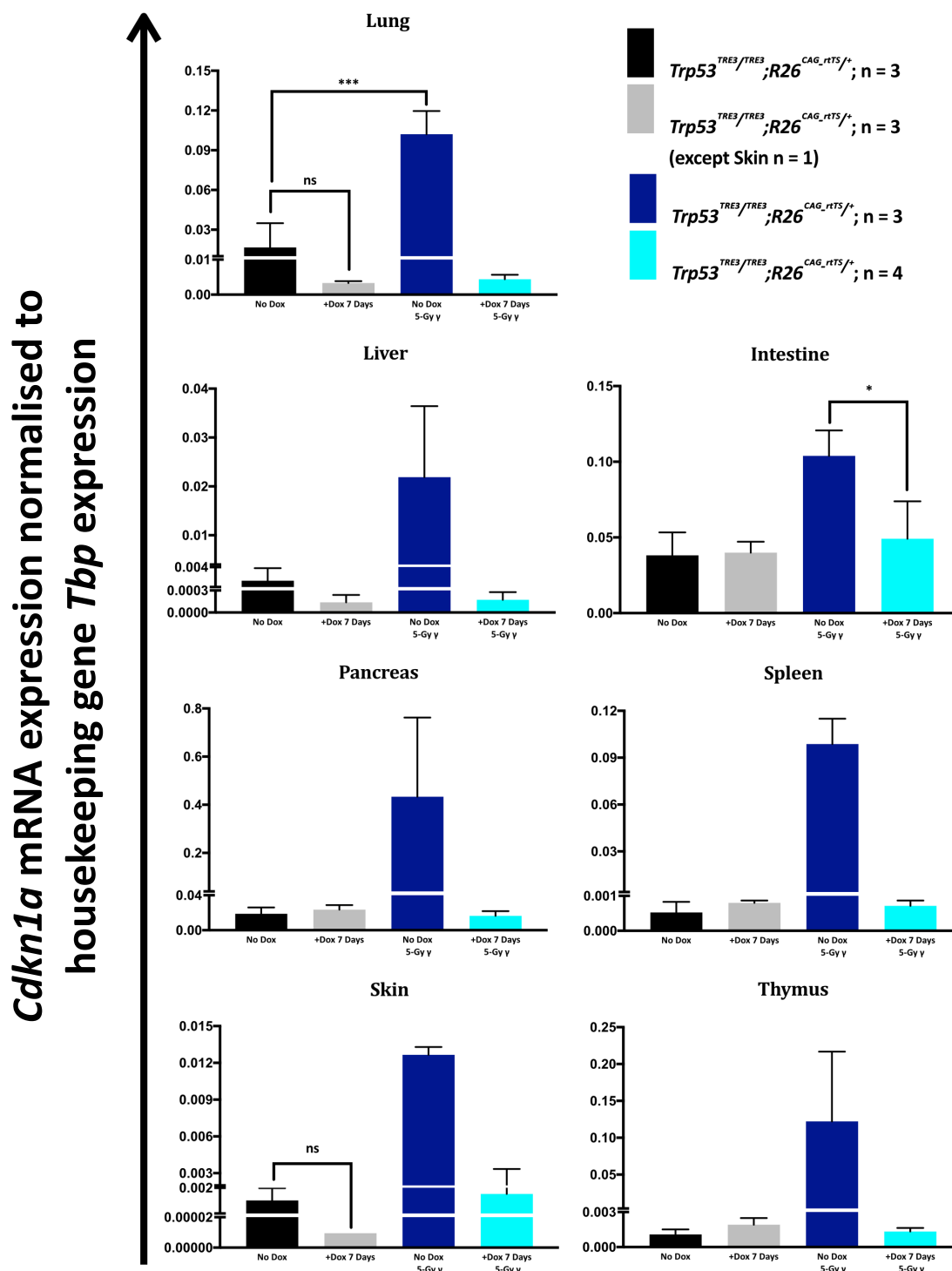


Figure 2.19. γ -irradiation induced *Cdkn1a* mRNA up-regulation is dependent on p53. Plotted are the mean quantified relative *Cdkn1a* mRNA levels of the indicated tissues of the animals in each treatment group (n = number of animals in the group) while error bar denotes the standard deviation. Note that the scale of the y-axis representing the relative mRNA level is not necessarily the same across the tissues. One-way ANOVA test was used to analyse the statistic significance of the differences between the treatment groups (ns = non significant; *: $p = 0.0186$; ***: $p = 0.0002$). Primers specific to *Cdkn1a* and *Tbp* mRNA were used in the qPCR analysis and their details are listed in **Table M.6b** in the **Methods and Materials** chapter.

Using this approach, the kinetics of recovery of p53 protein transcriptional activity in different tissues after removal of Dox treatment was investigated. In this experiment, *Trp53^{TRE3/TRE3;R26^{CAG-rtTS}/+}* mice received a 7-day Dox treatment, followed by withdrawal of Dox treatment for either 3 or 5 days before whole body, 5 Gy γ -irradiation. Tissues were collected for mRNA quantification 5 hours after irradiation. In this instance, *Bax* mRNA expression was used as the parameter to gauge p53 protein activities and the results are plotted in **Figure 2.20**. Consistent with the kinetics of p53 re-expression following Dox withdrawal (**Figure 2.14**), irradiation-dependent *Bax* expression was clearly seen in all tissues three days after removal of Dox treatment and was comparable to the level observed in WT mice (**Figure 2.20**).

p53 transcription activity recovered three days after Dox withdrawal

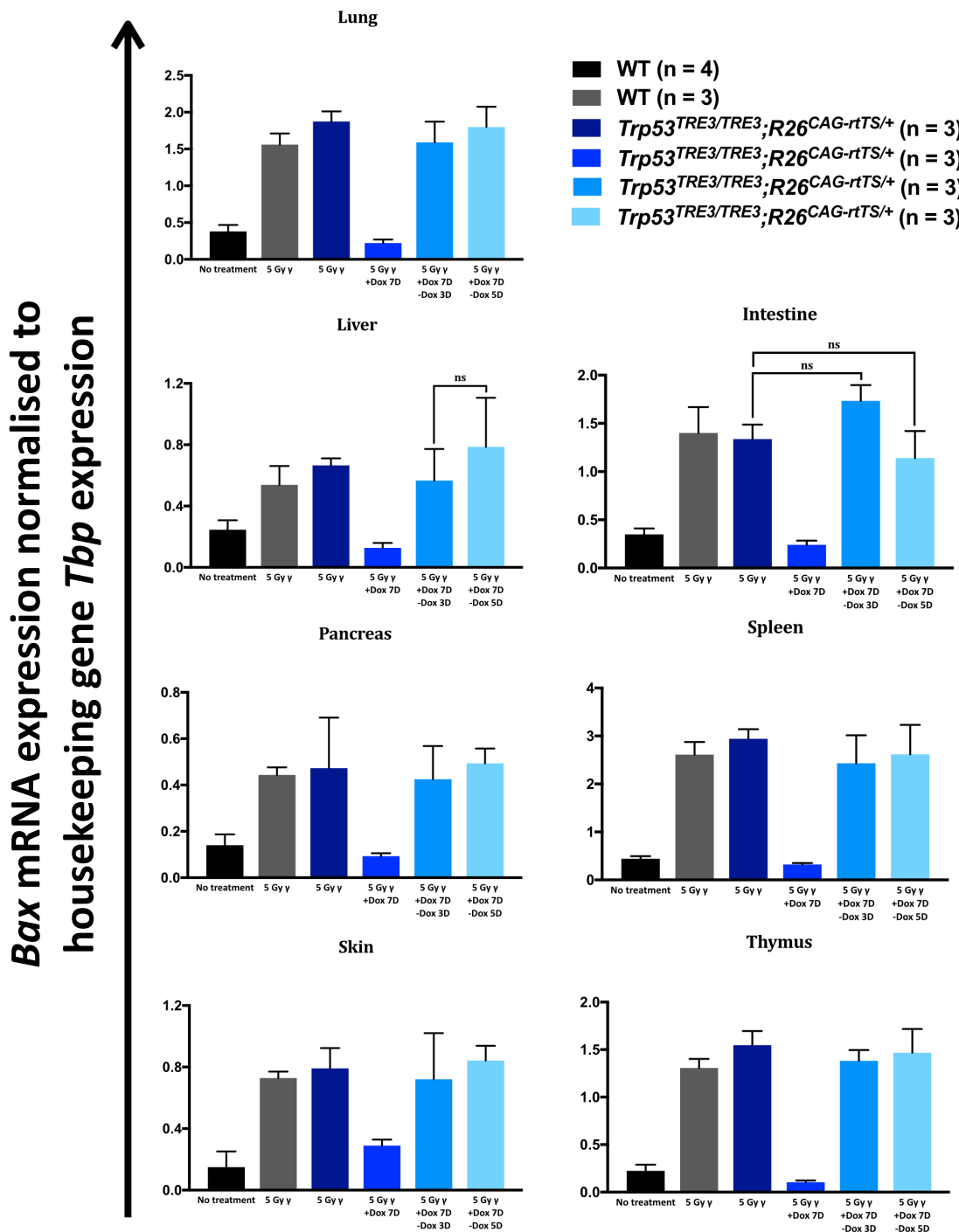


Figure 2.20. Recovery of p53 activity after removal of Dox treatment. *Bax* mRNA expression level was used as a parameter to assess how fast p53 activities recovered from repression after Dox treatment removal. Plotted are the mean quantified relative *Bax* mRNA levels of the indicated tissues of the animals in each treatment group (n = number of animals in the group) while error bar denotes the standard deviation. Note that the scale of the y-axis representing the relative mRNA level is not necessarily the same across the tissues. One-way ANOVA test was used to analyse the statistic significance of the differences between the treatment groups/timepoints (ns = non significant). Primers specific to *Bax* and *Tbp* mRNA were used in the qPCR analysis and their details are listed in **Table M.6b** in the **Methods and Materials** chapter.

2.4 The antisense gene *Wrap53*

Analysis of the gene structure of *Trp53* in mouse revealed that the antisense gene *Wrap53* is encoded in the promoter region of *Trp53*. This antisense gene encodes two functional mRNAs, namely *Wrap53 α* and *Wrap53 β* which share the first six exons. *Wrap53 α* is an antisense mRNA expressed following DNA damage signals that stabilises *Trp53* mRNA by complementarily binding to its 5' UTR (Mahmoudi et al. 2009). The other transcript encodes the *Wrap53 β* protein, also named TCAB1, which is involved in the maintenance of nuclear Cajal bodies, DNA repair and telomere elongation in human cell lines (Venteicher et al. 2009; Tycowski et al. 2009; Mahmoudi et al. 2010; Zhong et al. 2011; Henriksson et al. 2014; Freund et al. 2014). **Figure 2.21** illustrates *Wrap53*'s gene structure in mouse and expression of its gene products. In the mouse genome, *Trp53* and *Wrap53* do not overlap though their transcription start sites (TSS) are only 98 bp apart (NCBI). Although the exons of *Wrap53* were carefully avoided in placing the *TRE*, it is possible that expression of the gene is affected and/or subject to repression imposed by the *TRE* system. If so, it will be important to dissect the functional contribution of the antisense gene to results yielded from experiments using the system. To determine whether or not this is the case, I conducted some further experiments as described below.

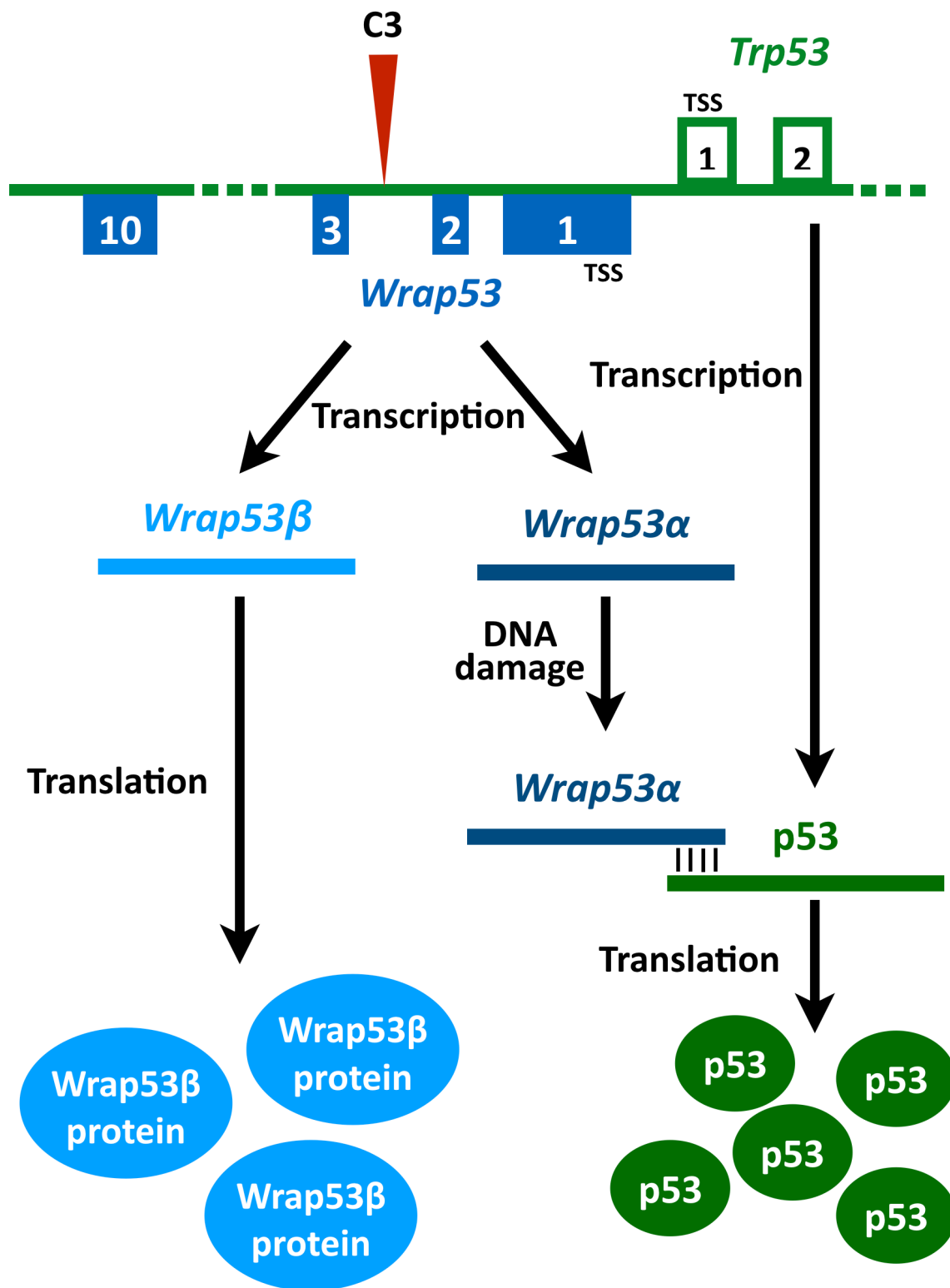


Figure 2.21. Reported functions of the *Wrap53* gene. The first mRNA transcript *Wrap53α* is antisense to the *p53* mRNA and, once expressed upon DNA damage signals, it binds to the 5' end of *p53* mRNA, stabilising it. The other transcript *Wrap53β* encodes the WD40 protein *Wrap53β* (or TCAB1), the human analog of which was reported to be involved in maintenance of nuclear Cajal bodies, DNA repair and telomere elongation, though no committed investigations on the mouse gene have been published. The two transcripts share the first 6 exons. The red pointer indicates the *TRE* insertion site C3; Deep blue boxes represent exons of *Wrap53*; Green empty boxes denote the first two exons, non-coding, of *Trp53*.

2.4.1 *Wrap53* mRNA expression *in vivo*

First, I asked whether *Wrap53* was expressed in mouse tissues and, if so, whether its expression was changed by the presence of the *TRE* alone and in the presence of rtTS and Dox. Since no reports have characterised *Wrap53* gene function in mice and no antibodies are available for the *Wrap53* β protein, expression of the gene was assessed at the mRNA level by qPCR. mRNA was isolated from various tissues from six-week old WT, and untreated and Dox-treated *Trp53^{TRE3/TRE3;R26^{CAG-rtTS/+}}* mice and total *Wrap53* α and β mRNA levels were determined by qPCR (**Figure 2.22**). It was not possible to quantify the level of the α transcript independent of β as the entirety of transcript α overlaps with the first six exons of transcript β . However, a pair of qPCR primers specific for transcript β were designed and used to determine its expression in the later part of this section. The plot in **Figure 2.22** shows that *Wrap53* was expressed to comparable levels in all tested tissues except skin, where the mRNA level was not detectable by the primers. It also indicates that the insertion of *TRE* in both alleles of the gene did not disrupt or reduce *Wrap53* mRNA expression in tissues. Note that in lungs the expression was slightly affected by the *TRE* insertion, though the reason for that and what it means biologically remains unclear. Importantly, this experiment showed that mRNA expression of the *Wrap53* gene was repressible by the *TRE* system upon Dox treatment.

To determine whether the repression of *Wrap53* α and *Wrap53* β both contributed to the observed reduction in total *Wrap53* mRNA, primers specific to *Wrap53* β (annealing to exon 7 and 8 respectively) were used to quantify its expression level (**Figure 2.23**). It is clear that *Wrap53* β was similarly expressed in the tissues and its expression was also repressed by the *TRE* system following administration of Dox. However, the expression level of *Wrap53* β quantified here is not directly comparable to the combined level reported in **Figure 2.22** because the primers used were unlikely to have exactly the same efficiency in the qPCR quantification. Without primers that recognise specifically the α transcript, it cannot be known

for certain whether *Wrap53 α* was also expressed and repressed by the system as it is possible that the expression detected in **Figure 2.22** was solely contributed to by *Wrap53 β* . However, the co-repression of *Wrap53 α* by the *TRE* system, if present, would be of less concern because it functions solely to regulate the *Trp53* mRNA level (Mahmoudi et al. 2009).

Wrap53 α and *Wrap53 β* mRNA expressed in tissues is repressible by *TRE* system upon Dox

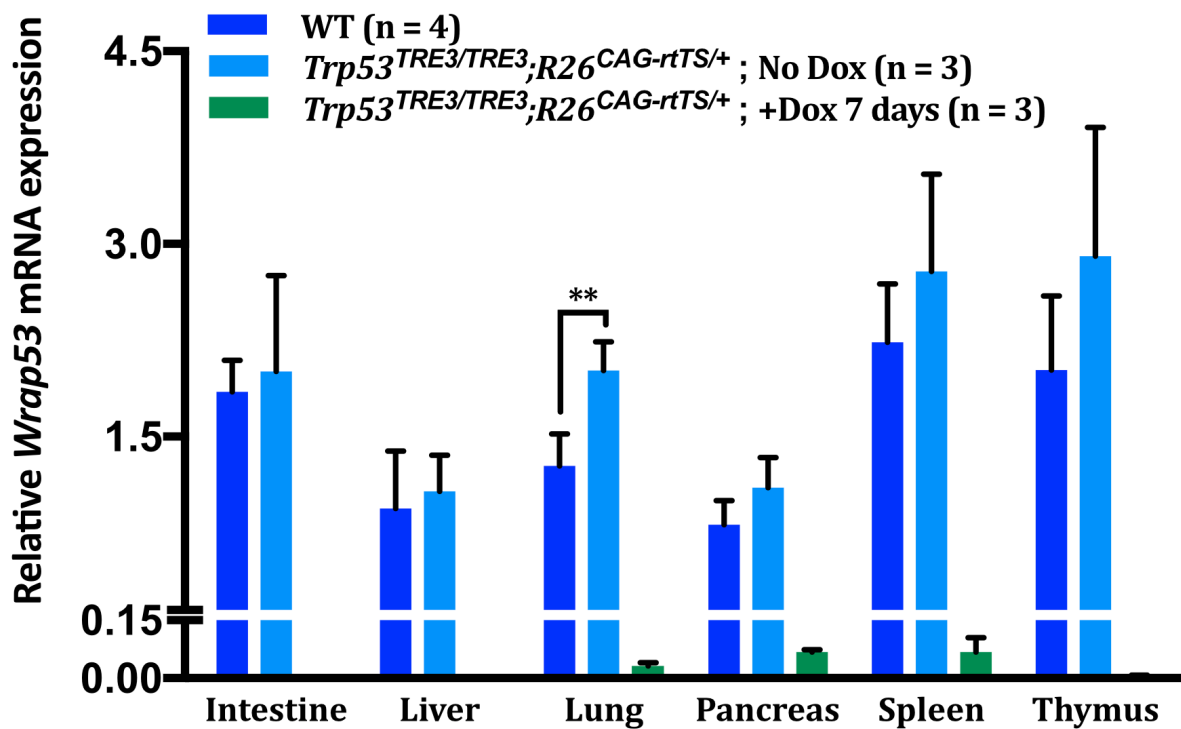


Figure 2.22. The *Wrap53* gene is expressed at mRNA level in all tissues except skin and is subject to repression by the *TRE* system upon Dox treatment. n denotes the number of animals in the genotype group. The quantification failed to detect any *Wrap53* expression in skin. A One-way ANOVA test was carried out to assess the statistical significance between WT and homozygous *TRE* lungs (**: $p = 0.0080$). Note that the primers used in the qPCR detected both transcript *Wrap53 α* and *Wrap53 β* and their details are listed in **Table M.6b** in the **Methods and Materials** chapter.

Wrap53 β mRNA expression is repressed by *TRE* system upon Dox

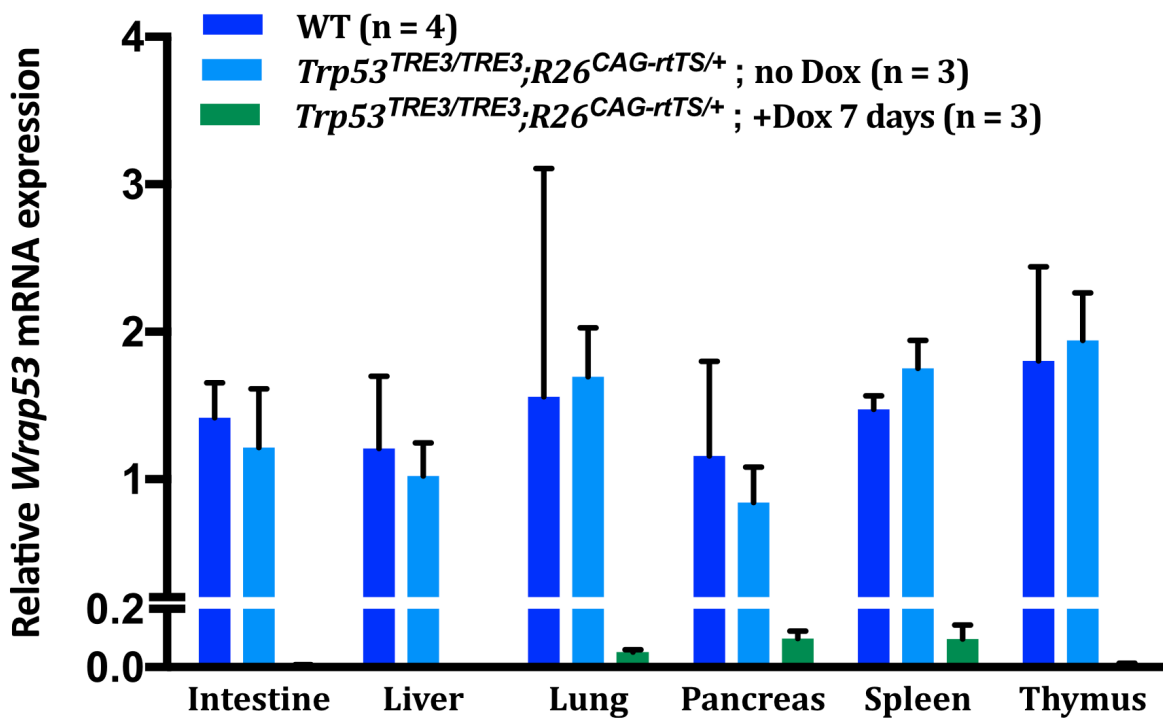


Figure 2.23. Transcript *Wrap53* β expressed in tissues is also subject to repression by the *TRE* system upon Dox treatment. n denotes the number of animals in the genotype group. The quantification failed to detect any *Wrap53* β expression in skin. The primers used are listed in Table M.6b in the Methods and Materials chapter.

2.4.2 Strategies to address the co-repression of *Wrap53*

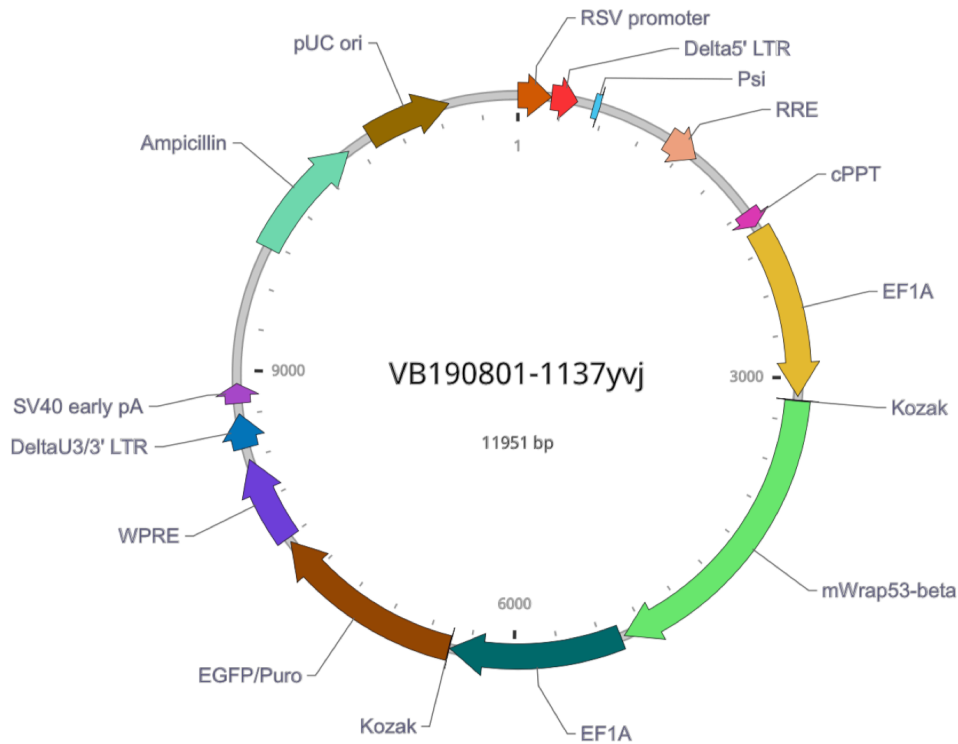
The capacity to rapidly and reversibly repress expression of endogenous *Trp53* displayed by the TRE-p53 model described in this thesis is undeniably an extremely valuable aid to understand when and how p53 exerts its physiological and tumour suppressor roles. It is a model far superior to the existing ones. However, co-repression of *Wrap53* by the *TRE* system has the potential to cloud experimental analyses of at least some of p53's functions and it will be important to be able to attribute experimental results to changes in *Trp53* alone. Given the circumstances, a feasible solution is to add in to the genome an extra copy of the *Wrap53* β with

expression matching the WT allele but not regulated by the *TRE* system. This could compensate for the repressed endogenous expression by the *TRE* system in the presence of Dox. The first assumption here is that the ectopic expression level brought in by the extra copy (in the absence of Dox) has no impact cellularly or physiologically. Secondly the designed knock-in of the gene expressed in all tissues in a manner, level-wise and temporally, comparable to the endogenous gene.

As a preliminary test of the strategy in the future, I will assess in MEFs the replacement of the repressed *Wrap53β* expression by introducing a constitutively expressed *Wrap53β* transgene by Lentivirus. To this end, the coding sequence of *Wrap53β* transcript was cloned into a Lentivirus vector under a constitutive promoter, which was outsourced to be carried out by AMSBIO Ltd. **Figure 2.24** shows a map of the Lentivirus DNA vector carrying the *Wrap53β* cDNA. The original 5' and 3' UTR of *Wrap53β* were included to preserve the post-transcriptional regulation of the transcript, if any. The first intron was also retained as other studies indicated that retention of an intron promoted successful mRNA processing of the ectopic coding sequences. Silent point mutations were introduced to the annealing sites of the qPCR primers used so that mRNA expressed from the *Wrap53β* transgene could be distinguished from the endogenous alleles in qPCR quantification. Finally, a FLAG-tag sequence was also added to the 5' end of exon 1 to identify the ectopic *Wrap53β* protein.

This Lentivirus construct will be used to introduce the *Wrap53β* transgene into *Trp53^{TRE3}/TRE3;R26^{CAG-rtTS}/+* MEFs and the expression of ectopic *Wrap53β* RNA and protein will be determined in the presence and absence of Dox. If successful, a similar construct could be used to introduce the *Wrap53β* transgene into *Trp53^{TRE3/TRE3};R26^{CAG-rtTS}/+* mice to compensate for the *TRE*-dependent repression in the presence of Dox.

(a)



(b)

Name	Position	Size (bp)	Type	Description
RSV promoter	1-229	229	Promoter	['Rous sarcoma virus enhancer/promoter']
Delta5' LTR	230-410	181	LTR	['Truncated HIV-1 5' long terminal repeat']
Psi	521-565	45	Miscellaneous	['HIV-1 packaging signal']
RRE	1075-1308	234	Miscellaneous	['HIV-1 Rev response element']
cPPT	1803-1920	118	Miscellaneous	['Central polypurine tract']
EF1A	1950-3128	1179	Promoter	['Human eukaryotic translation elongation factor 1 alpha1 promoter']
Kozak	3153-3158	6	Miscellaneous	['Kozak translation initiation sequence']

Name	Position	Size (bp)	Type	Description
mWrap53-beta	3159-5236	2078	ORF	None
EF1A	5261-6439	1179	misc_feature	None
Kozak	6440-6445	6	misc_feature	None
EGFP/Puro	6446-7762	1317	misc_feature	None
WPRE	7792-8389	598	Miscellaneous	['Woodchuck hepatitis virus posttranscriptional regulatory element']
DeltaU3/3' LTR	8471-8705	235	LTR	['Truncated HIV-1 3' long terminal repeat']
SV40 early pA	8778-8912	135	PolyA_signal	['Simian virus 40 early polyadenylation signal']
Ampicillin	9866-10726	861	ORF	['Ampicillin resistance gene']
pUC ori	10897-11485	589	Rep_origin	['pUC origin of replication']

Figure 2.24. *Wrap53 β* cDNA cloned in a Lentivirus DNA vector. (a) Map of the Lentivirus vector carrying the *Wrap53 β* cDNA. mWrap53-beta in the plasmid map denotes the *Wrap53 β* cDNA, which was cloned to carry the first intron and silent mutations that allow distinction from the transcript expressed from the endogenous gene following qPCR quantification. A FLAG-tag sequence was also cloned upstream of the 5' end of *Wrap53 β* cDNA, though it is not shown in the map. (b) Details of the plasmid components indicated in the map. Cloning of the plasmid was outsourced to AMSBIO Ltd.

2.5 Discussion

2.5.1 The TRE-p53 model and its applicability

The TRE-p53 mouse model allows rapid and reversible switching of endogenous *Trp53* expression and function. Administration of Dox to TRE-p53 mice led to systemic repression of p53 within 2 - 3 days while subsequent withdrawal of Dox treatment allows re-expression of *Trp53* in the same timeframe. Although not as rapidly as the tamoxifen-dependent switching of p53^{ERTam} protein activity (Christophorou et al. 2005), those animals are forced to develop in the absence of p53 function as tamoxifen causes abortion. In contrast, the TRE-p53 model allows normal p53 function during embryogenesis, thus ruling out the potential effect of the speculated compensatory signalling during embryogenesis (Danilova et al. 2008) but retaining the ability to regulate p53 in adult mice. Importantly, the introduction of the *TRE* did not appear to have any impact on the normal regulation of *Trp53* expression in the absence of Dox but rendered it sensitive to rapid repression by rtTS in the presence of Dox. Thus the TRE-p53 mouse model provides rapid switching of *Trp53* expression. Although experiments described here are based on systemic toggling of p53 in all tissues, tissue-specific expression of rtTS can provide analysis of individual tissues or cell lineages (e.g. tissue stem cells).

However, one caveat with the TRE-p53 model is the co-regulation of the closely located antisense *Wrap53* (see **Section 2.4.1**). While this might be problematic for some applications of the model, it is unlikely to affect analyses of well defined p53-specific functions, including activation of its target genes as demonstrated by the experiments reported in **Section 2.3.7**.

As described in **Section 2.4.2** ectopic expression of *Wrap53* could be used to compensate for any disruption of *Wrap53* functions in the presence of Dox. Alternatively, replacement of Dox-repressed endogenous *Trp53* expression in the TRE-p53 mice by ectopic p53 expression can be used to identify any effects of repressing *Wrap53* alone. This can be done by the use of the Rosa26-p53 mouse model constructed in my host laboratory (unpublished data), which has the full coding sequence of a *Trp53* transcript (including intron 4) knocked into

the constitutively and ubiquitously expressed *Rosa26* locus. The *in vivo* and *in vitro* expression from this ectopic allele of *Trp53* at both mRNA and protein level was comparable to the endogenous allele and able to compensate for loss of the endogenous *Trp53* allele completely, which suggested that the transcriptional control and all its isoform variants are largely dispensable for the gene's functions, and that the post-translational regulation is the arbiter of its activity.

2.5.2 Significance of the results in this Chapter

While confirming the functionality of the *TRE* system to rapidly regulate endogenous p53 expression and function, these TRE-p53 mice have already revealed novel findings regarding p53's expression and transcriptional activities in radio-sensitive and radio-resistant tissues. For example, previous reports using various approaches such as *lacZ* and *eGFP* reporter models to determine p53's expression and functions in tissues, (Komarova et al. 1997; Goh et al. 2012; Chen et al. 2015; Tanikawa et al. 2017) were largely confined to radio-sensitive tissues, notably spleen and thymus. Also, these studies were based on a comparison between WT and germline p53-deleted animals that were likely to have exhibited a compensated phenotype resulting from aberrant expression of the other p53-family proteins p63 and p73 during embryogenesis. Therefore, it is not clear whether phenotypes observed in adult germline p53 knockout mice accurately reflect acute loss of p53 function in adults (that have developed in the presence of normal p53). Moreover, the focus on radio-sensitive tissues where noticeable changes could be detected may overlook the more subtle effects of p53 in other tissues. The reported "tissue-specific" expression of p53 target genes including *Puma*, *Bax* and *Cdkn1a* in radio-sensitive tissues observed by comparing p53-WT vs germline p53-null animals might not be accurate (MacCallum et al. 1996; Komarova et al. 1997; Bouvard et al. 2000; Fei et al. 2002; Fei & El-Deiry 2003). Whereas some reports suggest p53 "selects to activate" some targets but not the others, e.g. *Puma* vs *Cdkn1a*, in certain conditions and tissues, others have inferred that p53 and its

pathways somehow “dictate” the outcome of DNA damage - apoptosis or growth arrest - and thus defining the radio-sensitivity of individual tissues. Experiments described in **Section 2.3.7** using the TRE-p53 model cast doubt on these interpretations. First, *Trp53* mRNA was expressed in all tested tissues (**Figure 2.12**, **Figure 2.15**, and **Figure 2.17**). Second, p53 was transcriptionally functional and capable of inducing *Bax*, *Puma* and *Cdkn1a*, upon DNA damage signals in all these tissues, irrespective of whether they were categorised as radio-sensitive or not. Induction of these genes was p53-dependent. Despite induction of the pro-apoptotic genes *Bax* and *Puma* in all tested tissues, radio-sensitive and radio-resistant alike, not all underwent apoptosis (IHC TUNNEL staining carried out on intestine, spleen, lungs, liver and skins confirmed that; data not shown). This is in agreement with the hypothesis that different cell types, or tissues, exhibit different thresholds for apoptosis and while p53 might shift the equilibrium, for example in response to DNA damage, it is not the sole determinant of cell fate. Furthermore, as both apoptotic and cell cycle arrest genes were induced by p53 upon irradiation in all tissues alike, the “binary decision” between growth arrest and apoptosis is clearly dependent on cell/tissue contexts rather than differential p53 activity in such contexts.

**BLANK
PAGE**

Chapter 3:

Investigation of *Trp53* functions

Although there are over 100,000 publications regarding p53, we are nowhere close to understanding even part of its functions as a tumour suppressor. How exactly does p53 distinguish tumorous growth from normal physiological process such as regeneration in wound-healing? And what is the timing of such function in tumourigenesis? Moreover, study of p53's physiological functions such as metabolism and autophagy have long been overshadowed by the overwhelming interests on the tumour suppressive function of p53 as well as the highly regarded proposed role of "guardian of the genome" (Lane 1992). This is partly due to the limitations and caveats of existing germline knockout and irreversible switchable mouse models of p53 (discussed in **Chapter 1**). To overcome these limitations and refocus to a more complete and comprehensive study of p53's functions, the TRE-p53 mouse model that allows rapid, reversible and non-invasive repression of p53 was developed. Using this model, I have investigated the impact of systemic denial of p53 functions on normal physiology in adult mice. I have also designed experiments to temporally dissect the impact of p53 loss on the genesis of skin squamous cells carcinomas.

3.1 Effect of systemic p53 denial in adulthood

3.1.1 Transient p53 denial in adult mice has no effect

The results in Chapter 2 clearly show that administration of doxycycline (Dox) for 7 days silences p53 expression in *Trp53^{TRE3/TRE3};R26^{CAG-rtTS/+}* mice. These mice exhibited no obvious health issues and their body condition (BC) scoring and weight tracking were no different to untreated *Trp53^{TRE3/TRE3};R26^{CAG-rtTS/+}* and wild type animals. Moreover, careful post-mortem examination did not reveal any morphological abnormalities. These results suggest that any physiological roles p53 plays in normal unchallenged adult tissues, if any, are likely too subtle to be revealed from the vantage point of the whole body physiological condition. Given majority of p53's functions involve its transcription activity, these functions may be revealed by comparing the transcriptome of tissues from the treated and untreated (and WT) animals.

3.1.2 Long-term *Trp53* repression in adults results in tumour formation

The question I asked here was what the impact would be when *Trp53* is repressed for the long-term in adulthood and how the observations would compare with germline p53 knockout mice. Reported by Donehower *et al.* in 1992, mice with homozygous germline deletion of p53 spontaneously develop tumours, usually lymphomas and thymomas. 74% of these mice developed tumours within 20 weeks on average (8 weeks the earliest), while no tumours were observed in WT mice after 9 months (Donehower *et al.* 1992). However, these mice lacked p53 during embryogenesis and it was unclear whether tumour formation results from loss of p53 during embryogenesis, during postnatal development or in adulthood or a combination of all three. Furthermore, any other phenotypes observed would be indicative of p53's physiological functions including for example cell metabolism, mitochondrial respiration and autophagy (Vousden & Ryan 2009; Matoba *et al.* 2006; Ryan 2011).

To address this question, five-week old *Trp53^{TRE3/TRE3};R26^{CAG-rtTS/+}* and wild type mice were administered Dox continuously (or not in the case of control animals). By 6.5 months of Dox administration, five out of twelve *Trp53^{TRE3/TRE3};R26^{CAG-rtTS/+}* mice (*Trp53*-repressed) developed severe symptoms such as a distended abdomen and rapid breathing and were euthanised. Three out of these five mice showed spontaneous tumours in the spleen and thymus, while no tumours were detected in the other two mice.

In addition, three apparently healthy experimental *Trp53^{TRE3/TRE3};R26^{CAG-rtTS/+}* mice (and two control mice) were sacrificed for analysis after 6 months of Dox administration. Despite no health concerns, two out of these three *Trp53^{TRE3/TRE3};R26^{CAG-rtTS/+}* mice had developed a single thymic lymphoma of a substantial size in their chest cavity (**Figure 3.1**). No other tumours or abnormalities were detected and all the other organs appeared the same as in the wild type control animals (not shown). To confirm that *Trp53* was repressed after 6 months of Dox treatment, mRNA was extracted from various tissues of these three mice and *Trp53* mRNA

quantified by qPCR (**Figure 3.2**). In all tissues analysed, including the thymoma, *Trp53* RNA expression was efficiently repressed. Note that no amplification product of *Trp53* mRNA was detected by qPCR on skin samples of the Dox-treated mice as the repressed mRNA level was too low to be detected (the relative *Trp53* mRNA level in skin of the non-treated mice ranged at the level of 10^{-6}).

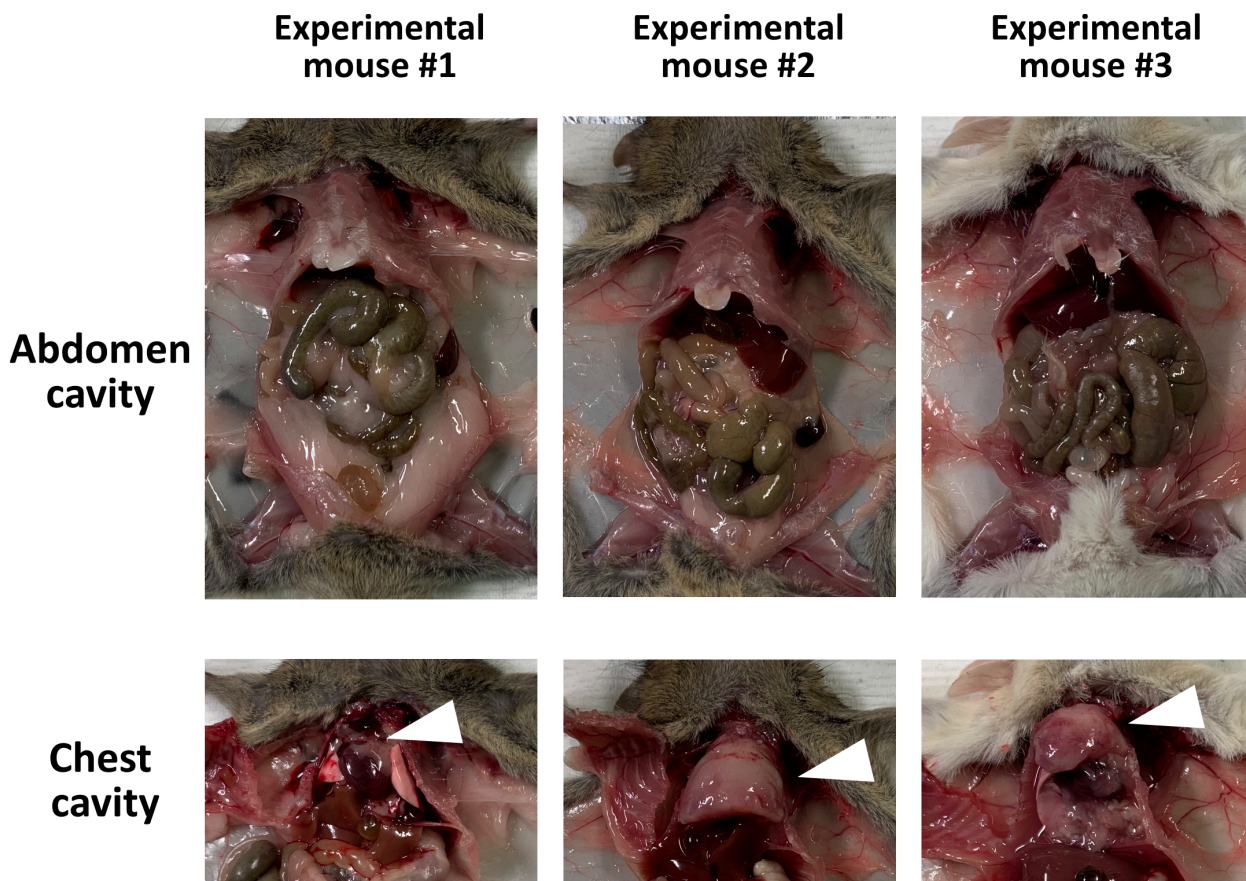


Figure 3.1. Autopsies revealed development of thymic lymphoma in two of the experimental mice after 6 months of Dox treatment. Two experimental mice (middle and right panels) developed a single, solid thymoma that filled almost the entire volume of the chest cavity. All other organs in these mice appeared normal without any tumour growth, so were all organs of experimental mouse #1. White pointers in the lower panel indicate the normal thymus (Expt mouse #1) and thymic lymphoma (Expt mouse #2 and #3).

Trp53 expression remained repressed in tissues after 6 months of Dox treatment

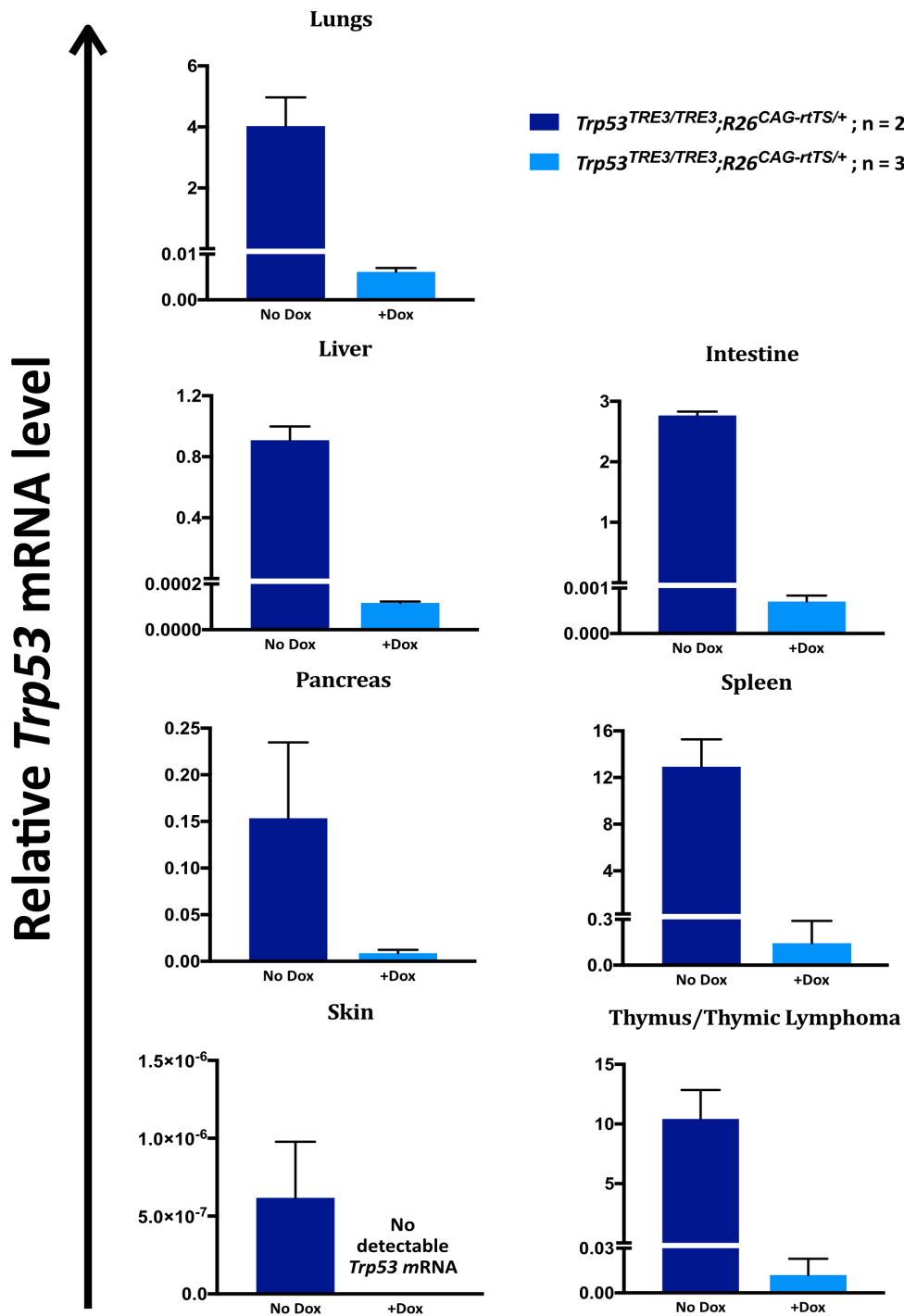


Figure 3.2. Long term repression of *Trp53* in tissues. Plotted were the mean quantified relative *Trp53* mRNA level in tissues of animals being treated with Dox for 6 months (n = number of animals in the treatment groups) while error bars denote standard deviation. The scale of the y-axis representing relative *Trp53* mRNA level is not necessarily the same across the tissues. Note that the qPCR failed to detect any *Trp53* mRNA in the skin of the Dox-treated animals, though it picked up signals of *Trp53* transcript at a relative level range of 10⁻⁶ in the control group. Note that 2 out of the 3 mice treated with Dox developed thymic lymphoma, which were analysed instead of thymus in these animals. Primers specific to *Trp53* and *Tbp* mRNA were used in the qPCR analysis and their details are listed in **Table M.6b** in the **Methods and Materials** chapter.

Table 3.1 summarises the post-mortem observations, symptoms and types of spontaneous tumours of the eight experimental mice that have been euthanised thus far. Five out of these eight mice developed spontaneous tumours, three with thymoma and two with splenic tumours. Of the remaining three mice none showed any evidence of tumours, although two of these mice exhibited health concerns before euthanasia. The remaining four experimental mice were still receiving Dox treatment when this thesis was written and appeared healthy and tumour-free.

Table 3.1. Summary of the euthanised mice that had received long term Dox treatment to repress *Trp53*

Animal count	Length of treatment	Observations	Spontaneous tumours
1	16 weeks	<ul style="list-style-type: none"> - Enlarged/inflated intestine - Otherwise normal - Culled sick 	- None observed upon autopsy
1	16 weeks	<ul style="list-style-type: none"> - Moribund - Laboured breathing - Culled sick 	- None observed upon autopsy
1	20 weeks	<ul style="list-style-type: none"> - Enlarged spleen - Culled sick 	- Spleen enlargement may be malignant
2*	24 weeks	<ul style="list-style-type: none"> - Appeared healthy - Sacrificed for analysis - Thymoma 	- Thymoma
1*	24 weeks	<ul style="list-style-type: none"> - Appeared healthy - Sacrificed for analysis 	- None observed upon autopsy
1	28 weeks	<ul style="list-style-type: none"> - Enlarged spleen - Culled sick 	- Spleen enlargement may be malignant
1	28 weeks	<ul style="list-style-type: none"> - Laboured breathing - Inactive - Thymoma - Culled sick 	- Thymoma

* Had appeared healthy before sacrificed for analyses

Several conclusions can be drawn from these experiments. First, Dox was capable of long-term repression of p53 expression in *Trp53^{TRE3/TRE3};R26^{CAG-rtTS/+}* mice. This also suggests that there is no strong selection to restore p53 expression, at least in the tissues examined. The model can therefore be used in long term experiments such as in tandem with the chemically induced skin cancer model (see **Section 3.3** below) (Hennings et al. 1985). Second, the occurrence of spontaneous tumourigenesis appeared to be consistent with observations in germline p53 knockout mice (Donehower *et al.* 1992), though only a limited sample size is reported here. Here, five out of twelve Dox-treated mice developed spontaneous tumours in 5 - 6.5 months, three mice with thymic lymphomas and two with splenic tumours, comparable to the latency and tumour spectrum observed by Donehower *et al.* A larger cohort of animals is needed to confirm these initial observations. Lastly, that no overt phenotype (other than spontaneous tumourigenesis) was observed in these mice suggests that any effect of p53 loss on normal physiological processes, if it exists, was too subtle to be discerned from gross anatomy. Detailed microscopic analysis will be required to determine such subtle effects. Likewise, transcriptomic analysis of tissues samples following both short-term and long-term Dox treatment may be informative.

3.2 Assessment of *Trp53*'s roles in early stage skin cancer

Despite p53's undeniable role in tumour suppression, it is still unclear when p53 is lost during tumourigenesis. For example, loss of p53 delays the formation of carcinogen-induced skin papillomas (Kemp et al. 1993). These, perhaps counter-intuitive, results suggest that retention of p53 in, at least some, proto- and nascent tumour cells is beneficial and is consistent with the observation that p53 inactivation is often associated with late stages of human cancers (Vogelstein et al. 1988; Ohue et al. 1994; Leslie et al. 2002). Why is *Trp53* not inactivated from the onset of tumourigenesis but in late stages? One possibility is that the oncogenic signals that trigger p53 (and would thereby normally engage tumour suppression) arise only at later stages

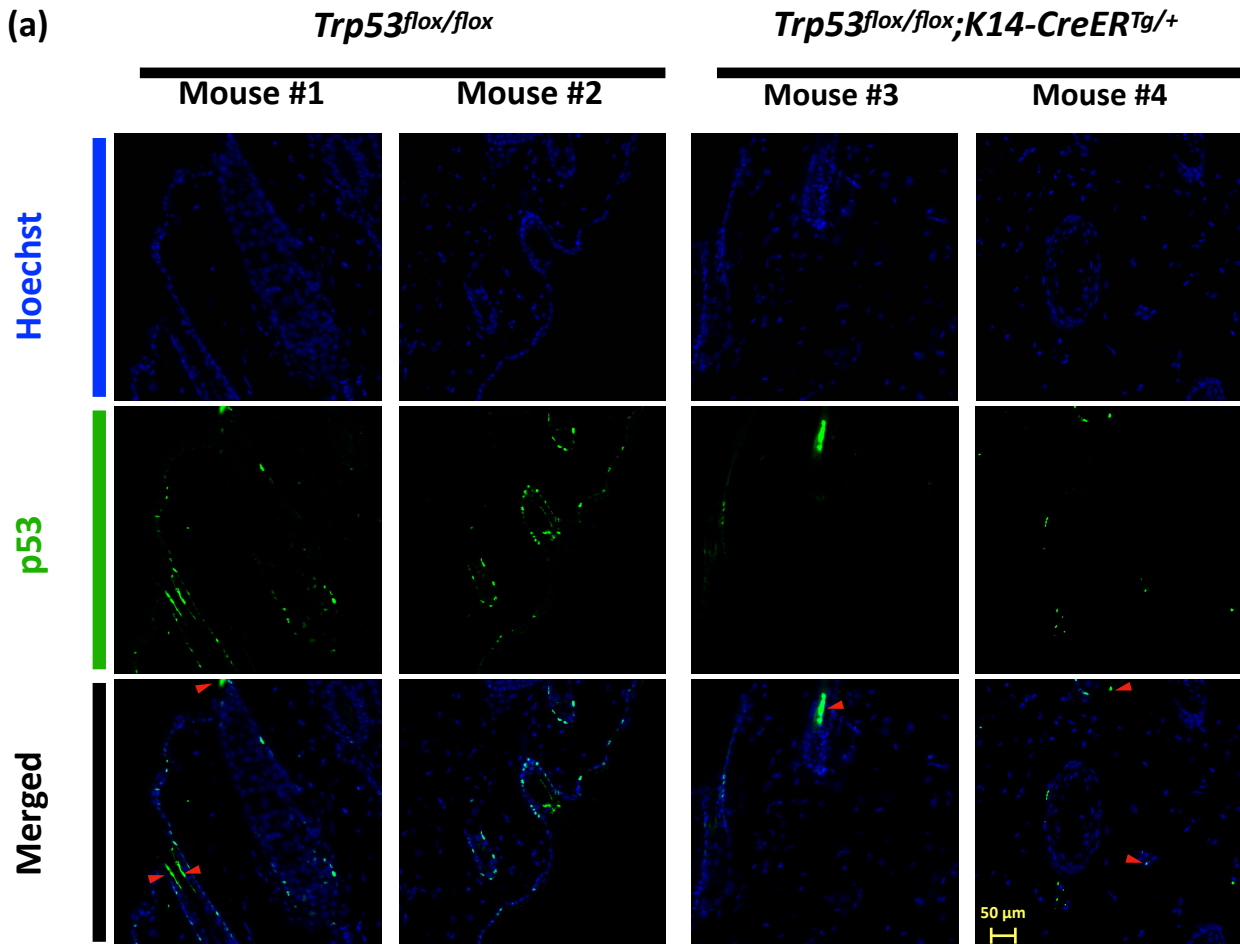
of tumour evolution and so there is no selective advantage to inactivate p53 present in nascent tumours. Alternatively, perhaps p53 confers some growth and/or survival advantage to early cancer cells that are likely to experience considerable stresses, both intracellular and micro-environmental. This notion is consistent with emerging roles of p53 in a range of physiological functions including regulation of cell metabolism, mitochondrial respiration and autophagy (Vousden & Ryan 2009; Matoba et al. 2006; Ryan 2011). Hence, retention of p53 physiological functions may be beneficial for nascent tumour cells to survive and proliferate amid various stresses associated with oncogenesis. Moreover, over half of the p53 pathway-inactivating mutations in human cancers spare p53 function but inactivate upstream or downstream components of the p53 tumour suppression pathway - potentially leaving some p53 functions intact (Junttila & Evan 2009). The ability to rapidly and reversibly regulate expression of endogenous p53 in *Trp53^{TRE3/TRE3};R26^{CAG-rtTS/+}* mice provides an ideal experimental platform to determine when and how p53 (or its inactivation) is required for carcinogen-induced skin papillomas and their subsequent transition to squamous cell carcinoma.

3.2.1 Temporal dissection of *Trp53* function in chemically induced skin cancer

Pending the generation of *Trp53^{TRE3/TRE3};R26^{CAG-rtTS/+}* mice, I investigated the role of p53 in early stage skin cancer using a Cre recombinase-dependent conditional p53 knockout mouse model, p53^{flox} (Jonkers et al. 2001). The p53^{flox} model has two advantages over germline p53-null models. First, inactivation of the *Trp53* gene can be induced at any time via tamoxifen-dependent activation of CreERT² recombinase. Second, tissue-specific inactivation of *Trp53* can be achieved by restricting CreERT² expression via the *K14* promoter to stratum basale of skin such as the inter-follicular epidermis (IFE) and the follicle bulge (FB) stem cells where chemically induced skin cancer originates (Vasioukhin et al. 1999; Lapouge et al. 2011; Abel et al. 2009). The chemically induced skin carcinogenesis model used in conjugation with the p53^{flox} model allowed visual monitoring of skin cancer development with or without *Trp53* inactivation.

Prior to the skin cancer experiment, the efficiency and cell type-specificity of *Trp53* inactivation by CreERT² was assessed. Five-week old *Trp53^{flox/flox}* and *Trp53^{flox/flox};K14-CreERTg/+* mice were treated with tamoxifen via Intraperitoneal (IP) injection for 5 consecutive days (1 mg per mouse per day) and then irradiated with 5-Gy of γ -irradiation. Dorsal skin samples were collected in 10% formalin 5 hours post irradiation and p53 protein expression in these samples was determined by immunofluorescence (IF) staining of tissue sections (**Figure 3.3a**). The IF staining clearly demonstrates significantly fewer p53-positive IFE and FB stem cells in tamoxifen treated animals, suggesting that *Trp53* had been excised in the majority of these cells (**Figure 3.3b**). However, the small number of p53-positive cells in the tamoxifen-treated *Trp53^{flox/flox};K14-CreERTg/+* animals, indicates incomplete penetrance of CreERT²-mediated *p53* excision.

I first attempted to recapitulate the experiments reported by Kemp *et al.* Thus, five-week old *Trp53^{flox/flox};K14-CreERTg/+* and control *Trp53^{flox/flox}* (*Trp53* allele intact) mice received daily IP injection of tamoxifen for 5 consecutive days (1 mg per mouse per day). One week later 100 μ g of the initiating agent 7,12-dimethylbenz[a]anthracene (DMBA) was topically administered to the shaved dorsal skin of all the mice. One week after DMBA administration, the promoting agent 12-O-tetradecanoylphorbol-13-acetate (TPA) was topically applied to the same dorsal area of the skin on every Monday, Wednesday and Friday for 18 weeks (5 μ g per mouse per dose). **Figure 3.4a** illustrates the timeline of this experiment. Emergence of lesions on the treated dorsal skin was monitored and the total number of tumours after 18 weeks of TPA treatment is shown in **Figure 3.4b**.



(b) Quantification of p53 positive nuclei upon 5 Gy γ -irradiation

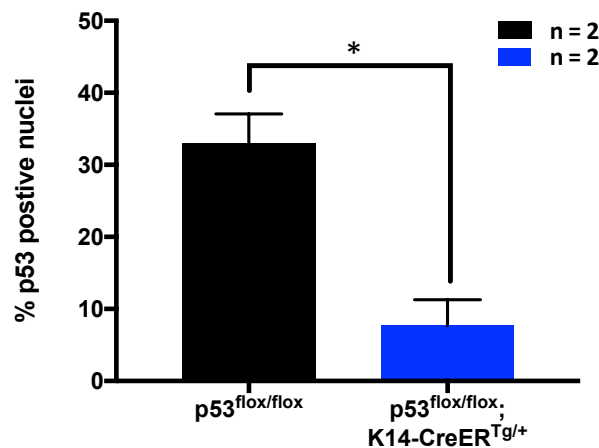
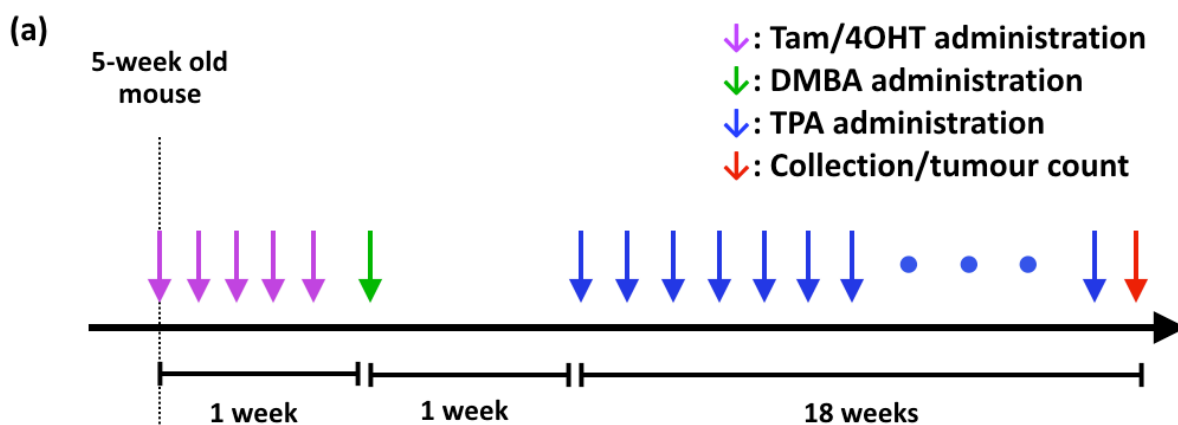


Figure 3.3. Inactivation of *Trp53* by Tam-activated CreERT² expressed in IFE and FB stem cells. (a) p53 expression in the nuclei of the IFE and FB cells was probed by IF staining with α -p53 antibody (CM5, Leica) and the total nuclei were visualised with Hoechst staining. Red pointers in the bottom panel indicate autofluorescence signals (e.g. from hair in follicles). Details of the antibodies used are listed in **Table M.10** in the **Methods and Materials** chapter. (b) Proportion of p53-positive nuclei post-irradiation over total nuclei was quantified in the IF-stained skin sections. Two sections from each animal were counted and the percentage averaged. Plotted is the mean value of % of p53-positive nuclei in the sections of the two animal and the error bars denote standard deviation. An unpaired t-test was used to assess the significance of the observed difference.



(b) **Conditional knockout of *Trp53* by skin-specific Cre impeded skin SCC development**

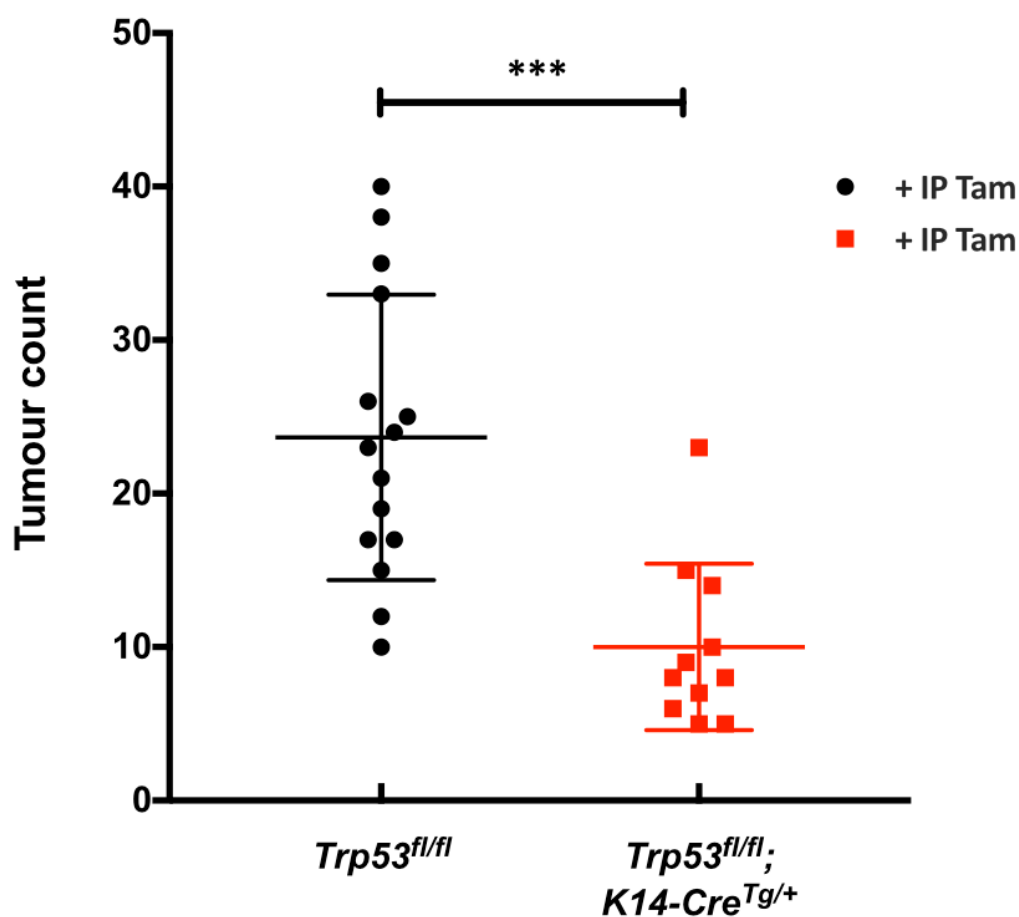
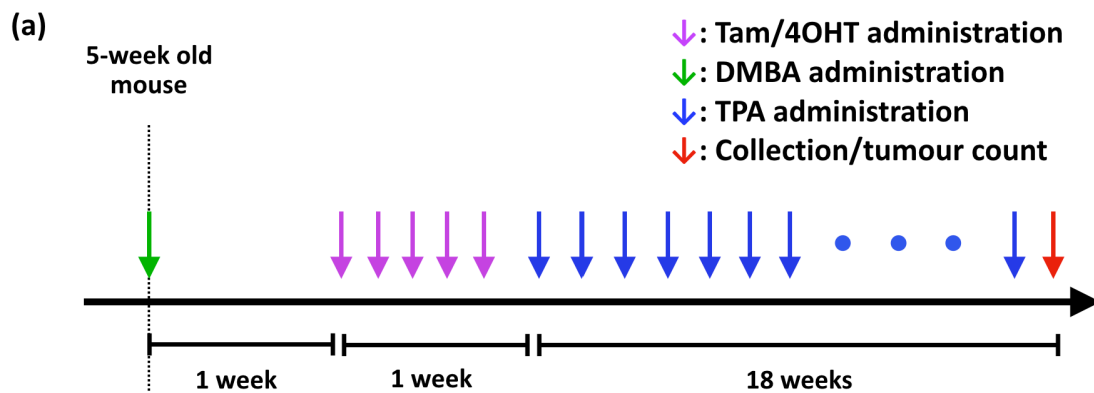


Figure 3.4. Cell type-specific knockout of *Trp53* by inducible CreER^{T2} hampered chemically induced skin SCC. (a) Timeline of the experiment. (b) Each dot represents the number of tumours on the dorsal skin of a mouse after 18 weeks of TPA treatment. p53 status of the skin basal layer (and thus tumours) of *Trp53^{fl/fl}* and *Trp53^{fl/fl};K14-CreER^{Tg/+}* was WT and null respectively after IP injection with Tam. The mean values of the genotype groups are shown with the standard deviations as error bar. A One-way ANOVA test was used to evaluate the statistical significance between the two groups and the *p*-value is indicated (***: *p* = 0.0007).

These data clearly demonstrate that mice in which *Trp53* was deleted by CreERT² in cells of the stratum basale developed fewer tumours compared to mice that retained intact *Trp53* before chemical induction of skin cancer. These findings, in agreement with Kemp CJ *et al*, implied that some functions of p53 are advantageous in papilloma genesis. Despite the apparent contradiction to the protein's prominent role as a tumour suppressor, the implication is understandable considering p53 tumour suppression was not engaged until late stage of tumorigenesis by a high level of oncogenic signals (Martins *et al.* 2006; Xue *et al.* 2007; Ventura *et al.* 2007; Feldser *et al.* 2010; Junttila & Evan 2009). Until that threshold is reached, other functions of p53 may promote survival of aberrantly proliferating (pre-)tumour cells by, for example, coping with transient metabolic stresses such as oxidative stresses and deprivation of nutrient, oxygen or growth factors and thus allowing adaptation and maintaining homeostasis (Humpton & Vousden 2016; Labuschagne *et al.* 2018). This interesting hypothesis had begun to gain more attention recently but had not yet been properly investigated in a tumorigenesis setting. In the following experiments, I further test this hypothesis using the skin carcinogenesis model.

I first attempted to pinpoint the period during which retention of p53 promotes papilloma genesis. This was achieved by delaying the inactivation of *Trp53* to different timepoints before papilloma emergence. I began with the timepoint of inactivating *Trp53* immediately after DMBA initiation. In this experiment, five-week old *Trp53^{flox/flox};K14-CreERTg/+* and control *Trp53^{flox/flox}* mice were treated first with DMBA by topical application on the dorsal skin, followed by IP injections of Tam 1 week later and then topical administration of TPA began for 18 weeks. Other than the reverse order of p53 inactivation and initiation by DMBA, the dose of chemicals used and treatment regime for this cohort of mice remained the same as the previous experiment. **Figure 3.5a** illustrates the timeline of this experiment. The number of papillomas after 18 weeks of TPA treatment is shown in **Figure 3.5b** and it appears that there was no difference in tumour emergence rate between the WT and *Trp53*-inactivated groups.

This result implies that the pro-survival functions of p53, whatever they are, only confers the survival and/or growth advantage to papilloma genesis in the initiation stage.



(b) *Trp53*-conferred survival and/or growth advantages appeared to confine in initiation stage

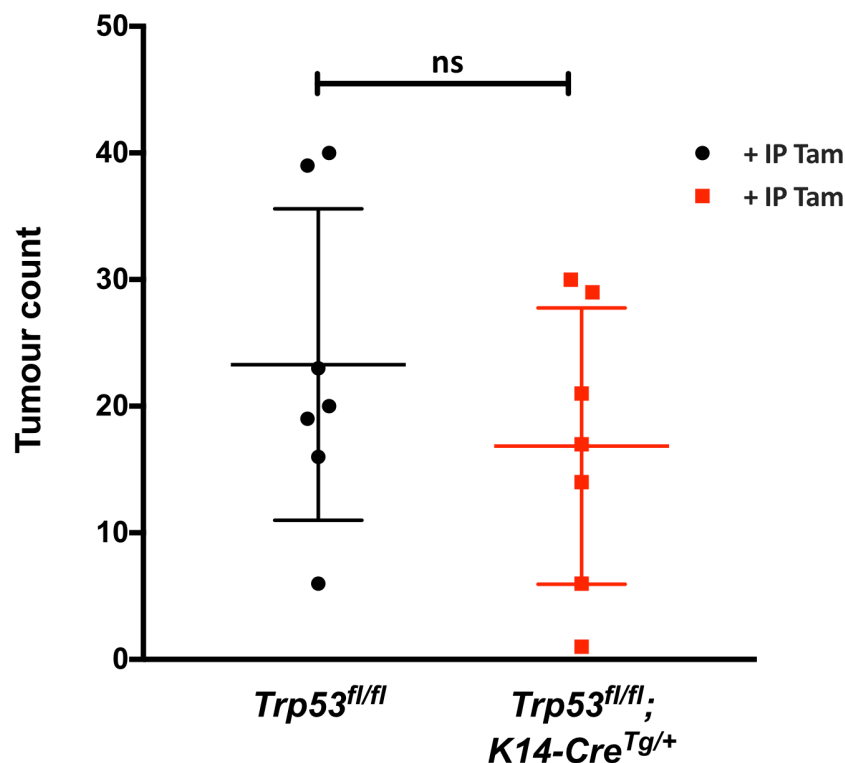


Figure 3.5. Inactivation of *Trp53* after the initiation by DMBA appeared not to confer a survival and/or growth advantage for papilloma development. (a) Timeline of the experiment. (b) Each dot represents the number of tumours on the dorsal skin of a mouse after 18 weeks of TPA treatment. p53 status of the skin basal layer (and thus tumours) of *Trp53^{fl/fl}* and *Trp53^{fl/fl};K14-CreER^{Tg/+}* was WT and null respectively after IP injection with Tam. The mean values of the genotype groups are shown with the standard deviations as error bar. A One-way ANOVA test was used to evaluate the statistical significance between the two groups and the *p*-value is indicated (ns = non significant).

Although this setting with the p53^{flox} model proved useful in finding out the starting point from which retention of p53 functions are important to skin cancer genesis, its irreversibility does not allow assessment of how long these functions will remain important along the trajectory of skin cancer evolution. The excision of *Trp53^{flox}* alleles by CreER^{T2} was also shown not to be fully penetrant in the target cells. Moreover, the use of a Cre recombinase had been proven to inflict significant DNA damage to recipient cells (Janbandhu et al. 2014) and would likely introduce noise and variations to analyses of the supposedly subtler and more transient functions of p53. The TRE-p53 model, on the other hand, can circumvent these issues and address the question properly and therefore was used from this stage on.

3.2.2 Refined temporal dissection of *Trp53*'s roles in chemically induced SCC

To address the questions with a cleaner and more refined approach, TRE-p53 was used in conjunction with the chemically induced skin cancer model. The rationale of the experiments in terms of p53 inactivation is the same as with the p53^{flox} model, except the inactivation is achieved by repression by the *TRE* system upon Dox treatment and is reversible upon Dox withdrawal. **Figure 3.6** illustrates the different timelines in which *Trp53* would be repressed by Dox to address the questions. Timeline **(a)** and **(b)** are the exact analogs of the experiment conducted in **Section 3.2.1 (Figure 3.4 and Figure 3.5 respectively)** and were included to confirm the function of the TRE-p53 system behaviour in comparison to the p53^{flox} model. Timeline **(c)** denotes the first of a series of experimental timelines in which *Trp53* is repressed specifically at different windows in papilloma genesis. These will unveil the exact period in which the pro-survival functions of p53 concerned is important for papilloma genesis. Detailed analysis of p53 function, including transcriptional and metabolic responses in lesions and tissues collected from these animals will be used to determine the “pro-tumour” activity of p53 in early lesion development. Depending on the results from timeline **(c)**, the involvement of these functions of p53 at more advanced stages of skin cancer development can also be investigated

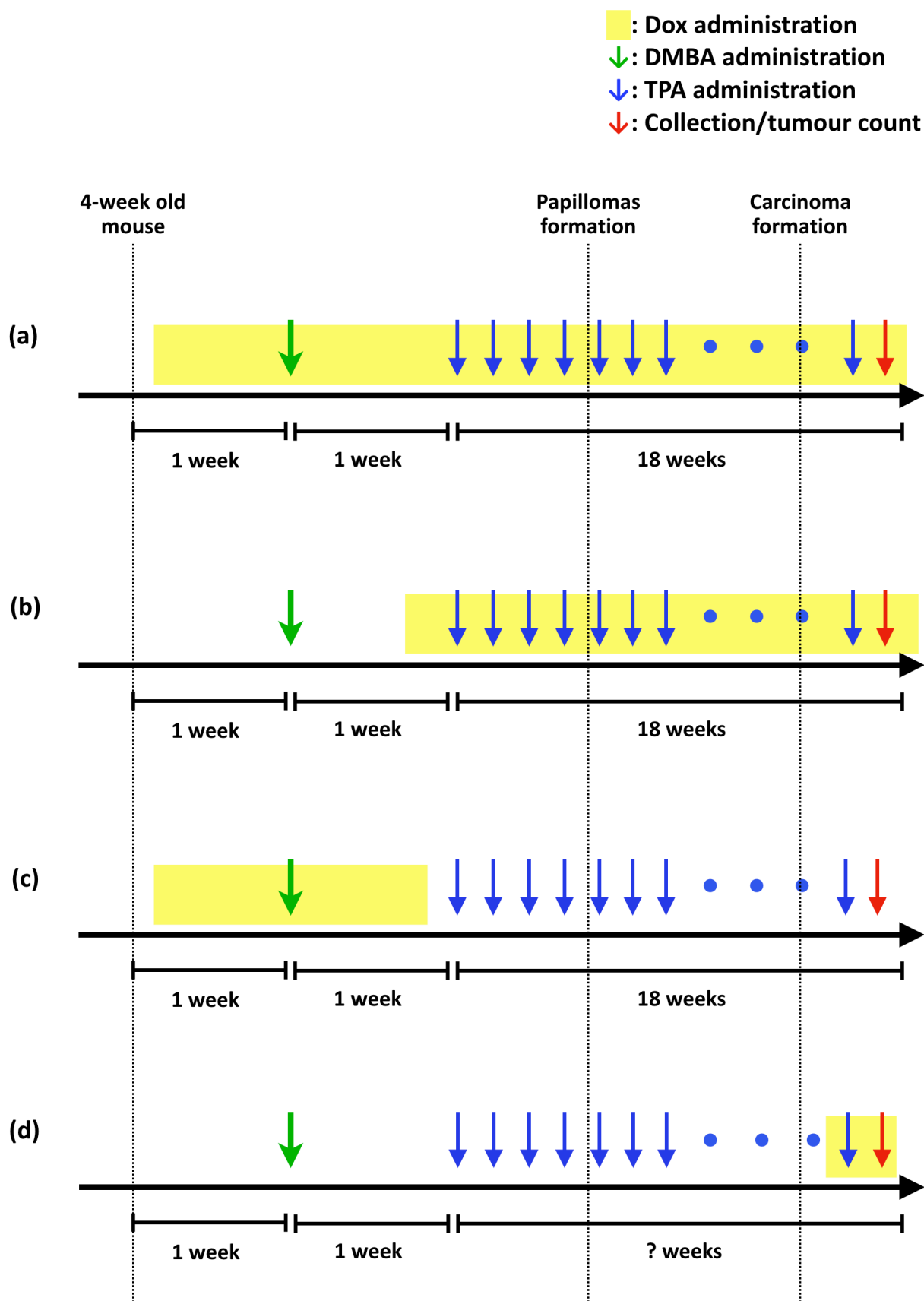


Figure 3.6. More flexible repression of *Trp53* by the *TRE* system allows more experiments of various timelines to address different questions. Timelines (a), (b) and (c) are ongoing while (d) will be conducted after results from Section 3.2.1 and (a) - (c) are analysed.

by, for example, briefly repressing *Trp53* in adenocarcinoma or carcinoma and assessing the immediate impact. Timeline **(d)** illustrates this experiment. This is to assess whether these “pro-tumour” functions of p53, if indeed advantageous for early stage lesions, will continue to be beneficial throughout tumorigenesis and at which point they will be outweighed by the protein’s tumour suppression function.

At the time of writing this thesis, experiments described in **Figures 3.6 (a), (b) and (c)** are ongoing. When the results from these experiments are analysed, further experiments will be designed and conducted.

3.2.3 Does p53 play a similar role in other cancers?

Though frequently mutated in human cancers, the majority of the mutations found in *TP53* are missense mutations rather than nonsense or frameshift mutations that are often found in the other tumour suppressor genes such as *RB* and *APC* (Leslie et al. 2002; Soussi 2005). One possible reason for this is that such missense mutations while inactivating p53’s tumour suppressor role retains at least some of its stress response activity, for example, in nascent tumour cells. However, there is no direct evidence for this, partly since most experiments have been focused on the role of p53 in tumour suppression. In the murine *Kras^{G12D}*-driven model of lung cancer, for example, investigators modelled the human disease by inactivating *Trp53* from the onset (Jackson et al. 2005). Though this yielded tumours of late stages that resembled the human disease at an equivalent stage, it likely shortcuts the development of the early stage tumour during which p53 might have contributed pro-survival and/or growth functions and thus is retained. The preliminary data presented in **Section 3.2** suggests that p53 does indeed influence the development and progression of early skin papillomas. While the p53-dependent “pro-tumour” mechanisms are unclear, it will be important to determine whether this is a common feature of early tumours other than those

induced by chemical carcinogenesis in the skin. Precise temporal regulation of p53 expression afforded by the TRE-p53 model will be invaluable in this pursuit.

Coupled with different mouse tumour models such as the lung *Kras*^{G12D} model, the TRE-p53 system can be used to address the question with a similar approach as in **Section 3.2**. However, another initial parameter is needed to assess the effect of *Trp53* inactivation in early lesions of these tumour models as tumour progression cannot be visually monitored.

**BLANK
PAGE**

Overall Conclusion

OVERALL CONCLUSION

This project was set out to address questions regarding physiological and tumourigenic functions of p53 that had not been properly addressed due to the limitations of the existing *in vivo* model of p53. To achieve such aim, I have built a novel switchable genetic mouse model of p53, TRE-p53, which allows rapidly reversible repression of the gene on transcription level. More specifically, when the repression system is not activated, *Trp53^{TRE}* expression is no different from wild type *in vivo* while repression of *Trp53^{TRE}* expression to over 98 - 99% is efficiently achieved when the repression system is activated through administration of Dox.

In **Chapter 2**, the *in vivo* experiments conducted using the model showed that p53 is expressed and functional as mediator of DNA damage response, transcriptionally activating *Bax*, *Puma* and *Cdkn1a*, in response to whole-body γ -radiation in different tissues.

In **Chapter 3**, short-term systemic repression of p53 using the TRE-p53 model revealed no significant impact on the physiology of adult mouse. On the other hand, long-term systemic repression of p53 in adult mouse led to susceptibility towards tumourigenesis, despite no other physiological symptoms were observed. The spectrum and latency of tumours developed mirrored that of the germline p53-null mice (Donehower et al. 1992). Using the p53^{Flox} model in conjunction with the chemically induced skin squamous cell carcinoma model, I confirmed that the absence of p53 impedes papilloma development triggered by the chemical carcinogen DMBA/TPA, in agreement with the Kemp report published in the 90s (Kemp et al. 1993).

In the future, the TRE-p53 model will be used to address more questions about the biology of p53 such as its less understood role in tissue homeostasis, autophagy and metabolic regulation. I also aim to address the fundamental questions regarding p53 in tumourigenesis, including in particular whether p53 inactivation is a driver mutation in tumorigenesis or a merely mutation-permissive event as well as what p53 activating signals, if any, are present in tumours that develop without p53. Answers to these questions will provide valuable insights to further understanding of p53's functions in normal physiology and carcinogenesis.

List of Reference

LIST OF REFERENCE

- Abel, E.L. et al., 2009. Multi-stage chemical carcinogenesis in mouse skin: Fundamentals and applications. *Nature protocols*, 4(9), pp.1350–1362.
- Alarcón, R. et al., 1999. Hypoxia Induces p53 Accumulation through MDM2 Down-Regulation and Inhibition of E6-mediated Degradation. *Cancer Research*, 59(24), pp.6046–6051.
- American Society of Cancer, 2009. *History of Cancer*, Available at: <https://www.cancer.org/cancer/cancer-basics/history-of-cancer.html>.
- An, W., Kim, J. & Roeder, R.G., 2004. Ordered cooperative functions of PRMT1, p300, and CARM1 in transcriptional activation by p53. *Cell*, 117(6), pp.735–748.
- Anderson, M.E. et al., 1997. Reciprocal interference between the sequence-specific core and nonspecific C-terminal DNA binding domains of p53: implications for regulation. *Molecular and Cellular Biology*, 17(11), pp.6255–6264.
- Antoniades, H.N. et al., 1994. p53 expression during normal tissue regeneration in response to acute cutaneous injury in swine. *Journal of Clinical Investigation*, 93(5), pp.2206–2214.
- Aoyama, M. et al., 2005. Simple and straightforward construction of a mouse gene targeting vector using in vitro transposition reactions. *Nucleic Acids Research*, 33(5), pp.e52–e52.
- Aranda-Anzaldo, A. & Dent, M.A.R., 2003. Developmental noise, ageing and cancer. *Mechanisms of Ageing and Development*, 124(6), pp.711–720.
- Aranda-Anzaldo, A. & Dent, M.A.R., 2007. Reassessing the role of p53 in cancer and ageing from an evolutionary perspective. *Mechanisms of Ageing and Development*, 128(4), pp.293–302.
- Armstrong, J.F. et al., 1995. High-frequency developmental abnormalities in p53-deficient mice. *Current Biology*, 5(8), pp.931–936.
- Ayed, A. et al., 2001. Latent and active p53 are identical in conformation. *Nature structural biology*, 8(9), pp.756–760.
- Baatout, S. et al., 2002. Developmental abnormalities induced by X-irradiation in p53 deficient mice. *In vivo (Athens, Greece)*, 16(3), pp.215–221.
- Baker, S.J. et al., 1989. Chromosome 17 deletions and p53 gene mutations in colorectal carcinomas. *Science*, 244(4901), pp.217–221.
- Balagurumoorthy, P. et al., 1995. Four p53 DNA-binding domain peptides bind natural p53-response elements and bend the DNA. *Proceedings of the National Academy of Sciences of the United States of America*, 92(19), pp.8591–8595.

- Bao, J. et al., 2013. Incomplete cre-mediated excision leads to phenotypic differences between Stra8-iCre; Mov10l1lox/lox and Stra8-iCre; Mov10l1lox/ Δ mice. *Genesis*, 51(7), pp.481–490.
- Baptiste, N. et al., 2002. The proline-rich domain of p53 is required for cooperation with anti-neoplastic agents to promote apoptosis of tumor cells. *Oncogene*, 21(1), pp.9–21.
- Barak, Y. et al., 1993. mdm2 expression is induced by wild type p53 activity. *European Molecular Biology Organization*, 12(2), pp.461–468.
- Bargonetti, J. et al., 1991. Wild-type but not mutant p53 immunopurified proteins bind to sequences adjacent to the SV40 origin of replication. *Cell*, 65(6), pp.1083–1091.
- Bartkova, J. et al., 2005. DNA damage response as a candidate anti-cancer barrier in early human tumorigenesis. *Nature*, 434(7035), pp.864–870.
- Bauer, J.H. et al., 2005. Neuronal expression of p53 dominant-negative proteins in adult *Drosophila melanogaster* extends life span. *Current biology : CB*, 15(22), pp.2063–2068.
- Belyi, V.A. et al., 2010. The Origins and Evolution of the p53 Family of Genes. *Cold Spring Harbor Perspectives in Biology*, 2(6), pp.a001198–a001198.
- Ben David, Y. et al., 1988. Inactivation of the p53 oncogene by internal deletion or retroviral integration in erythroleukemic cell lines induced by Friend leukemia virus. *Oncogene*, 3(2), pp.179–185.
- Bondar, T. & Medzhitov, R., 2010. p53-mediated hematopoietic stem and progenitor cell competition. *Cell stem cell*, 6(4), pp.309–322.
- Bourdon, J.-C. et al., 2005. p53 isoforms can regulate p53 transcriptional activity.
- Bouvard, V. et al., 2000. Tissue and cell-specific expression of the p53-target genes: bax, fas, mdm2 and waf1/p21, before and following ionising irradiation in mice. *Oncogene*, 19(5), pp.649–660.
- Böttger, V. et al., 1999. Comparative study of the p53-mdm2 and p53-MDMX interfaces. *Oncogene*, 18(1), pp.189–199.
- Brugarolas, J. et al., 1995. Radiation-induced cell cycle arrest compromised by p21 deficiency. *Nature*, 377(6549), pp.552–557.
- Budanov, A.V., 2011. Stress-Responsive Sestrins Link p53 with Redox Regulation and Mammalian Target of Rapamycin Signaling. *ANTIOXIDANTS REDOX SIGNALING*, 15(6), pp.1679–1690.
- Burns, T.F., Bernhard, E.J. & El-Deiry, W.S., 2001. Tissue specific expression of p53 target genes suggests a key role for KILLER/DR5 in p53-dependent apoptosis in vivo. *Oncogene*, 20(34), pp.4601–4612.

LIST OF REFERENCE

- Cancer Research UK, 2019. Cancer in the UK 2019. Available at: http://https://www.cancerresearchuk.org/sites/default/files/state_of_the_nation_april_2019.pdf
- Canman, C.E. et al., 1998. Activation of the ATM kinase by ionizing radiation and phosphorylation of p53. *Science*, 281(5383), pp.1677–1679.
- Carter, S. & Vousden, K.H., 2009. Modifications of p53: competing for the lysines. *Current Opinion in Genetics & Development*, 19(1), pp.18–24.
- Chehab, N.H. et al., 1999. Phosphorylation of Ser-20 mediates stabilization of human p53 in response to DNA damage. *Proceedings of the National Academy of Sciences of the United States of America*, 96(24), pp.13777–13782.
- Chen, L. et al., 2015. BAC transgenic mice provide evidence that p53 expression is highly regulated in vivo. *Cell death & disease*, 6(9), pp.e1878–e1878.
- Chen, T.-H. et al., 2017. The p53 gene with emphasis on its paralogues in mosquitoes. *Journal of microbiology, immunology, and infection*, 50(6), pp.747–754.
- Cho, S.-Y. et al., 2012. Doxorubicin induces the persistent activation of intracellular transglutaminase 2 that protects from cell death. *Molecules and Cells*, 33(3), pp.235–241.
- Cho, Y. et al., 1994. Crystal structure of a p53 tumor suppressor-DNA complex: understanding tumorigenic mutations. *Science*, 265(5170), pp.346–355.
- Christophorou, M.A. et al., 2005. Temporal dissection of p53 function in vitro and in vivo. *Nature Genetics*, 37(7), pp.718–726.
- Christophorou, M.A. et al., 2006. The pathological response to DNA damage does not contribute to p53-mediated tumour suppression. *Nature*, 443(7108), pp.214–217.
- Clarke, A.R. et al., 1993. Thymocyte apoptosis induced by p53-dependent and independent pathways. *Nature*, 362(6423), pp.849–852.
- Colaluca, I.N. et al., 2008. NUMB controls p53 tumour suppressor activity. *Nature*, 451(7174), pp.76–80.
- Craig, A.L. et al., 1999. Dephosphorylation of p53 at Ser20 after cellular exposure to low levels of non-ionizing radiation. *Oncogene*, 18(46), pp.6305–6312.
- Crighton, D. et al., 2006. DRAM, a p53-Induced Modulator of Autophagy, Is Critical for Apoptosis. *Cell*, 126(1), pp.121–134.

- Danilova, N., Sakamoto, K.M. & Lin, S., 2008. p53 family in development. *Mechanisms of development*, 125(11-12), pp.919–931.
- de Oca Luna, R.M., Wagner, D.S. & Lozano, G., 1995. Rescue of early embryonic lethality in mdm2-deficient mice by deletion of p53. *Nature*, 378(6553), pp.203–206.
- Delphin, C. et al., 1997. The in vitro phosphorylation of p53 by calcium-dependent protein kinase C--characterization of a protein-kinase-C-binding site on p53. *European Journal of Biochemistry*, 245(3), pp.684–692.
- Do, H. & Kim, W., 2018. Roles of Oncogenic Long Non-coding RNAs in Cancer Development. *Genomics & Informatics*, 16(4), p.e18.
- Donehower, L.A. et al., 1992. Mice deficient for p53 are developmentally normal but susceptible to spontaneous tumours. *Nature*, 356(6366), pp.215–221.
- Dornan, D. et al., 2003. The Proline Repeat Domain of p53 Binds Directly to the Transcriptional Coactivator p300 and Allosterically Controls DNA-Dependent Acetylation of p53. *Molecular and Cellular Biology*, 23(23), pp.8846–8861.
- Du, W. & Searle, J.S., 2009. The rb pathway and cancer therapeutics. *Current drug targets*, 10(7), pp.581–589.
- Dumaz, N. & Meek, D.W., 1999. Serine 15 phosphorylation stimulates p53 transactivation but does not directly influence interaction with HDM2. *European Molecular Biology Organization*, 18(24), pp.7002–7010.
- Dumaz, N. et al., 2001. Critical roles for the serine 20, but not the serine 15, phosphorylation site and for the polyproline domain in regulating p53 turnover. *Biochemical Journal*, 359(2), pp.459–464.
- Efeyan, A. et al., 2006. Tumour biology: Policing of oncogene activity by p53. *Nature*, 443(7108), pp.159–159.
- El-Deiry, W., 1993. WAF1, a potential mediator of p53 tumor suppression. *Cell*, 75(4), pp.817–825.
- El-Deiry, W.S. et al., 1992. Definition of a consensus binding site for p53. *Nature Genetics*, 1(1), pp.45–49.
- Eliyahu, D. et al., 1984. Participation of p53 cellular tumour antigen in transformation of normal embryonic cells. *Nature*, 312(5995), pp.646–649.
- Eliyahu, D. et al., 1989. Wild-type p53 can inhibit oncogene-mediated focus formation. *Proceedings of the National Academy of Sciences of the United States of America*, 86(22), pp.8763–8767.

LIST OF REFERENCE

- Eliyahu, D., Michalovitz, D. & Oren, M., 1985. Overproduction of p53 antigen makes established cells highly tumorigenic. *Nature*, 316(6024), pp.158–160.
- Espinosa, J.M. & Emerson, B.M., 2001. Transcriptional regulation by p53 through intrinsic DNA/chromatin binding and site-directed cofactor recruitment. *Molecular Cell*, 8(1), pp.57–69.
- Fei, P. & El-Deiry, W.S., 2003. P53 and radiation responses. *Oncogene*, 22(37), pp.5774–5783.
- Fei, P., Bernhard, E.J. & El-Deiry, W.S., 2002. Tissue-specific induction of p53 targets in vivo. *Cancer Research*, 62(24), pp.7316–7327.
- Feldser, D.M. et al., 2010. Stage-specific sensitivity to p53 restoration during lung cancer progression. *Nature*, 468(7323), pp.572–575.
- Feng, X. et al., 2011. p53 directly suppresses BNIP3 expression to protect against hypoxia-induced cell death. *European Molecular Biology Organization*, 30(16), pp.3397–3415.
- Finlan, L. & Hupp, T.R., 2004. The N-terminal interferon-binding domain (IBiD) homology domain of p300 binds to peptides with homology to the p53 transactivation domain. *The Journal of biological chemistry*, 279(47), pp.49395–49405.
- Finlay, C.A., Hinds, P.W. & Levine, A.J., 1989. The p53 proto-oncogene can act as a suppressor of transformation. *Cell*, 57(7), pp.1083–1093.
- Finucane, D.M. et al., 1999. Bax-induced caspase activation and apoptosis via cytochrome c release from mitochondria is inhibitable by Bcl-xL. *The Journal of biological chemistry*, 274(4), pp.2225–2233.
- Fitzgerald, A.L. et al., 2015. Reactive oxygen species and p21Waf1/Cip1 are both essential for p53-mediated senescence of head and neck cancer cells. *Cell death & disease*, 6(3), pp.e1678–e1678.
- Flatt, P.M. et al., 2000. p53-dependent expression of PIG3 during proliferation, genotoxic stress, and reversible growth arrest. *Cancer Letters*, 156(1), pp.63–72.
- Fodde, R., 2002. The APC gene in colorectal cancer. *European journal of cancer (Oxford, England : 1990)*, 38(7), pp.867–871.
- Freund, A. et al., 2014. Proteostatic control of telomerase function through TRiC-mediated folding of TCAB1. *Cell*, 159(6), pp.1389–1403.
- Gamper, A.M. & Roeder, R.G., 2008. Multivalent binding of p53 to the STAGA complex mediates coactivator recruitment after UV damage. *Molecular and Cellular Biology*, 28(8), pp.2517–2527.

- Gamper, I. et al., 2017. Determination of the physiological and pathological roles of E2F3 in adult tissues. *Scientific reports*, 7(1), pp.9932–15.
- Garcia-Cao, I., 2002. `Super p53' mice exhibit enhanced DNA damage response, are tumor resistant and age normally. *European Molecular Biology Organization*, 21(22), pp.6225-6235.
- Gentry, A. & Venkatachalam, S., 2005. Complicating the role of p53 in aging. *Aging Cell*, 4(3), pp.157–160.
- Gibson, D.G. et al., 2009. Enzymatic assembly of DNA molecules up to several hundred kilobases. *Nature Methods*, 6(5), pp.343–345.
- Goh, A.M. et al., 2012. Using targeted transgenic reporter mice to study promoter-specific p53 transcriptional activity. *Proceedings of the National Academy of Sciences*, 109(5), pp.1685–1690.
- Gorgoulis, V.G., Vassiliou, L. & Karakaidos, P., 2005. Activation of the DNA damage checkpoint and genomic instability in human precancerous lesions. *Nature*, 434(7035), pp.907-913.
- Gossen, M. & Bujard, H., 1992. Tight control of gene expression in mammalian cells by tetracycline-responsive promoters. *Proceedings of the National Academy of Sciences*, 89(12), pp.5547–5551.
- Götz, C. et al., 1999. Protein kinase CK2 interacts with a multi-protein binding domain of p53. *Molecular and cellular biochemistry*, 191(1-2), pp.111–120.
- Grossman, S.R., 2001. p300/CBP/p53 interaction and regulation of the p53 response. *European Journal of Biochemistry*, 268(10), pp.2773–2778.
- Hall, P.A. et al., 1993. High levels of p53 protein in UV-irradiated normal human skin. *Oncogene*, 8(1), pp.203–207.
- Hammond, E.M. et al., 2002. Hypoxia Links ATR and p53 through Replication Arrest. *Molecular and Cellular Biology*, 22(6), pp.1834–1843.
- Haupt, Y. et al., 1997. Mdm2 promotes the rapid degradation of p53. *Nature*, 387(6630), pp.296–299.
- Hennings, H. et al., 1985. Induction of papillomas with a high probability of conversion to malignancy. *Carcinogenesis*, 6(11), pp.1607–1610.
- Henriksson, S. et al., 2014. The scaffold protein WRAP53 β orchestrates the ubiquitin response critical for DNA double-strand break repair. *Genes & Development*, 28(24), pp.2726–2738.
- Hollstein, M. et al., 1991. p53 mutations in human cancers. *Science*, 253(5015), pp.49–53.

LIST OF REFERENCE

- Horn, H.F. & Vousden, K.H., 2007. Coping with stress: multiple ways to activate p53. *Oncogene*, 26(9), pp.1306–1316.
- Hu, W. et al., 2007. p53 regulates maternal reproduction through LIF. *Nature*, 450(7170), pp.721–724.
- Humpton, T.J. & Vousden, K.H., 2016. Regulation of Cellular Metabolism and Hypoxia by p53. *Cold Spring Harbor Perspectives in Medicine*, 6(7), p.a026146.
- Hupp, T.R. & Lane, D.P., 1994. Allosteric activation of latent p53 tetramers. *Current biology : CB*, 4(10), pp.865–875.
- Hupp, T.R. et al., 1992. Regulation of the specific DNA binding function of p53. *Cell*, 71(5), pp.875–886.
- Hyunhee Do, W.K., 2018. Roles of Oncogenic Long Non-coding RNAs in Cancer Development. *Genomics & Informatics*, 16(4), p.e18.
- Ito, A. et al., 2002. MDM2-HDAC1-mediated deacetylation of p53 is required for its degradation. *European Molecular Biology Organization*, 21(22), pp.6236–6245.
- Jackson, E.L. et al., 2005. The Differential Effects of Mutant p53 Alleles on Advanced Murine Lung Cancer. *Cancer Research*, 65(22), pp.10280–10288.
- Jain, A.K. & Barton, M.C., 2018. p53: emerging roles in stem cells, development and beyond. *Development*, 145(8), p.dev158360.
- Janbandhu, V.C., Moik, D. & Fässler, R., 2014. Cre recombinase induces DNA damage and tetraploidy in the absence of loxP sites. *Cell cycle*, 13(3), pp.462–470.
- Jayaraman, J. & Prives, C., 1995. Activation of p53 sequence-specific DNA binding by short single strands of DNA requires the p53 C-terminus. *Cell*, 81(7), pp.1021–1029.
- Jenkins, J.R., Rudge, K. & Currie, G.A., 1984. Cellular immortalization by a cDNA clone encoding the transformation-associated phosphoprotein p53. *Nature*, 312(5995), pp.651–654.
- Jenkins, J.R., Rudge, K., Redmond, S., et al., 1984. Cloning and expression analysis of full length mouse cDNA sequences encoding the transformation associated protein p53. *Nucleic Acids Research*, 12(14), pp.5609–5626.
- Jones, R.G. et al., 2005. AMP-Activated Protein Kinase Induces a p53-Dependent Metabolic Checkpoint. *Molecular Cell*, 18(3), pp.283–293.
- Jones, S.N. et al., 1995. Rescue of embryonic lethality in Mdm2-deficient mice by absence of p53. *Nature*, 378(6553), pp.206–208.

- Jonkers, J. et al., 2001. Synergistic tumor suppressor activity of BRCA2 and p53 in a conditional mouse model for breast cancer. *Nature Genetics*, 29(4), pp.418–425.
- Joruiz, S.M. & Bourdon, J.-C., 2016. p53 Isoforms: Key Regulators of the Cell Fate Decision. *Cold Spring Harbor Perspectives in Medicine*, 6(8), p.a026039.
- Jozefczuk, J., Drews, K. & Adjaye, J., 2012. Preparation of mouse embryonic fibroblast cells suitable for culturing human embryonic and induced pluripotent stem cells. *Journal of visualized experiments : JoVE*, (64).
- Jung, H. et al., 2013. TXNIP maintains the hematopoietic cell pool by switching the function of p53 under oxidative stress. *Cell Metabolism*, 18(1), pp.75–85.
- Junttila, M.R. & Evan, G.I., 2009. p53 — a Jack of all trades but master of none. *Nature Reviews Cancer*, 9(11), pp.821–829.
- Junttila, M.R. et al., 2010. Selective activation of p53-mediated tumour suppression in high-grade tumours. *Nature*, 468(7323), pp.567–571.
- Kamijo, T. et al., 1997. Tumor suppression at the mouse INK4a locus mediated by the alternative reading frame product p19ARF. *Cell*, 91(5), pp.649–659.
- Kamijo, T. et al., 1998. Functional and physical interactions of the ARF tumor suppressor with p53 and Mdm2. *Proceedings of the National Academy of Sciences of the United States of America*, 95(14), pp.8292–8297.
- Kastan, M.B. et al., 1992. A mammalian cell cycle checkpoint pathway utilizing p53 and GADD45 is defective in ataxia-telangiectasia. *Cell*, 71(4), pp.587–597.
- Kaufman, M.H. et al., 1997. Analysis of fused maxillary incisor dentition in p53-deficient exencephalic mice. *Journal of anatomy*, 191 (Pt 1)(1), pp.57–64.
- Kemp, C.J. et al., 1993. Reduction of p53 gene dosage does not increase initiation or promotion but enhances malignant progression of chemically induced skin tumors. *Cell*, 74(5), pp.813–822.
- Kenzelmann Broz, D. et al., 2013. Global genomic profiling reveals an extensive p53-regulated autophagy program contributing to key p53 responses. *Genes & Development*, 27(9), pp.1016–1031.
- Kern, S.E. et al., 1991. Identification of p53 as a sequence-specific DNA-binding protein. *Science*, 252(5013), pp.1708–1711.

LIST OF REFERENCE

- Komarova, E.A. et al., 1997. Transgenic mice with p53-responsive lacZ: p53 activity varies dramatically during normal development and determines radiation and drug sensitivity in vivo. *European Molecular Biology Organization*, 16(6), pp.1391–1400.
- Kondo, S., 1998. Apoptotic repair of genotoxic tissue damage and the role of p53 gene. *Mutation research*, 402(1-2), pp.311–319.
- Kubbutat, M.H.G., Jones, S.N. & Vousden, K.H., 1997. Regulation of p53 stability by Mdm2. *Nature*, 387(6630), pp.299–303.
- Labuschagne, C.F., Zani, F. & Vousden, K.H., 2018. Control of metabolism by p53 – Cancer and beyond. *Biochimica et Biophysica Acta (BBA) - Reviews on Cancer*, 1870(1), pp.32–42.
- Lakin, N.D. & Jackson, S.P., 1999. Regulation of p53 in response to DNA damage. *Oncogene*, 18(53), pp.7644–7655.
- Lambert, P.F. et al., 1998. Phosphorylation of p53 serine 15 increases interaction with CBP. *The Journal of biological chemistry*, 273(49), pp.33048–33053.
- Lane, D.P., 1992. Cancer. p53, guardian of the genome. *Nature*, 358(6381), pp.15–16.
- Lane, D.P. & Crawford, L.V., 1979. T antigen is bound to a host protein in SV40-transformed cells. *Nature*, 278(5701), pp.261–263.
- Lane, D.P. et al., 2010. Mdm2 and p53 are highly conserved from placozoans to man. *Cell cycle*, 9(3), pp.540–547.
- Lapouge, G. et al., 2011. Identifying the cellular origin of squamous skin tumors. *Proceedings of the National Academy of Sciences*, 108(18), pp.7431–7436.
- Laptenko, O. et al., 2015. The p53 C terminus controls site-specific DNA binding and promotes structural changes within the central DNA binding domain. *Molecular Cell*, 57(6), pp.1034–1046.
- Le Cam, L. et al., 2006. E4F1 is an atypical ubiquitin ligase that modulates p53 effector functions independently of degradation. *Cell*, 127(4), pp.775–788.
- Lee, J.H. et al., 2003. In vivo p53 function is indispensable for DNA damage-induced apoptotic signaling in Drosophila. *FEBS letters*, 550(1-3), pp.5–10.
- Lee, J.H. et al., 2010. The p53-inducible gene 3 (PIG3) contributes to early cellular response to DNA damage. *Oncogene*, 29(10), pp.1431–1450.

- Lemon, B. & Tjian, R., 2000. Orchestrated response: a symphony of transcription factors for gene control. *Genes & Development*, 14(20), pp.2551–2569.
- Leslie, A. et al., 2002. The colorectal adenoma–carcinoma sequence. *British Journal of Surgery*, 89(7), pp.845–860.
- Li, J. et al., 2004. Hypoxia-induced nucleophosmin protects cell death through inhibition of p53. *The Journal of biological chemistry*, 279(40), pp.41275–41279.
- Li, M. et al., 2003. Mono- versus polyubiquitination: differential control of p53 fate by Mdm2. *Science*, 302(5652), pp.1972–1975.
- Lin, T. et al., 2005. p53 induces differentiation of mouse embryonic stem cells by suppressing Nanog expression. *Nature Cell Biology*, 7(2), pp.165–171.
- Linzer, D.I. & Levine, A.J., 1979. Characterization of a 54K dalton cellular SV40 tumor antigen present in SV40-transformed cells and uninfected embryonal carcinoma cells. *Cell*, 17(1), pp.43–52.
- Linzer, D.I., Maltzman, W. & Levine, A.J., 1979. The SV40 A gene product is required for the production of a 54,000 MW cellular tumor antigen. *Virology*, 98(2), pp.308–318.
- Littlewood, T.D. et al., 1995. A modified oestrogen receptor ligand-binding domain as an improved switch for the regulation of heterologous proteins. *Nucleic Acids Research*, 23(10), pp.1686–1690.
- Liu, Y. et al., 2009. p53 regulates hematopoietic stem cell quiescence. *Cell stem cell*, 4(1), pp.37–48.
- Lowe, S.W., Ruley, H.E., et al., 1993. p53-dependent apoptosis modulates the cytotoxicity of anticancer agents. *Cell*, 74(6), pp.957–967.
- Lowe, S.W., Schmitt, E.M., et al., 1993. p53 is required for radiation-induced apoptosis in mouse thymocytes. *Nature*, 362(6423), pp.847–849.
- MacCallum, D.E. et al., 1996. The p53 response to ionising radiation in adult and developing murine tissues. *Oncogene*, 13(12), pp.2575–2587.
- Mahmoudi, S. et al., 2010. WRAP53 is essential for Cajal body formation and for targeting the survival of motor neuron complex to Cajal bodies. T. Misteli, ed. *PLoS Biology*, 8(11), p.e1000521.
- Mahmoudi, S. et al., 2009. Wrap53, a Natural p53 Antisense Transcript Required for p53 Induction upon DNA Damage. *Molecular Cell*, 33(4), pp.462–471.
- Maier, B. et al., 2004. Modulation of mammalian life span by the short isoform of p53. *Genes & Development*, 18(3), pp.306–319.

LIST OF REFERENCE

- Malkin, D. et al., 1990. Germ line p53 mutations in a familial syndrome of breast cancer, sarcomas, and other neoplasms. *Science*, 250(4985), pp.1233–1238.
- Maltzman, W. & Czyzyk, L., 1984. UV irradiation stimulates levels of p53 cellular tumor antigen in nontransformed mouse cells. *Molecular and Cellular Biology*, 4(9), pp.1689–1694.
- Martins, C.P., Brown Swigart, L. & Evan, G.I., 2006. Modeling the therapeutic efficacy of p53 restoration in tumors. *Cell*, 127(7), pp.1323–1334.
- Matallanas, D. et al., 2007. RASSF1A elicits apoptosis through an MST2 pathway directing proapoptotic transcription by the p73 tumor suppressor protein. *Molecular Cell*, 27(6), pp.962–975.
- Matoba, S. et al., 2006. p53 regulates mitochondrial respiration. *Science*, 312(5780), pp.1650–1653.
- Matsuda, T. & Cepko, C.L., 2007. Controlled expression of transgenes introduced by in vivo electroporation. *Proceedings of the National Academy of Sciences of the United States of America*, 104(3), pp.1027–1032.
- McKinney, K. et al., 2004. p53 linear diffusion along DNA requires its C terminus. *Molecular Cell*, 16(3), pp.413–424.
- Melino, G. et al., 2004. p73 Induces apoptosis via PUMA transactivation and Bax mitochondrial translocation. *The Journal of biological chemistry*, 279(9), pp.8076–8083.
- Mendrysa, S.M. et al., 2006. Tumor suppression and normal aging in mice with constitutively high p53 activity. *Genes & Development*, 20(1), pp.16–21.
- Metzger, D. & Chambon, P., 2001. Site- and Time-Specific Gene Targeting in the Mouse. *Methods*, 24(1), pp.71–80.
- Mills, A.A. et al., 1999. p63 is a p53 homologue required for limb and epidermal morphogenesis. *Nature*, 398(6729), pp.708–713.
- Ming, L. et al., 2008. Sp1 and p73 activate PUMA following serum starvation. *Carcinogenesis*, 29(10), pp.1878–1884.
- Miyashita, T. & Reed, J.C., 1995. Tumor suppressor p53 is a direct transcriptional activator of the human bax gene. *Cell*, 80(2), pp.293–299.
- Momand, J. et al., 1992. The mdm-2 oncogene product forms a complex with the p53 protein and inhibits p53-mediated transactivation. *Cell*, 69(7), pp.1237–1245.

- Mowat, M. et al., 1985. Rearrangements of the cellular p53 gene in erythroleukaemic cells transformed by Friend virus. *Nature*, 314(6012), pp.633–636.
- Murphy, D.J. et al., 2008. Distinct thresholds govern Myc's biological output in vivo. *Cancer Cell*, 14(6), pp.447–457.
- Nakamura, E., Nguyen, M.T. & Mackem, S., 2006. Kinetics of tamoxifen-regulated Cre activity in mice using a cartilage-specific CreERT to assay temporal activity windows along the proximodistal limb skeleton. *Developmental Dynamics*, 235(9), pp.2603–2612.
- Nakano, K. & Vousden, K.H., 2001. PUMA, a novel proapoptotic gene, is induced by p53. *Molecular Cell*, 7(3), pp.683–694.
- National Center for Biotechnology Information (NCBI)[Internet]. Bethesda (MD): National Library of Medicine (US), National Center for Biotechnology Information; [1988] – [cited 2017 Apr 06] . Available from: <https://www.ncbi.nlm.nih.gov/>
- Nie, L., Sasaki, M. & Maki, C.G., 2007. Regulation of p53 nuclear export through sequential changes in conformation and ubiquitination. *The Journal of biological chemistry*, 282(19), pp.14616–14625.
- Nigro, J.M. et al., 1989. Mutations in the p53 gene occur in diverse human tumour types. *Nature*, 342(6250), pp.705–708.
- Ohue, M., Tomita, N. & Monden, T., 1994. A frequent alteration of p53 gene in carcinoma in adenoma of colon. *Cancer Research*, 54(17), pp.4798–4804.
- Oltvai, Z.N., Milliman, C.L. & Korsmeyer, S.J., 1993. Bcl-2 heterodimerizes in vivo with a conserved homolog, Bax, that accelerates programmed cell death. *Cell*, 74(4), pp.609–619.
- Pan, Y. et al., 2004. p53 cannot be induced by hypoxia alone but responds to the hypoxic microenvironment. *Oncogene*, 23(29), pp.4975–4983.
- Pankow, S. & Bamberger, C., 2007. The p53 tumor suppressor-like protein nvp63 mediates selective germ cell death in the sea anemone *Nematostella vectensis*. S. Rutherford, ed. *PLoS one*, 2(9), p.e782.
- Pavletich, N.P., Chambers, K.A. & Pabo, C.O., 1993. The DNA-binding domain of p53 contains the four conserved regions and the major mutation hot spots. *Genes & Development*, 7(12B), pp.2556–2564.
- Pomerantz, J. et al., 1998. The Ink4a tumor suppressor gene product, p19Arf, interacts with MDM2 and neutralizes MDM2's inhibition of p53. *Cell*, 92(6), pp.713–723.

LIST OF REFERENCE

- Quelle, D.E. et al., 1995. Alternative reading frames of the INK4a tumor suppressor gene encode two unrelated proteins capable of inducing cell cycle arrest. *Cell*, 83(6), pp.993–1000.
- Raj, N. & Attardi, L.D., 2017. The Transactivation Domains of the p53 Protein. *Cold Spring Harbor Perspectives in Medicine*, 7(1), p.a026047.
- Rajagopalan, S. et al., 2009. Interaction between the transactivation domain of p53 and PC4 exemplifies acidic activation domains as single-stranded DNA mimics. *The Journal of biological chemistry*, 284(32), pp.21728–21737.
- Rutkowski, R., Hofmann, K. & Gartner, A., 2010. Phylogeny and function of the invertebrate p53 superfamily. *Cold Spring Harbor Perspectives in Biology*, 2(7), pp.a001131–a001131.
- Ryan, K.M., 2011. p53 and autophagy in cancer: Guardian of the genome meets guardian of the proteome. *European Journal of Cancer*, 47(1), pp.44–50.
- Sah, V.P. et al., 1995. A subset of p53-deficient embryos exhibit exencephaly. *Nature Genetics*, 10(2), pp.175–180.
- Saifudeen, Z. et al., 2009. p53 regulates metanephric development. *Journal of the American Society of Nephrology : JASN*, 20(11), pp.2328–2337.
- Sakaguchi, K. et al., 2000. Damage-mediated phosphorylation of human p53 threonine 18 through a cascade mediated by a casein 1-like kinase. Effect on Mdm2 binding. *The Journal of biological chemistry*, 275(13), pp.9278–9283.
- Sakamuro, D. et al., 1997. The polyproline region of p53 is required to activate apoptosis but not growth arrest. *Oncogene*, 15(8), pp.887–898.
- Sarkisian, C.J. et al., 2007. Dose-dependent oncogene-induced senescence in vivo and its evasion during mammary tumorigenesis. *Nature Cell Biology*, 9(5), pp.493–505.
- Schon, O. et al., 2002. Molecular Mechanism of the Interaction between MDM2 and p53. *Journal of Molecular Biology*, 323(3), pp.491–501.
- Shieh, S.-Y. et al., 1997. DNA Damage-Induced Phosphorylation of p53 Alleviates Inhibition by MDM2. *Cell*, 91(3), pp.325–334.
- Siegl, C. et al., 2014. Tumor suppressor p53 alters host cell metabolism to limit *Chlamydia trachomatis* infection. *Cell reports*, 9(3), pp.918–929.
- Siliciano, J.D. et al., 1997. DNA damage induces phosphorylation of the amino terminus of p53. *Genes & Development*, 11(24), pp.3471–3481.

- Silva, J. et al., 2008. Promotion of reprogramming to ground state pluripotency by signal inhibition. M. A. Goodell, ed. *PLoS Biology*, 6(10), p.e253.
- Sodir, N.M. et al., 2011. Endogenous Myc maintains the tumor microenvironment. *Genes & Development*, 25(9), pp.907–916.
- Sogame, N., Kim, M. & Abrams, J.M., 2003. Drosophila p53 preserves genomic stability by regulating cell death. *Proceedings of the National Academy of Sciences of the United States of America*, 100(8), pp.4696–4701.
- Solozobova, V. & Blattner, C., 2011. p53 in stem cells. *World Journal of Biological Chemistry*, 2(9), pp.202-214
- Soucek, L. & Evan, G.I., 2010. The ups and downs of Myc biology. *Current Opinion in Genetics & Development*, 20(1), pp.91–95.
- Soucek, L. et al., 2011. Modeling pharmacological inhibition of mast cell degranulation as a therapy for insulinoma. *Neoplasia*, 13(11), pp. 1093-1100.
- Soucek, L. et al., 2008. Modelling Myc inhibition as a cancer therapy. *Nature*, 455(7213), pp.679–683.
- Soussi, T., 2005. The p53 pathway and human cancer. *British Journal of Surgery*, 92(11), pp.1331–1332.
- Srivastava, S. et al., 1990. Germ-line transmission of a mutated p53 gene in a cancer-prone family with Li-Fraumeni syndrome. *Nature*, 348(6303), pp.747–749.
- Suh, E.-K. et al., 2006. p63 protects the female germ line during meiotic arrest. *Nature*, 444(7119), pp.624–628.
- Tafvizi, A. et al., 2011. A single-molecule characterization of p53 search on DNA. *Proceedings of the National Academy of Sciences*, 108(2), pp.563–568.
- Tago, K., Chiocca, S. & Sherr, C.J., 2005. Sumoylation induced by the Arf tumor suppressor: a p53-independent function. *Proceedings of the National Academy of Sciences of the United States of America*, 102(21), pp.7689–7694.
- Takimoto, R. & El-Deiry, W.S., 2001. DNA replication blockade impairs p53-transactivation. *Proceedings of the National Academy of Sciences of the United States of America*, 98(3), pp.781–783.
- Tanikawa, C. et al., 2017. The Transcriptional Landscape of p53 Signalling Pathway. *EBioMedicine*, 20, pp.109–119.
- Tateossian, H. et al., 2015. Interactions between the otitis media gene, Fbxo11, and p53 in the mouse embryonic lung. *Disease models & mechanisms*, 8(12), pp.1531–1542.

LIST OF REFERENCE

- Thut, C.J. et al., 1995. p53 transcriptional activation mediated by coactivators TAFII40 and TAFII60. *Science*, 267(5194), pp.100–104.
- Tosoni, D. et al., 2015. The Numb/p53 circuitry couples replicative self-renewal and tumor suppression in mammary epithelial cells. *The Journal of cell biology*, 211(4), pp.845–862.
- Tovy, A. et al., 2017. p53 is essential for DNA methylation homeostasis in naïve embryonic stem cells, and its loss promotes clonal heterogeneity. *Genes & Development*, 31(10), pp.959–972.
- Tschaharganeh, D.F. et al., 2014. p53-Dependent Nestin Regulation Links Tumor Suppression to Cellular Plasticity in Liver Cancer. *Cell*, 158(3), pp.579–592.
- Tycowski, K.T. et al., 2009. A conserved WD40 protein binds the Cajal body localization signal of scaRNP particles. *Molecular Cell*, 34(1), pp.47–57.
- Tyner, S.D. et al., 2002. p53 mutant mice that display early ageing-associated phenotypes. *Nature*, 415(6867), pp.45–53.
- Unger, T. et al., Critical role for Ser20 of human p53 in the negative regulation of p53 by Mdm2. *European Molecular Biology Organization*, 18(7), pp.1805-1814.
- Vasioukhin, V. et al., 1999. The magical touch: genome targeting in epidermal stem cells induced by tamoxifen application to mouse skin. *Proceedings of the National Academy of Sciences of the United States of America*, 96(15), pp.8551–8556.
- Venot, C. et al., 1998. The requirement for the p53 proline-rich functional domain for mediation of apoptosis is correlated with specific PIG3 gene transactivation and with transcriptional repression. *European Molecular Biology Organization*, 17(16), pp.4668–4679.
- Venteicher, A.S. et al., 2009. A human telomerase holoenzyme protein required for Cajal body localization and telomere synthesis. *Science*, 323(5914), pp.644–648.
- Ventura, A. et al., 2007. Restoration of p53 function leads to tumour regression in vivo. *Nature*, 445(7128), pp.661–665.
- Vogelstein, B. et al., 1988. Genetic Alterations during Colorectal-Tumor Development. *New England Journal of Medicine*, 319(9), pp.525–532.
- Vousden, K.H. & Ryan, K.M., 2009. p53 and metabolism. *Nature Reviews Cancer*, 9(10), pp.691–700.
- Waga, S. et al., 1994. The p21 inhibitor of cyclin-dependent kinases controls DNA replication by interaction with PCNA. *Nature*, 369(6481), pp.574–578.

- Walker, K.K. & Levine, A.J., 1996. Identification of a novel p53 functional domain that is necessary for efficient growth suppression. *Proceedings of the National Academy of Sciences of the United States of America*, 93(26), pp.15335–15340.
- Wang, Q. et al., 2017. The p53 Family Coordinates Wnt and Nodal Inputs in Mesendodermal Differentiation of Embryonic Stem Cells. *Cell stem cell*, 20(1), pp.70–86.
- Wang, Y. et al., 1993. p53 domains: identification and characterization of two autonomous DNA-binding regions. *Genes & Development*, 7(12B), pp.2575–2586.
- Wolf, D. & Rotter, V., 1984. Inactivation of p53 gene expression by an insertion of Moloney murine leukemia virus-like DNA sequences. *Molecular and Cellular Biology*, 4(7), pp.1402–1410.
- Wolf, D. & Rotter, V., 1985. Major deletions in the gene encoding the p53 tumor antigen cause lack of p53 expression in HL-60 cells. *Proceedings of the National Academy of Sciences of the United States of America*, 82(3), pp.790–794.
- Wu, X. et al., 1993. The p53-mdm-2 autoregulatory feedback loop. *Genes & Development*, 7(7a), pp.1126–1132.
- Xue, W. et al., 2007. Senescence and tumour clearance is triggered by p53 restoration in murine liver carcinomas. *Nature*, 445(7128), pp.656–660.
- Yang, A. & McKeon, F., 2000. p63 and p73: p53 mimics, menaces and more. *Nature Review Molecular Cell Biology*, pp.1–9.
- Yang, A. et al., 1999. p63 is essential for regenerative proliferation in limb, craniofacial and epithelial development. *Nature*, 398(6729), pp.714–718.
- Yang, A. et al., 2000. p73-deficient mice have neurological, pheromonal and inflammatory defects but lack spontaneous tumours. *Nature*, 404(6773), pp.99–103.
- Yonish-Rouach, E. et al., 1991. Wild-type p53 induces apoptosis of myeloid leukaemic cells that is inhibited by interleukin-6. *Nature*, 352(6333), pp.345–347.
- Yoon, K.-A., Nakamura, Y. & Arakawa, H., 2004. Identification of ALDH4 as a p53-inducible gene and its protective role in cellular stresses. *Journal of human genetics*, 49(3), pp.134–140.
- Zhang, Y., Xiong, Y. & Yarbrough, W.G., 1998. ARF promotes MDM2 degradation and stabilizes p53: ARF-INK4a locus deletion impairs both the Rb and p53 tumor suppression pathways. *Cell*, 92(6), pp.725–734.

LIST OF REFERENCE

- Zhong, F. et al., 2011. Disruption of telomerase trafficking by TCAB1 mutation causes dyskeratosis congenita. *Genes & Development*, 25(1), pp.11–16.
- Zindy, F. et al., 1998. Myc signaling via the ARF tumor suppressor regulates p53-dependent apoptosis and immortalization. *Genes & Development*, 12(15), pp.2424–2433.
- Zhu, J. et al., 1999. Differential regulation of cellular target genes by p53 devoid of the PXXP motifs with impaired apoptotic activity. *Oncogene*, 18(12), pp.2149–2155.

THE END